# PCRedux package - an overview

The PCRedux package authors

2022-05-12

## Contents

The PDF version of this document is available **online supplement**.

# 1 Aims of the `PCRedux` package

A review of the literature (PubMed, Google Scholar; 1984-01-01 - 2022-05-12) and discussion with peers revealed that there is no open source software package to calculate predictors from quantitative PCR amplification curves for machine learning applications. A predictor is a quantifiable *informative* property of an amplification curve. In particular, there is no information available about predictors that can be used from amplification curves apart from measures that describe quantification points, amplification efficiencies and signal levels. Although several amplification curve data sets are available, no curated labeled data sets labels are described in the literature or repositories such as GitHub[1], Bitbucket[2], SourceForge[3] or Kaggle[4].

Therefore, the aim of the package was to:

1. create a collection of classified amplification curve data,
2. propose algorithms that can be used to calculate predictors from amplification curves,
3. evaluate pipelines that can be used for an automatic classification of amplification curves based on the curve shape and
4. to bundle the findings in a public repository open source software and open data package.

# 2 Introduction to the Detection and Quantification of Nucleic Acids and the Relation to Machine Learning

In subsection 2.1 the reader finds a concise introduction to nucleic acids, including nucleic acid detection methods for the analysis of forensic sample material. Special intention is paid to the quantitative Polymerase Chain Reaction (qPCR), since this method is the *de facto* standard for the detection and high-precision quantification of nucleic acids.

The focus of this study is the development of statistical and bioinformatical algorithms for the `PCRedux` software (version 1.1.2). This software can be used to automatically calculate putative predictors (*features*) from qPCR amplification curves. A predictor herein refers to a quantifiable *informative* property of an amplification curve, employable for data mining, machine learning applications and classification tasks.

[1] https://github.com/
[2] https://bitbucket.org/
[3] https://sourceforge.net/
[4] https://www.kaggle.com/

The subsection 3.1 deals with elements of the software engineering (e. g., continuous integration, Donald Knuth's *Literate Programming*, unit testing) used within the `PCRedux` software. The subsection 3.2 gives an introduction into qPCR data, their analysis and explains why there is a need for the `PCRedux` software. In addition, the data analysis using machine learning is concisely described, after which the work focuses on the analysis of the measured data.

The proposed algorithms were partially tested with machine learning methods. For this purpose, a brief introduction to the subject *machine learning* is given in subsubsection 3.2.1, and results from the belonging chapters are applied.

The details for statistical analyses of qPCR amplification curves are presented in subsubsection 3.2.4 ff. This covers the description of the curvature and the challenges of the calculations.

All scientific and engineering work depends on data. In particular, *open data* are becoming a cornerstone in science. As data sets of classified amplification curves were not available anywhere else, subsection 3.5 summarizes the aggregation, maintenance, and distribution of classified qPCR amplification curve data sets. The manual classification of amplification curves is a time-consuming and error prone task when working with large data sets. To facilitate the manual analysis procedure, helper tools are presented in subsection 3.4. In particular, a novel approach for *curve-shape based group classification* is shown.

An achievement of this study is the extensive portfolio of statistical algorithms for predictor calculation. Central findings of the research are presented in subsection 3.3.

It is expected that these implementations will allow the automatic analysis of large data sets for machine learning applications. The expectations of the findings are critically discussed in section 5.

## 2.1 Bioanalytical Methods for the Detection and Quantification of Nucleic Acids

Nucleic acids are biopolymers composed of nucleotides and allow organisms to transfer genetic information. The nucleotides (e. g., *G* for guanine, *C* for cytosine) are arranged in a specific order (sequence). Strands of complementary nucleotide pairs (e. g., G:::C) form stable hybrids. These can be differentiated based on their sequences by the analytical methods presented below. There are two types of nucleic acids:

- deoxyribonucleic acid (DNA) and
- ribonucleic acid (RNA).

The latter has further subtypes such as micro-RNA (Berg, Tymoczko, and Stryer 2002). Jeffreys, Wilson, and Thein (1985) set a milestone for analytical forensics by showing how to create DNA profiles (*DNA fingerprints*) from different sequences in forensic trace analysis, human identification and parenthood testing. This was made possible since short detection probes made of DNA were used to detect sets of hypervariable mini-satellites, which are specific for individuals and even twins.

Beyond any doubt is the detection and quantification of nucleic acids a cornerstone in trace analysis. There are plenty of methods to detect and quantify nucleic acids. Nowadays, nucleic acids can be used

- to differentiate between human and non-human,
- to distinguish individuals or
- to differentiate body fluids

as exemplary shown by Vennemann and Koppelkamm (2010); Halpern and Ballantyne (2011); Geng, Novak, and Mathies (2014); Silva et al. (2015) and Sauer, Reinke, and Courts (2016). Provided, that the nucleic acid is in solution, methods described in subsubsection 2.1.1 ff. are commonly used.

### 2.1.1 Photometric Determination and Fluorescence Determination of Nucleic Acids

DNA has a maximum absorbency of light at a wavelength of 254 - 260 nm. The DNA can be quantified photometrically, using Lambert-Beer's law (Beer 1852), in a quartz or plastic cuvette. This quantitative method gives the total DNA content in the sample. Herewith, differentiation of specific sequences or the determination of sequence copy numbers is impossible.

There are several fluorescent dyes that bind specifically to nucleic acids for fluorescence determination (e. g., ethidium bromide, SYTO-9, PicoGreen and SYBR® Green (Karsai et al. 2002)). For quantification, the DNA is mixed with the fluorescence dye that binds to the DNA backbone. DNA without the dye binding has no fluorescence. The fluoresce signal intensity is measured upon binding of the dye to the nucleic acid, where the intensity is proportional to the quantity of DNA in the sample. This method gives information about the total DNA content in the sample but allows no differentiation of specific sequences, or the determination of sequence copy numbers.

Fluorescent labeled detection probes have been developed that specifically bind to a target sequence. Examples include *hybridization probes*, *hydrolysis probes* and *molecular beacons* (Rödiger et al. 2014; Halpern and Ballantyne 2011). Once calibrated with standards of known quantities, this enables a precise (sequence-specific) quantification (Singer et al. 1997).

Both principles are used in melting curve analysis, which involves the monitoring of the temperature-dependent dissociation of double stranded nucleic acids (subsubsection 2.1.2).

### 2.1.2 Melting Curve Analysis of Nucleic Acids

**Melting curve analysis** is an analytical method to determine the melting temperature of a double-stranded nucleic acid. The melting temperature ($T_m$) is the temperature at which 50% of nucleic acid is denatured. The temperature dependent denaturation of the nucleic acids is continuously monitored during the melting curve analysis, for which either photometric determination or fluorescence determination are used. The energy required to break hybrids of double-stranded nucleic acids depends on the length of the sequence, the

GC content and the reaction environment (e. g., salt concentration, pH) (Rödiger, Böhm, and Schimke 2013; Rödiger, Burdukiewicz, et al. 2015).

### 2.1.3 Solid-phase Determination of Nucleic Acids

Solid-phase technologies such as **microbead assays** and **microarrays** have been developed to capture specific target sequences from a solution. In this case, target specific nucleic acid capture probes (e. g., DNA, RNA) are immobilized on a solid phase such as a glass slide or microbeads. The target sequences need to be labeled by a biochemical reaction (e. g., by a fluorescence dye) and are subsequently hybridized to the corresponding capture probe. This binding event can be quantified with specific readers or fluorescence microscopy (Rödiger et al. 2014).

### 2.1.4 Methods based on Nucleic Acid Amplification - Applications of qPCRs

The most common used method for nucleic acid detection and quantification is the **polymerase chain reaction (PCR)**. PCR is a biochemical reaction that is used to enzymatically synthesize multiple identical copies of a DNA sequence by a DNA polymerase (e. g., *Taq* polymerase). This is possible by annealing two DNA primer molecules, single stranded (18 - 35 nucleotide long) DNA sequences, which are complementary to the target stand. The primers bind under temperature controlled conditions specific to the target sequence and function as starter molecule for the DNA synthesis by the DNA polymerase.

A DNA polymerase is a transferase (e. g., *Taq* polymerase) that covalently attaches (phosphodiester bonds) nucleotides (e. g., guanine and cytosine) at the 5'-end starting from the primer. This results in a complementary strand of the template DNA. This process is repeated multiple times to synthesize the DNA copies. The product formation can be analyzed, for example, by agarosegel electrophoresis, or capillary electrophoresis. In both cases, the DNA is separated by size. To visualize specific detection probes, DNA labeling dyes or combination of detection probes and dyes, can be used. (Halpern and Ballantyne 2011; Westermeier 2004)

The PCR is the recommended procedure for short tandem repeat (STR) analysis. Short tandem repeats play a pivotal role in forensics, since they are a gold standard for DNA profiling in forensic casework (Oorschot, Ballantyne, and Mitchell 2010; Geng, Novak, and Mathies 2014).

With the **quantitative PCR** (qPCR) technology, the number of start copies of a target nucleic acid sequence in a genomic or complementary DNA sample can be quantified. qPCR uses the same biochemical principles as PCR. This is possible because the amplification reaction is continuously monitored in each thermo-cycle (Higuchi et al. 1993; Rutledge and Côté 2003). The resulting kinetics of the amplification process are described in subsubsection 3.2.4. To quantify the DNA copies, the amplification reaction of the unknown DNA sample is compared with a sample whose concentration is known (e. g. internal standard, dilution series).

qPCR is widely employed for gene expression analysis (GEA) and quantification of human nuclear DNA and mitochondrial DNA from forensic evidence (Alonso and García 2007), analysis of gene expression (Pabinger et al. 2014; George et al. 2016) in personalized medicine and forensics (Dvinge and Bertone 2009; Lynch and Fleming 2019; Pabinger et al. 2014). Also, the relationship between (poly)pharmacy and clinical consequences (Maher, Hanlon, and Hajjar 2014; Caudle et al. 2019; Rao et al. 2018; Mestdagh et al. 2016; Giuliano et al. 2017; Meyer et al. 2017; Lee et al. 2017) is studied by qPCR. It is also essential for high-throughput technology validation (e. g., next generation sequencing (RNA-seq) and validation of sequencing libraries) (Olagnier, Chiang, and Hiscott 2017; Gracz et al. 2015; Fischer et al. 2016; Nassirpour et al. 2014). To make data-scientific steps of qPCR reproducible and to accurately reflect the questions asked is not trivial Taylor et al. (2019).

qPCR was used in this work to generate amplification curve data sets. In the later chapters, this work will only focus on qPCR technology.

In the Life Science sector, qPCR has become indispensable. For one, qPCR is used to investigate biological relationships by gene expression analysis. The qPCR is also used for the preparation and post-processing of NGS experiment (Nassirpour et al. 2014; Cristino et al. 2011). The RNA-Seq assumes that all transcripts can be sequenced unbiased. In reality, certain DNA sequences (e. g., GC-rich regions) are more poorly processed

and so their quantity is often underestimated. Normalization of RNA-Seq data is based on the assumption that each sample contains the equal total amount of expressed mRNA, which does not necessarily have to be the case. NGS data are derived by mapping the sequenced DNA fragments to a genome reference. Here, mutations and single nucleotide polymorphisms (SNPs) are sometimes ignored. As a consequence, results vary depending on which mismatches are allowed. The qPCR is used for qualitative and quantitative characterization of the material to be sequenced. Moreover, qPCR is a highly sensitive method for checking the "library DNA" of NGS reactions. Analysis of sequencing data is not the end of an NGS experiment, and sequence variations or expression changes need to be verified reliably. qPCR is used to confirm found differences in the follow-up. There are undisputed qualities of qPCR in terms of sensitivity and specificity. The above described problems play only a minor role in qPCR. For this reason, qPCR is usually used for validation of NGS experiments. In particular, the technical progress of commercially available qPCR technologies has led to the development of easy-to-use devices that enable users to compile large volumes of data on their specific research questions. This involves the requirement to evaluate data objectively and reproducibly (Rödiger, Burdukiewicz, et al. 2015).

The **digital PCR** (dPCR) is a variation of the PCR which predates qPCR. Due to the technical complexity of dPCRs, it was predominantly used in academia. Technical advances make it widely available to the mass market since 2008. The biochemical foundation of dPCR is similar to qPCR, but the reaction mix is partitioned into thousands of small partitions (nanoliter volume). These partitions separate the amplification reactions ("clonal amplification"), which in combination with Poisson statistics, enables an absolute quantification of DNA (Pabinger et al. 2014; Burdukiewicz et al. 2016).

An alternative to PCR is **isothermal amplification**. Isothermal amplification is a continuous reaction at a constant temperature (isothermal) and involves enzymes that differ from the conventional PCRs. An example is the loop-mediated amplification (LAMP) (Rödiger et al. 2011) that is gaining interest in forensics for point-of-care testing and microfluidic devices. Recent advances in the development of technologies for bioanalytical microfluidic devices, medium-throughput and high-throughput technologies were achieved. A device for forensic applications was shown for the analysis of STRs, but also for quantitative assays (Horsman et al. 2007).

Modern **DNA sequencing**, often referred to as next generation sequencing (NGS), is a technology that provides the exact sequence of large and complex mixtures of DNA sequences. NGS is also a quantitative method since the number of target sequences can be counted. As of completion of this study, this method is still laborious and not ubiquitously available in forensic laboratories (Yang, Xie, and Yan 2014).

All the above methods are used for DNA typing, to distinguish individuals according to their DNA profile, to determine the origin of body fluids or to analyze the temporal course of expression of inflammatory mediators in wound tissue (Curran 2009; Alonso and García 2007; Swango et al. 2007; Sauer, Reinke, and Courts 2016; Martins et al. 2015; Wurmb-Schwark et al. 2002). One further application of PCR is the analysis of short tandem repeat (STR) loci (Halpern and Ballantyne 2011).

# 3 Concepts and Methods

The following sections describe the biostatistical approaches and working principles

- for *data management*,
- *literate programming*,
- *open data* and
- *reproducible research*

as recommended by Wilson et al. (2017). The proposed work-flow for the study is to:

1. define the biostatistical problem exemplified by the curvature of amplification curve data,
2. collect and prepare the amplification curve data,
3. develop tools for the manual amplification curve classification,
4. develop algorithms that can calculate predictors of amplification curve data,
5. apply machine learning algorithms from predictors of the curvature,

6. improve the results and finally
7. present the results as part of an open source software package for reproducible research.

For the generation of negative amplification curves, a set of experiments was conducted to amplify sequences of the Human papillomaviruses (HPV). The availability of negative amplification curves is limited, since in most cases only a few negative controls are included in qPCR experiments. The findings and data set used in this study were made available as open data bundled in the open source software package called `PCRedux` (https://CRAN.R-project.org/package=PCRedux).

All statistical analyses were performed using `RKWard` (Rödiger et al. 2012) v. $\geq$ 0.7.0z+0.7.1+devel1. `RKWard` is an integrated development environment and graphical user interface for the `R` (v. 4.0.4) statistical computing language. It has been shown that `R` is a powerful environment for reproducible and transparent data analysis in a highly customizable cross-platform environment (Rödiger, Burdukiewicz, et al. 2015).

## 3.1 Development, Implementation and Installation

`PCRedux` is an open source software package (MIT license[5]) for the statistical computing language `R`. Data with sigmoid curves are common in bioanalytical methods, such as in the widely used real-time PCR (qPCR), applied in human diagnostics, life sciences and forensics (Martins et al. 2015; Sauer, Reinke, and Courts 2016). qPCR amplification curves are an example for sigmoid shaped curves, for which `PCRedux` contains functions to calculate predictors and classify data sets for machine learning applications.

All technical and experimental aspects should be performed under principles that follow good practices of reproducible research. Here, numerous authors addressed the matter for experimental design and data report. Examples are the *Minimum Information for Publication of Quantitative PCR Experiments* guidelines (MIQE) and the *Real-time PCR Data Markup Language* (RDML). MIQE is a recommended standard of the minimum information for publication of quantitative real-time PCR experiments guidelines and RDML is a data exchange format (Bustin 2017; Rödiger, Burdukiewicz, et al. 2015; Rödiger et al. 2017).

The development of scientific software is a complex process, in particular, when a developer team works in different time zones with no face-to-face meetings. End users need releases with stable software that delivers reproducible results and developers need well documented software to modify the software to their needs.

Under the umbrella *Agile Software Development* and *Extreme Programming*, several principles were proposed to deliver high quality software that meet the needs of end users and developers. This includes version control, collaborative editing, unit testing and continuous integration (Lanubile et al. 2010; Myers et al. 2004; Rödiger, Burdukiewicz, et al. 2015). The core contributors are listed in the DESCRIPTION file of the `PCRedux` package. The following paragraphs describe methods applied for the `PCRedux` package.

### 3.1.1 Version Control and Continuous Integration

The development of the `PCRedux` package started 2017 with the submission of a functional, yet immature source code, to GitHub (GitHub, Inc.). GitHub is a web-based version control repository hosting service. Both distributed version control and source code management are based on Git (Lanubile et al. 2010). Additional functionality of GitHub includes the administration of access management, bug tracking, moderation of predictor requests, task management, some metrics for the software development, and wikis. The source code of `PCRedux` is available at:

https://github.com/devSJR/PCRedux/

Continuous integration development team members (incl. coders, artists, translators) can commit and integrate their contributions several times a day. An automated build and test system verifies each integration and gives the development team members a timely feedback about the effect of their commit. In contrast to deferred integration, this leads to a reduced number of integration problems and less workload as most errors are solved shortly after they were integrated (Myers et al. 2004).

[5]https://opensource.org/licenses/MIT

TravisCI was chosen as continues integration service for `PCRedux`. The TravisCI server communicates with the GitHub version control system and manages the `PCRedux` package building process. Continuous interaction is available for the `R` releases *oldrel*, *release* and *devel*. The history of the build tests are available at:

https://travis-ci.org/devSJR/PCRedux

### 3.1.2 Naming Convention and Literate Programming

`PCRedux` is an R ($\geq$ v. 3.3.3) package, written as an *S3* object system. *S3* has characteristics of object orientated programming, but eases the development due to the use of the naming conventions (Brito 2008). In most places functions and parameter names are written as underscore separated (underscore_sep), which is a widely used style in `R` packages (Bååth 2012). This convention had to be violated in coding sections where functionality from other packages was used.

By convention, it was specified that functions from the `PCRedux` package shall be reported in the form `functionname()` (e. g., `qPCR2fdata()`) and functions from other packages in the form `functionname()` [`packagename`] (e. g., `pcrfit()` [`qpcR`]).

Literate programming, as proposed by Knuth (1984), is a concept where the logic of the source code and documentation is integrated in a single file. Markup conventions (e. g., '#') define in literate programming on how to typeset the documentation. This produces outputs in a typesetting language such as the lightweight markup language **Markdown**, or the document preparation system LaTeX.

The `roxygen2`, `rmarkdown` and `knitr` packages were used to write the documentation in-line with code for the `PCRedux` package.

### 3.1.3 Installation of the `PCRedux` Package

The development version of `PCRedux` can be installed using the `devtools` package.

```
# Install devtools, if not already installed.
install.packages("devtools")

# Install PCRedux
devtools::install_github("devSJR/PCRedux")
```

`PCRedux` is available as stable version from the **C**omprehensive `R` **A**rchive **N**etwork (CRAN) at https://CRAN.R-project.org/package=PCRedux. Package published at CRAN undergo intensive checking procedures. In addition, CRAN tests whether the package can be built for common operating systems and whether all version dependencies are solved. To install `PCRedux` first install `R` ($\geq$ v. 3.3.3). Then start `R` and type in the prompt:

```
# Select your local mirror
install.packages("PCRedux")
```

The `PCRedux` package should just install. If this failed make sure that write access is permitted to the destination directory and that all package dependencies are met.

```
# The following command points to the help for download and install of packages
# from CRAN-like repositories or from local files.
?install.packages()
```

If this fails try to follow the instructions given by De Vries and Meys (2012).

R CMD check

Results from CRAN check can be found at

http://cran.us.r-project.org/web/checks/check_results_PCRedux.html.

### 3.1.4 Unit Testing of the PCRedux Package

Module testing, better known as unit testing, is an approach to simplify the refactoring of source code during software development. Unit testing is not a guarantee for error-free software. The goal is to minimize errors and regressions. It is also intended to ensure that the numerical results from the calculations are reproducible and of high quality. An unintended behavior of the software should be detected at the latest during the package building process (Myers et al. 2004).

*Checkpoints* are used to check whether the software performs calculations and data transformations correctly for all builds. For this, numerous (logical) queries have to be defined by the developer in advance, referred to as *expectations*. It should be ensured that as many errors as possible are covered. A logical query can be, for example, whether the calculation has a numeric or Boolean value as output. If the data type is incorrect during output, this is a sufficient termination criterion. Or it can be checked whether the length of the result vector is correct after the calculation. There are different approaches for unit tests in `R`, including the packages `RUnit`, `covr`, `svUnit` and `testthat` (Wickham (2011)).

The package `testthat` was used in `PCRedux` because it could well be implemented and its maintenance is relatively simple. The logic is that an *expectation* defines how the result, class or error in the corresponding unit (e. g., function) should behave. Unit tests can be found in the `/test/testthat` subdirectory of the `PCRedux` package. They are run automatically during the creation of the package. The following example for the `qPCR2fdata()` function (for details see subsubsection 3.6.2) uses the `test_that()` [`testthat`] function with the *expectations* that:

- an object of class *fdata* is created (see Febrero-Bande and Oviedo de la Fuente (2012) for details of the class *fdata*),
- the parameter `rangeval` has a length of two,
- the second value of parameter `rangeval` is 49 (last cycle number) and *whether the object structure of the `qPCR2fdata()` function does not change if the parameter `preprocess=TRUE` is set.

```
# Expectations used for the unit testing of the qPCR2fdata() function.
library(PCRedux)

context("qPCR2fdata")

test_that("qPCR2fdata gives the correct dimensions and properties", {
    library(qpcR)
    res_fdata <- qPCR2fdata(testdat)
    res_fdata_preprocess <- qPCR2fdata(testdat, preprocess = TRUE)

    expect_that(res_fdata, is_a("fdata"))
    expect_that(length(res_fdata$rangeval) == 2 &&
    res_fdata$rangeval[2] == 49, is_true())

    expect_that(res_fdata_preprocess, is_a("fdata"))
    expect_that(length(res_fdata_preprocess$rangeval) == 2 &&
    res_fdata_preprocess$rangeval[2] == 49, is_true())
})
```

Further unit tests were implemented for all functions of the `PCRedux` package. The coverage of the `PCRedux` package can be calculated by the `package_coverage()` [`covr`] function (Hester 2018) or visually analyzed via web-interface at:

https://codecov.io/gh/devSJR/PCRedux/list/master/.

## 3.2 Analysis of Sigmoid-Shaped Curves for Data Mining and Machine Learning Applications

The following sections describe `PCRedux` regarding the analysis, numerical description and predictor calculation from a sigmoid curve. A predictor herein refers to a quantifiable *informative* property of a sigmoid curve. The predictors (subsection 3.3), sometimes referred to as descriptors, can be used for applications such as data mining, machine learning and automatic classification (e. g., negative or positive amplification).

Machine learning is a scientific discipline that deals with the use of simple to sophisticated algorithms to learn from large volumes of data. A number of approaches to machine learning exist. Supervised learning algorithms are trained with data which contain correct answers (Zielesny 2011; Walsh, Pollastri, and Tosatto 2015; Fernandez-Delgado et al. 2014). This allows to create models that assign the data to the answers and use these for further processing and predictions (Tolson 2001). Unsupervised algorithms learn from data without answers. They use large, diverse data sets for self-improvement. Neural networks or artificial neural networks are a type of machine learning that roughly resembles the function of human neurons. They are computer programs that use several levels of nodes (neurons), work in parallel for learning, recognize patterns and make decisions in a human-like manner (Günther and Fritsch 2010). Deep Learning uses a deep neural network with many neuronal layers and an extensive volume of data (Shin et al. 2016). They solve complex, non-linear problems and are responsible for groundbreaking innovations through artificial intelligence, such as the processing of a natural language or images (Tolson 2001). Applications in the life sciences have already been described for each of these methods. There appears to be no study that uses machine learning for the classification of amplification curves, based on interpretable feature, in a scientific setting.

The determination of quantification points such as the Cq value is a typical task during the analysis of qPCR experiments. This is briefly described in dedicated sections (subsubsection 3.2.3ff.).

Characteristics of amplification curves that can be used for the statistical and analytical description are discussed (subsubsection 3.3.1) more in detail. The examples described focus on the concepts for **binary (dichotomous) classification** (Kruppa et al. 2014) as negative or positive. The mere binary classification into classes "positive" or "negative" is not necessarily the aim of the `PCRedux` package. Instead, it is aimed to provide a tool set for automatic **multicategory (polychotomus) classification** of amplification curves by any class conceivable. Such classification could be used for the quality of an amplification curve as negative, ambiguous and positive (Figure 1A & B). A definition for binary (dichotomous) classification and multicategory (polychotomus) classification is presented in Kruppa et al. (2014).

### 3.2.1 Relation of Machine Learning to the Classification of Amplification Curves

Data mining and machine learning can be used for descriptive and predictive tasks during the analysis of complex data sets. Data mining uses specific methods from statistical inference, software engineering and domain knowledge to get a better understanding of the data, and to extract *hidden knowledge* from the preprocessed data (Kruppa et al. 2014; Herrera et al. 2016). All this implies that a human being interacts with the data at the different stages of the whole process as part of the workflow in data mining. Elements of the data mining process are the preprocessing of the data, the description of the data, the exploration of the data and the search for connections and causes.

The availability of classified amplification curve data sets and technologies for the classification of amplification curves is of high importance to train and validate models. This is dealt with in subsection 3.5 and subsection 3.4, respectively.

For machine learning, the type of learning task is the first thing that needs to be defined. The learning task can be a classification, clustering or regression problem. Next, suitable algorithms can be selected depending on the task. In the case of classification problems, it is attempted to predict a *discrete valued* output. The labels ($y$) are usually categorical and represent a finite number of classes (e. g. "negative", "positive" $\rightarrow$ binary classification). With regression tasks, it is attempted to predict a *continuously valued* output. Clustering is primarily about forming groups (clusters) based on their similarities. Examples are presented in the following and following chapters.

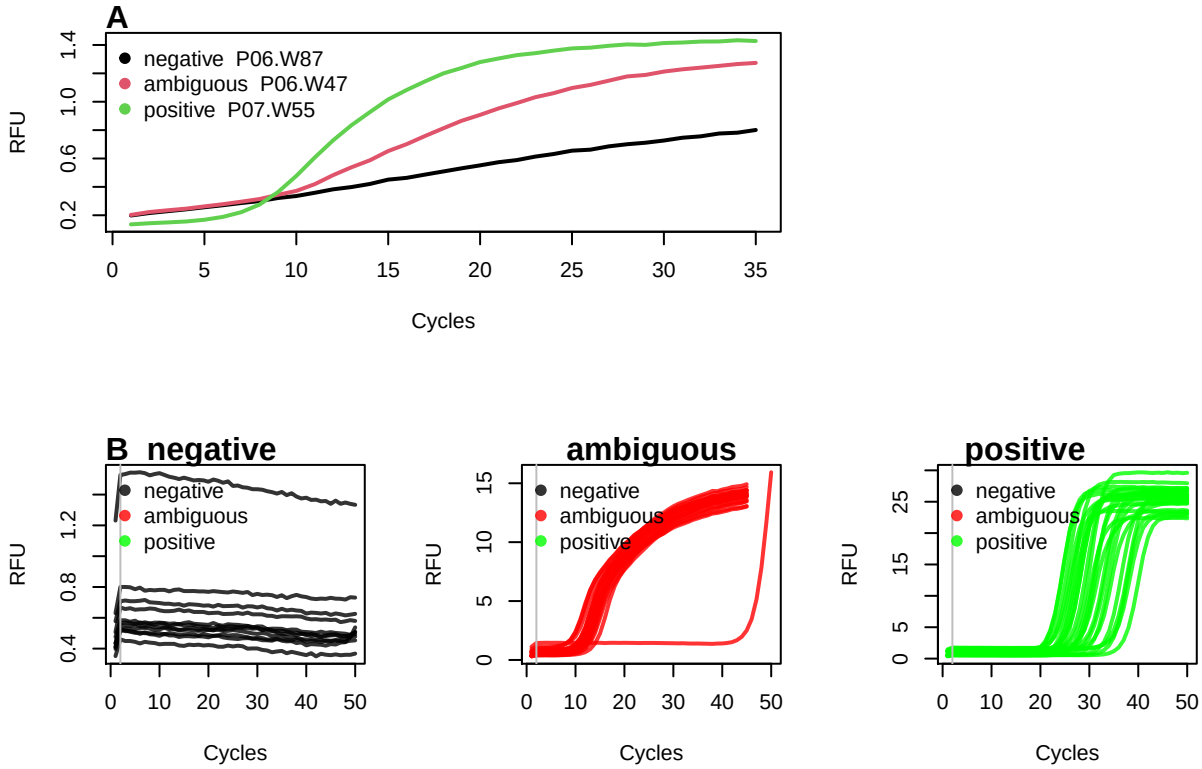


Figure 1: Examples of negative, ambiguous and positive amplification curves. A) A negative (black), ambiguous (red) and positive (green) amplification curve were selected from the 'htPCR' data set. The negative amplification curve is non-sigmoid and has a positive trend. The ambiguous amplification curve is similar to a sigmoidic amplification curve, but shows a positive slope in ground phase (cycle 1 $\rightarrow$ 5). The positive amplification curve (green) is sigmoid. It starts with a flat baseline (cycle 5 $\rightarrow$ 25). This is followed by the exponential phase (cycle 5 $\rightarrow$ 25) and ends in a flat plateau phase (cycle 26 $\rightarrow$ 35). B) Amplification curves of the 'vermeulen1' data set were divided into groups with *negative*, *ambiguous* and *positive* classification. Negative amplification curves have a low signal level. Interesting is the spontaneous increase (probably due to a sensor calibration) in cycles 1 to 2 followed by a linear signal decrease. In principle, the ambiguous amplification curves have a sigmoid curve shape. However, the plateau phase is fairly broad. One of the ambiguous amplification curves begins to rise sharply at Cycle 45. The positive amplification curves have a characteristic sigmoid curve shape.

In contrast, machine learning uses instructions and data in software modules to create models that can be used to make predictions on novel data. In machine learning, the human being is much less necessary in the entire process. Processes (algorithms) are used to create models with tunable parameters. These models automatically adapt their performance to the information (predictors) from the data. Well-known examples of machine learning technologies are Decision Trees (DT), Boosting, Random Forests (RF), Support Vector Machines (SVM), generalized linear models (GLM), logistic regression (LR) and deep neural networks (DNN) (Lee 2010). The three following concepts of machine learning are frequently described in the literature:

*Supervised learning*: These algorithms (e. g., SVM, DT, RF) learn from a training data set of labeled and annotated data (e. g., "positive" and "negative"). Classified training data can be created by one or more individuals. It is used for building a generalized model of all data. These algorithms use error or reward signals to evaluate the quality of a found solution (Bischl et al. 2010; Greene et al. 2014; Igual and Seguí 2017). Binomial logistic regression[6] (also referred to as logit regression or logit model) is used to gain knowledge about a binary relationship, by fitting a regression model $y = f(x)$. $y$ is a categorical variable with two states (negative $\rightarrow$ 0, positive $\rightarrow$ 1). Typically, this model is used for predicting $y$ with a mixture of $n$ continuous and categorical predictors (features) $x_{i1}, \ldots, x_{k1}, (i = 1, \ldots, n)$.

The logit model is a robust and versatile classification method to explain a dependent binary variable. Their codomain of real numbers is limited to [0,1], hence probabilities can be employed. The logistical distribution function $F(\eta)$, also known as the response function, is strictly monotone increasing and limited to this range.

$\eta_i$ establishes the link between the probability of the occurrence and the independent variables. For this reason, $\eta_i$ is referred to as a link function. The distribution function of the normal distribution is an alternative to the logistical distribution function. By using the normal distribution, the Probit model is obtained. However, since this is more difficult to interpret, it is less widely used in practice. Since probabilities are used, it is possible to make a prediction about the probability of occurrence of an event.

For example, when analyzing amplification curves, diagnosis can be made whether a reaction was unsuccessful (0) or successful (1). For the prediction, independent metric variables (predictors) are used. The metric variables have interpretable distances with a defined order. Their codomain is [-$\infty$,$\infty$]. The logistic distribution function on the independent variables determines the probability for $Y_i = 0$ or $Y_i = 1$. A logistic regression model can be formulated as follows:

$F(\eta) = \frac{1}{1+exp(-\eta)}$

The logistic regression analysis is based on the maximum-likelihood estimation (MLE). In contrast to linear regression, the probability for $Y = 1$ is not modeled from explanatory variables. Rather, the logarithmic chance (logit) is used for the occurrence of $Y = 1$. The term *chance* refers to the ratio of the probability of occurrence of an event (e. g., amplification curve is positive) and the counter-probability (e. g., amplification curve is negative) of an event.

*Unsupervised learning*: Algorithms, such as k-means clustering, kernel density estimation, or Principal Component Analysis learn from training data sets of unlabeled or non-annotated data to find hidden structures according to geometric or statistical criteria (Bischl et al. 2010; Greene et al. 2014; Igual and Seguí 2017).

*Reinforcement Learning*: The algorithms learn by reinforcement from *criticism*. The criticisms inform the algorithm about the quality of the solution found but nothing about how to improve. These algorithms search by iterations the improved solution in the entire solution space (Bischl et al. 2010; Igual and Seguí 2017).

[6]Logistical regression can also be used to predict a dependent variable that can assume more than two states. In this case, it is called a multinomial logistic regression. An example would be the classification $y$ of amplification curves as *slightly noisy*, *medium noisy* or *heavily noisy*.

### 3.2.2 Why is there a need for the PCRedux software?

The binary classification of an amplification curve is feasible using bioanalytical methods such as melting curve analysis (Rödiger, Böhm, and Schimke 2013) or electrophoretic separation (Westermeier 2004). However, this is not always possible or desirable.

- Melting curve analysis is used in some qPCRs as a post-processing step to identify samples which contain the specific target sequence (*positive*) based on a specific melting temperature. However, some detection probe systems like hydrolysis probes do not permit such classification. Moreover, nucleic acids with similar biochemical properties but different sequences may have the same melting temperature.
- An electrophoretic separation (classification of target DNA sequences by size and quantity) often requires too much effort for experiments with high sample throughput.
- There are mathematical qPCR analysis algorithms such as `linreg` (Ruijter et al. 2009) that require information on whether an amplification curve is negative or positive for subsequent calculation.
- Raw data of amplification curves can be fitted with sigmoid functions. Sigmoid functions are non-linear, real-valued, have an S-shaped curvature (Figure 3) and can be differentiated (e. g., first derivative maximum, with one local minimum and one local maximum). With the obtained model, predictions can be made. For example, the position of the second derivative maximum can be calculated from this (subsubsection 3.2.4). In the context of amplification curves, the second derivative maximum is commonly used to describe the relationship between the cycle number and the PCR product formation (subsubsection 3.2.4). All software assume that the amplification resembles a sigmoid curve shape (ideal positive amplification reaction), or a flat low line (ideal negative amplification reaction). For example, Ritz and Spiess (2008) published the `qpcR` `R` package that contains functions to fit several multi-parameter models. This includes the five-parameter Richardson function (Richards 1959) (Equation 3). The `qpcR` package (Ritz and Spiess 2008) contains an amplification curve test via the `modlist()` function. The parameter `check="uni2"` offers an analytical approach, as part of a method for the kinetic outlier detection. It tries to checks for a sigmoid structure of the amplification curve. Then, `modlist()` tests for the location of the first derivative maximum and the second derivative maximum. However, multi-parameter functions fit "successful" in most cases including noise and give false positive results. This will be shown in later sections. This is exemplary shown in later sections in combination with the `amptester()` [`chipPCR`] function (Rödiger, Burdukiewicz, and Schierack 2015), which uses fixed thresholds and frequentist inference to identify amplification curves that exceed the threshold (↦ classified as positive). However, the analysis can also lead to false-positive classifications as exemplified in the example below and in Figure 2. Therefore, additional classification concepts would be beneficial.

```
# Load the qpcR package for the model fit.
library(qpcR)
library(chipPCR)
```

```
## Warning in .recacheSubclasses(def@className, def, env): undefined subclass
## "numericVector" of class "Mnumeric"; definition not updated
```

```
# Select one positive and one negative amplification curve from the PCRedux
# package.

amp_data <- PCRedux::RAS002[, c("cyc", "A01_gDNA.._unkn_B.Globin",
                                "B07_gDNA.._unkn_HPRT1")]

colnames(amp_data) <- c("cyc", "positive", "negative")

# Arrange graphs in an matrix and set the plot parameters. An plot the positive
# and negative amplification curve.
hight <- c(3100, 4100)

plot(NA, NA, xlim = range(amp_data[, "cyc"]),
       ylim = range(amp_data[, c("positive", "negative")]),
```

```
        xlab = "Cycles", ylab = "RFU", main = "")

# Apply the amptester() function from the chipPCR package to the amplification
# curve data and write the results to the main of the plots.

for (i in 2:3) {
    res.ampt <-  suppressMessages(amptester(amp_data[, i]))

    # Make a logical connection by two tests (shap.noisy, lrt.test and
    # tht.dec) of amptester to decide if an amplification reaction is
    # positive or negative.
    decision <- ifelse(!res.ampt@decisions[1] &&
    res.ampt@decisions[2] &&
    res.ampt@decisions[4],
    "positive", "negative"
    )
    # The amplification curves were fitted (l7 model) with pcrfit() function.
    # The Cq was determined with the efficiency() function.

    fit <- pcrfit(data = amp_data, cyc = 1, fluo = i, model = l7)
    res <- efficiency(fit, plot = FALSE)
    lines(predict(fit), pch = 19, lty = 1, xlab = "Cycles", ylab = "RFU",
          main = "", col = i - 1)
    abline(h = res[["fluo"]], col = "grey")
    points(res[["cpD2"]], res[["fluo"]], pch = 19)

    legend(1, hight[i-1], paste0(colnames(amp_data)[i],
                                 "  curve ->  Decision: ",
                                 decision, "    Cq: ", res[["cpD2"]]),
           bty = "n", cex = 1, col = "red"
          )
}
```

- The analysis and classification of sigmoid data (e. g., quantitative PCR) is a manageable task if the data volume is low, or dedicated analysis software is available. An example for a low number of amplification curves is shown in Figure 4A. All 65 curves exhibit a sigmoid curve shape. It is trivial to classify them as positive by hand. In contrast, the vast number of amplification curves in Figure 4B is barely manageable with a reasonable effort by simple visual inspection. These data originate from a high-throughput experiment that encompasses in total 8858 amplification curves of which only 200 are shown. A manual analysis of the data is time-consuming and prone to errors. Even for an experienced user, it is difficult to classify the amplification curves unambiguously and reproducible as will be later shown in subsection 3.5.
- qPCRs are performed in thermo-cyclers, which are equipped with a real-time monitoring technology. There are numerous commercial manufactures producing thermo-cyclers (Table 5). An example for a thermo-cycler that originated in a scientific project is the VideoScan technology (Rödiger, Schierack, et al. 2013). Most of the thermo-cyclers have a thermal block with wells at certain positions. Reaction vessels containing the PCR mix are inserted into the wells. There are also thermo-cyclers that use capillary tubes that are heated and cooled by air (e. g., Roche Light Cycler 1.0). The thermo-cycler raises and lowers the temperature in the reaction vessels in discrete, pre-programmed steps so that PCR cycling can take place. Instruments with a real-time monitoring functionality have sensors to measure changes of the fluorescence intensity in the reaction vessel. All thermo-cycler systems use software to processes the amplification curves. Plots of the fluorescence observations versus cycle number obtained from two different qPCR systems are shown in Figure 4A and B. The thermo-cyclers produce different amplification curve shapes even with the same sample material and PCR mastermix

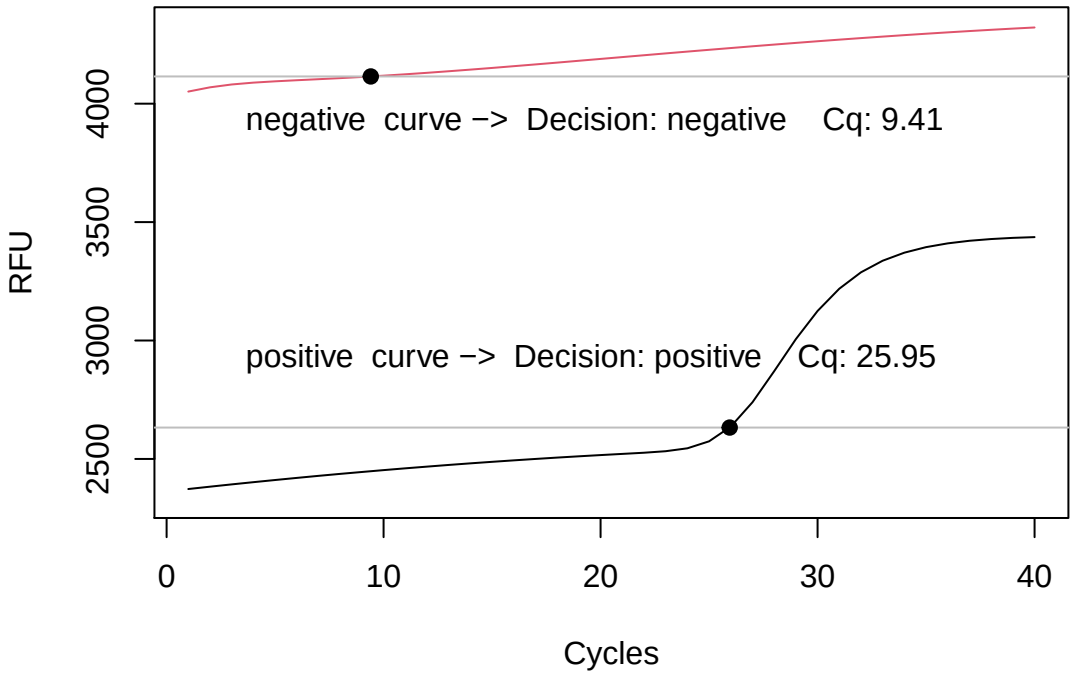


Figure 2: Incorrect model adjustment for amplification curves. A positive (black), and a negative (red) amplification curve were randomly selected from the 'RAS002' data set. The positive amplification curve has a baseline signal of about 2500 RFU and has a definite sigmoidal shape. The negative amplification curve has a baseline signal of approx. 4200 RFU, but only moderately positive slope (no sigmoidal shape). A logistic function with seven parameters ('l7') has been fitted to both amplification curves. A Cq value of 25.95 was determined for the positive amplification curve. The negative amplification curve had a Cq value of 9.41. However, it can be seen that the latter model fitting is not appropriate for calculating a trustworthy Cq value. An automatic calculation without user control would give a false-positive result.

because of their technical design, sensors, and software. These factors need to be taken into account during the development of analysis algorithms.

### 3.2.3 Software for the Analysis of Amplification Curve Data

There are several open source and closed source software tools for the analysis of qPCR data (Pabinger et al. 2014). The software packages deal for example with

- missing values and non-detects (McCall et al. 2014),
- noise and artifact removal (Rödiger, Burdukiewicz, and Schierack 2015; Rödiger, Burdukiewicz, et al. 2015; Spiess et al. 2015, 2016),
- inter-run calibration (Ruijter et al. 2015),
- normalization (Rödiger, Burdukiewicz, and Schierack 2015; Ruijter et al. 2013; Feuer et al. 2015; Matz, Wright, and Scott 2013),
- quantification cycle estimation (Ritz and Spiess 2008; Ruijter et al. 2013),
- amplification efficiency estimation (Ritz and Spiess 2008; Ruijter et al. 2013),
- data exchange (Lefever et al. 2009; Perkins et al. 2012; Rödiger et al. 2017),
- relative gene expression analysis (Dvinge and Bertone 2009; Pabinger et al. 2009; Neve et al. 2014) and
- data analysis pipelines (Pabinger et al. 2009; Ronde et al. 2017; Mallona, Weiss, and Egea-Cortines 2011; Mallona et al. 2017).

However, a bottleneck of qPCR data analysis is the lack of predictors and software to build classifiers for amplification curves. A classifier herein refers to a vector of predictors that can be used to distinguish the amplification curves only by their shape. A predictor, also referred to as *feature*, is an entity that characterizes an object. A few potential predictors for amplification curves are described in the literature. These include:

- the starting point (*takeoff*) of the amplification curve,
- the Cq value and amplification efficiency, and
- the signal level (e. g., slope and intercept of the ground phase).

These alone are presumably not enough to describe amplification curves sufficiently. The number of predictors should be large enough to describe the object accurately and small enough to not interfere with the learning process with redundant information ("overtraining"). There are no references of algorithms in the scientific literature for the calculation of additional predictors from amplification curves. This makes studies on machine learning and modeling difficult.

### 3.2.4 Principles of Amplification Curve Data Analysis and Predictor Calculation

The shape of a positive amplification curve is in most cases sigmoidal. Many factors such as the sample quality, qPCR chemistry, and technical problems (e. g., sensor errors) contribute to various curve shapes (Ruijter et al. 2014). The curvature of the amplification curve can be used as a quality measure. For example, fragmentation, inhibitors and sample material handling errors during the extraction can be identified. The kinetic of fluorescence emission is proportional to the quantity of the synthesized DNA. Typical amplification curves have three phases.

1. **Ground phase**: This phase occurs during the first cycles of the PCR, where the fluorescence emission is in most cases flat. Here, noise but no product formation is detected by the sensor system and the PCR product signal is an insignificantly small component of the total signal. This is often referred to as base-line or background signal. Apparently, there is only a phase shift or no signal at all, primarily due to the limited sensitivity of the instrument. Even in a perfect PCR reaction (double amplification per cycle), qPCR instruments cannot detect the fluorescence signal from the amplification. Fragmentation, inhibitors and sample handling errors would result in a prolonged ground phase. Nevertheless, this may indicate some typical properties of the qPCR system or probe system. In many instruments, this phase is used to determine the base-line level for the calculation of the Cycle threshold (Ct). The Ct value is considered statistically relevant as an increase outside of the noise range (threshold) when coming from the amplicon. In some qPCR systems, a flat amplification signal is expected in this phase. Slight deviations from this trend are presumably due to changes (e. g., disintegration of probes) in the

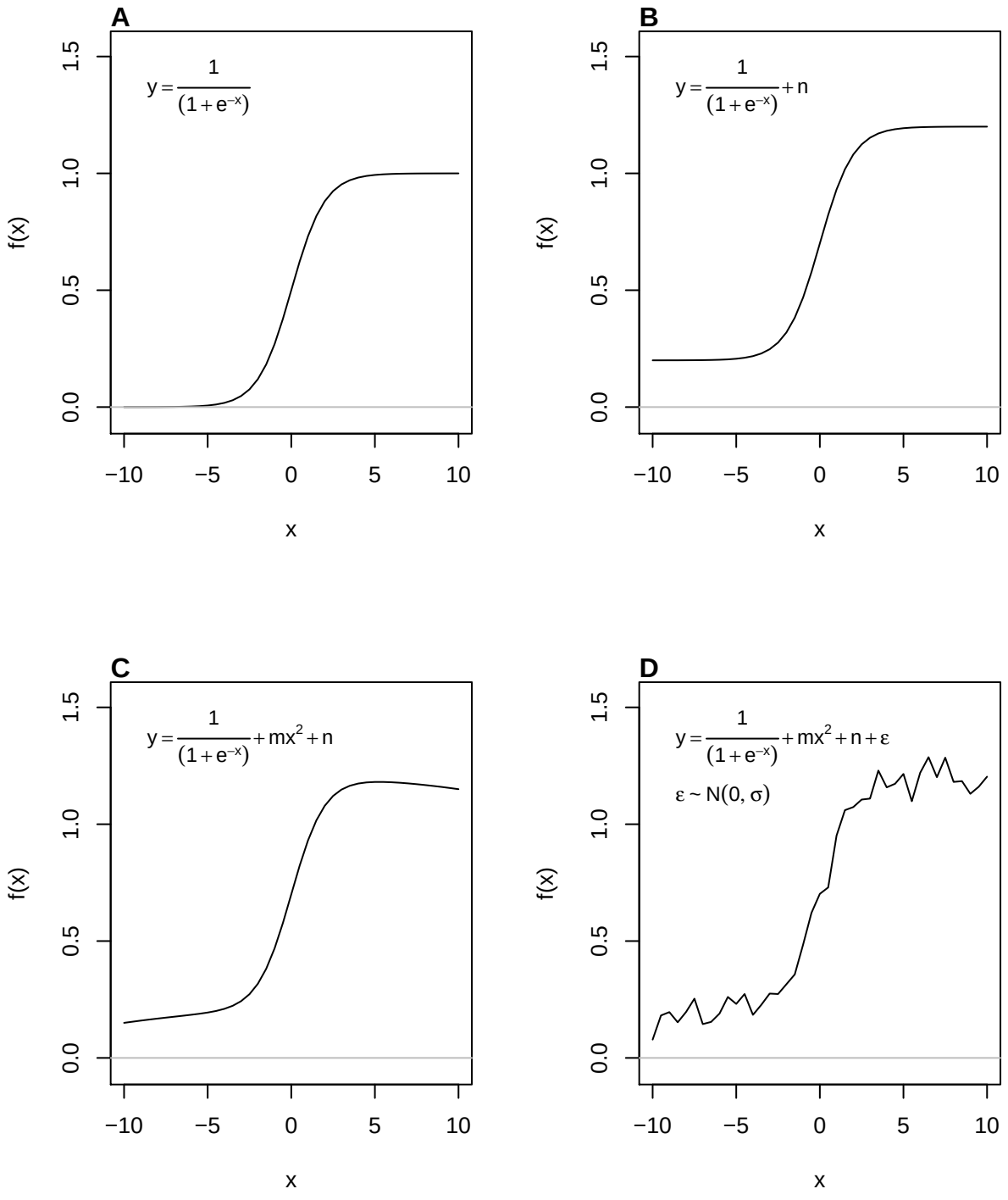


Figure 3: A) Model function of a one-parameter sigmoid function. B) Model function of a sigmoid function with an intercept $n = 0.2$ RFU (shift in base-line). C) Model function of a sigmoid function with an intercept ($n$ ~0.2 RFU) and a square portion $m * x^2, m = -0.0005, n = 0.2RFU$ (hook-effect-like). D) Model function of a sigmoid function with an intercept ($n$) and a square portion of $m * x^2$ and additional noise $\epsilon$ (normal distributed, $\mu = 0.01, \sigma = 0.05$).

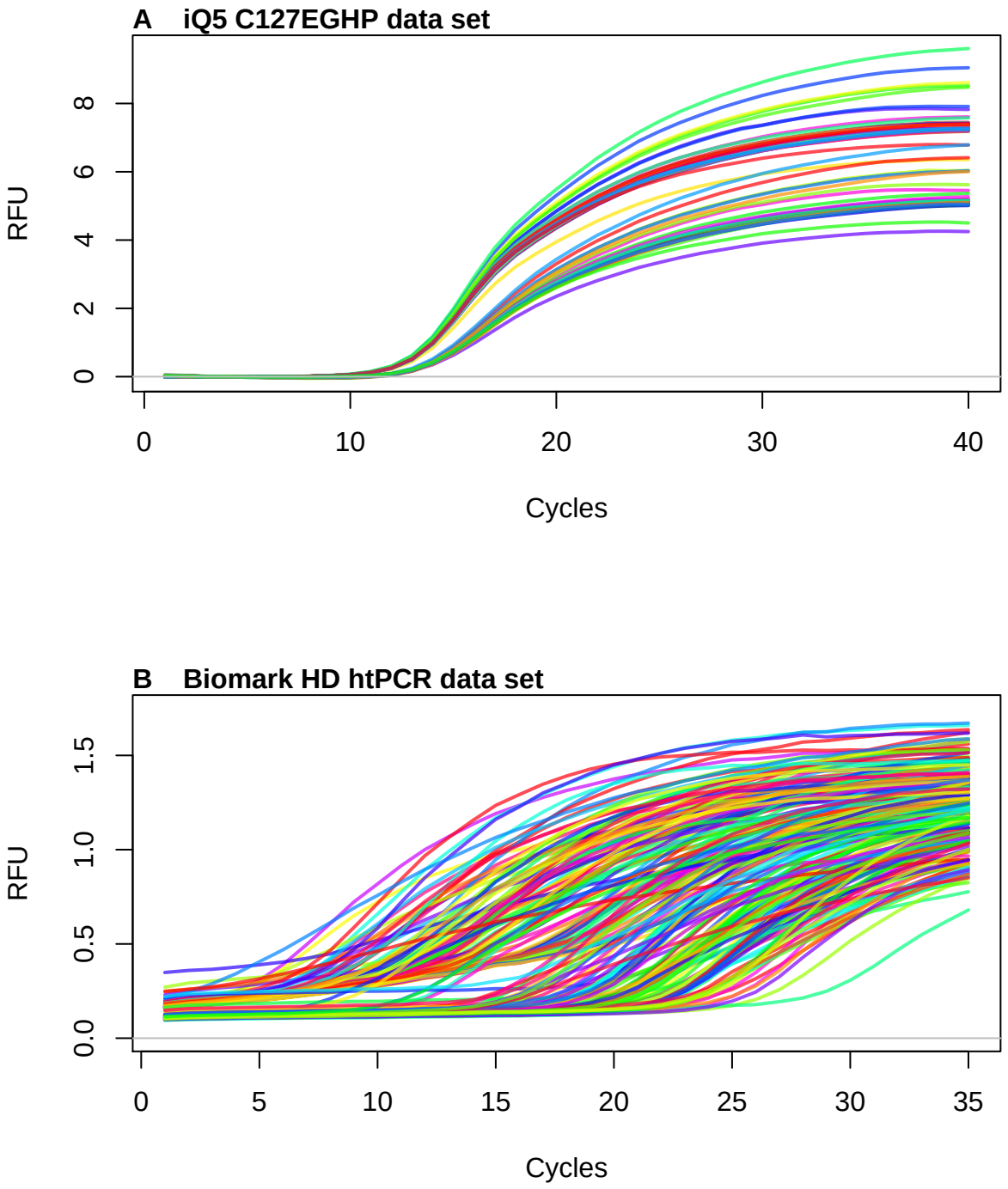


Figure 4: Amplification curve data from an iQ5 (Bio-Rad) thermo-cycler and a high throughput experiment in the Biomark HD (Fluidigm). A) The 'C127EGHP' data set with 64 amplification curves was produced in a conventional thermo-cycler with a 8 x 12 PCR grid. B) The 'htPCR' data set, which contains 8858 amplification curves, was produced in a 95 x 96 PCR grid. Only 200 amplification curves are shown. In contrast to 'A)' have all amplification curves in 'B)' an off-set (intercept) between 0.09 and 0.40 RFU.

fluorophores. Background correction algorithms are often used here to ensure that flat amplification curves without slope are generated. However, this can result in errors and inevitably leads to a loss of information via the waveform of the raw data (Nolan, Hands, and Bustin 2006). The slope, level and variance of this phase can serve as predictors.

2. **Exponential phase**: This phase follows the ground phase and is also called *log-linear phase*. It is characterized by a strong increase of the emitted fluorescence as the DNA amount roughly doubles in each cycle under ideal conditions and when the amount of the synthesized fluorescent labeled PCR product is high enough to be detected by the sensor system. This phase is used for the calculation of the quantification point (Cq) and curve specific amplification efficiency. The most important measurement from qPCRs is the Cq, which signifies the PCR cycle for which the fluorescence exceeds a `threshold value`. However, there is an ongoing debate as to what a significant and robust threshold value is. An overview and performance comparison of Cq methods is given in Ruijter et al. (2013). There are several mathematical methods to calculate the Cq.
    - The 'classical' threshold value (cycle threshold, Ct) is the intersection between a manually defined straight horizontal line with the quasi-linear phase in the exponential amplification phase (Figure 6A & B). This simple to implement method requires that amplification curves are properly baselined prior to analysis. The Ct method makes the assumption that the amplification efficiency (~ slope in the log-linear phase) is equal across all compared amplification curves (Ruijter et al. 2013). Evidently, this is not always case as exemplified in Figure 5C. The Ct method is widely used presumably due to the familiarity of users with this approach (e. g., chemical analysis procedures). However, this method is statistically unreliable (Ruijter et al. 2013; Spiess et al. 2015, 2016). Moreover, the Ct method gives no stable in predictions if different users are given the same data set to be analyzed. *Therefore, this method is not used within the `PCRedux` package.*
    - Another Cq method uses the maximum of the second derivative (SDM) (Rödiger, Burdukiewicz, et al. 2015) (Figure 6C). In all cases, the Cq value can be used to calculate the concentration of target sequence in a sample (low Cq →high target concentration). In contrast, negative or ambiguous amplification curves loosely resemble noise. This noise may appear linear or exhibit a curvature similar to a specific amplification curve (Figure 1). This however, may result in faulty interpretation of the amplification curves. Fragmentation, inhibitors and sample handling errors would decrease the slope of the amplification curve (Spiess, Feig, and Ritz 2008; Ritz and Spiess 2008). The slope and its variation can be considered as predictors. Since the Cq depends on the initial template amount and amplification efficiency, there is no immediate use of the Cq as an predictor.
3. **Plateau phase**: This phase follows the exponential phase and is a consequence of the exhaustion of limited reagents (incl. primers, nucleotides, enzyme activity) in the reaction vessel, limiting the amplification reaction, so that the theoretical maximum amplification efficiency (doubling per cycle) no longer prevails. This turning point, and the progressive limitation of resources, finally leads to a plateau. In the plateau phase, there is in some cases a signal decrease called *hook effect* (subsubsection 3.2.2 and (Barratt and Mackay 2002; Isaac 2009; Burdukiewicz et al. 2018)). The slope (*hook effect*), level and variation can be considered as predictors.

If the amplification curve has only a slight positive slope and no perceptible/measureable exponential phase, it can be assumed that the amplification reaction did not occur (Figure 5B). Causes may include poor specificity of the PCR primers (non-specific PCR products), degraded sample material, degraded probes or detector failures. If a lot of input DNA is present in a sample, the amplification curve starts to increase in early PCR cycles (1 - 12 cycles). Some PCR devices have a software that corrects this feature without rechecking, resulting in an amplification curve with a negative trend.

The discussed phases are considered as regions of interest (ROI). As an example, the *ground phase* is in the head area, while the *plateau phase* is in the tail area. The *exponential phase* is located between these two ROIs.

The amplification curve shape, the amplification efficiency and the Cq value are important measures to judge the outcome of a qPCR reaction. In all phases of PCR, the curves should be smooth. Possible artifacts in the curves may be due to unstable light sources from the instrument or problems during sample preparation,

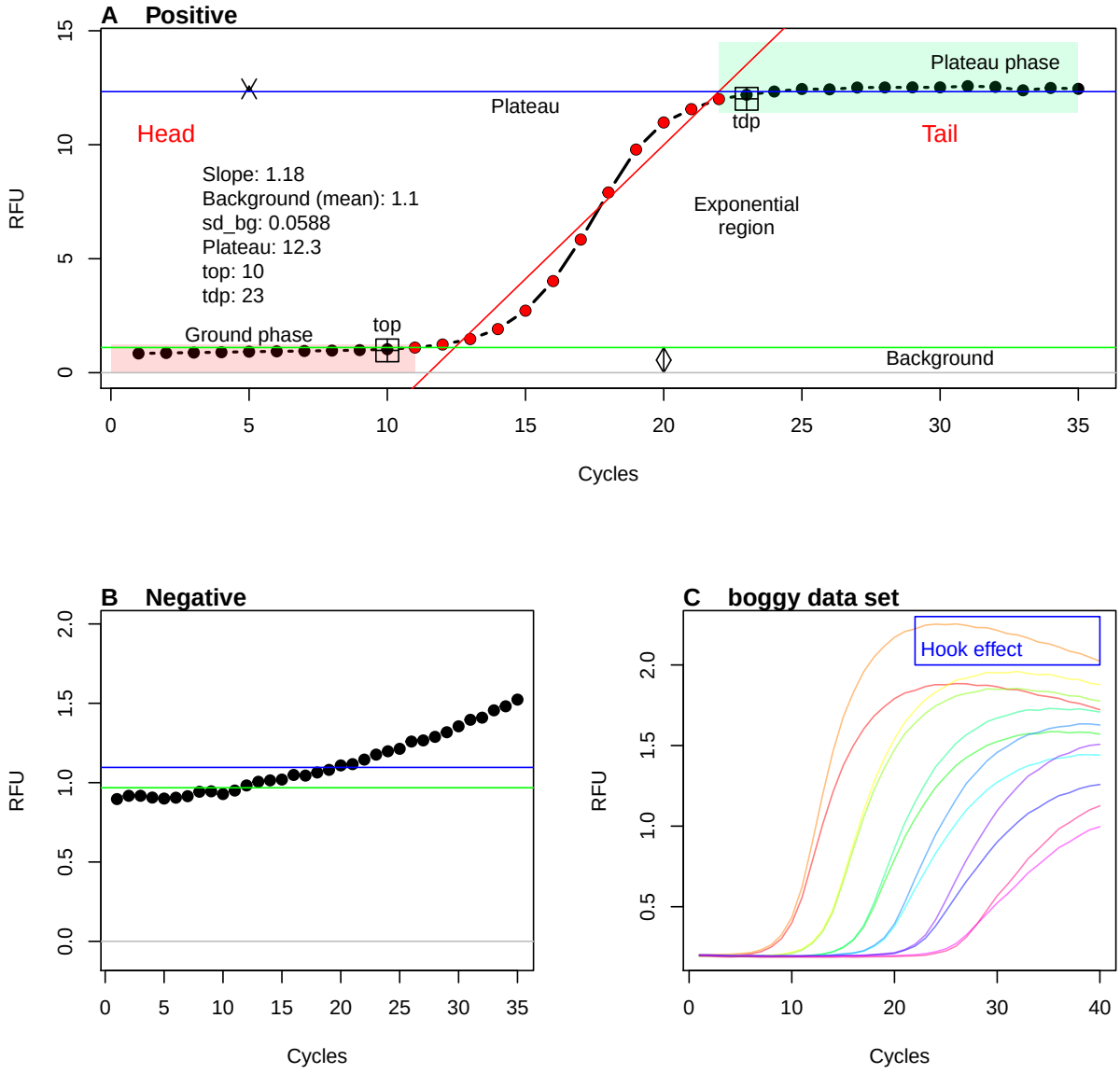


Figure 5: Phases of amplification curves as Region of Interest (ROI). For amplification curves, the fluorescence signal (RFU, relative fluorescence units) of the reporter dye is plotted against the cycle number. Positive amplification curves possess three ROIs: ground phase, exponential phase and plateau phase. These ROIs can be used to determine predictors such as the takedown point ('tdp') or the standard deviation within the ground phase ('sd_bg'). The exponential range (red dots) is used to determine the Cq values and amplification efficiency (not shown). A linear regression model (red) can be used to calculate the slope in this region. B) PCRs without amplification reaction usually show a flat (non-sigmoides) signal. C) The exponential phase of PCR reactions can vary greatly depending on the DNA starting quantity and other factors. Amplification curves that appear in later cycles often have a lower slope in the exponential phase.

such as the presence of bubbles in the reaction vessel, incorrectly assigned dye detectors, errors during the calibration of dyes for the instrument, errors during the preparation of the PCR master mix, sample degradation, lack of a sample in the PCR, too much sample material in the PCR mix or a low detection probe concentration (Ruijter et al. 2009, 2014; Spiess et al. 2015). Smoothing and filtering cause alterations to the raw data that affects the Cq value and the amplification efficiency.

Most commercial qPCR systems do not display the raw data of the amplification curves on the screen. Instead, raw data are often processed by the instrument software to remove fluorophore-specific effects and noise in all ROIs. Commonly employed preprocessing step of qPCR is smoothing and filtering to remove noise, where the latter can have different causes (Spiess et al. 2015).

The ordinate often does not display the measured fluorescence, but rather the change in fluorescence per cycle ($\Delta RFU = RFU_{cycle+1} - RFU_{cycle}$). Some qPCR systems display periodicity in the amplification curve data, thereby exposing the risk of introducing artificial shifts in the Cq values (Spiess et al. 2016).

In particular the cycle threshold method (Ct method) (subsubsection 3.2.4) is affected by these factors (Spiess et al. 2015, 2016). Therefore, it is advisable to clarify in advance, which processing steps the amplification curves have been subjected to. Failure to do so may result in misinterpretations and incorrect amplification curve fitting models (Nolan, Hands, and Bustin 2006; Rödiger, Burdukiewicz, et al. 2015; Rödiger, Burdukiewicz, and Schierack 2015; Spiess et al. 2015).

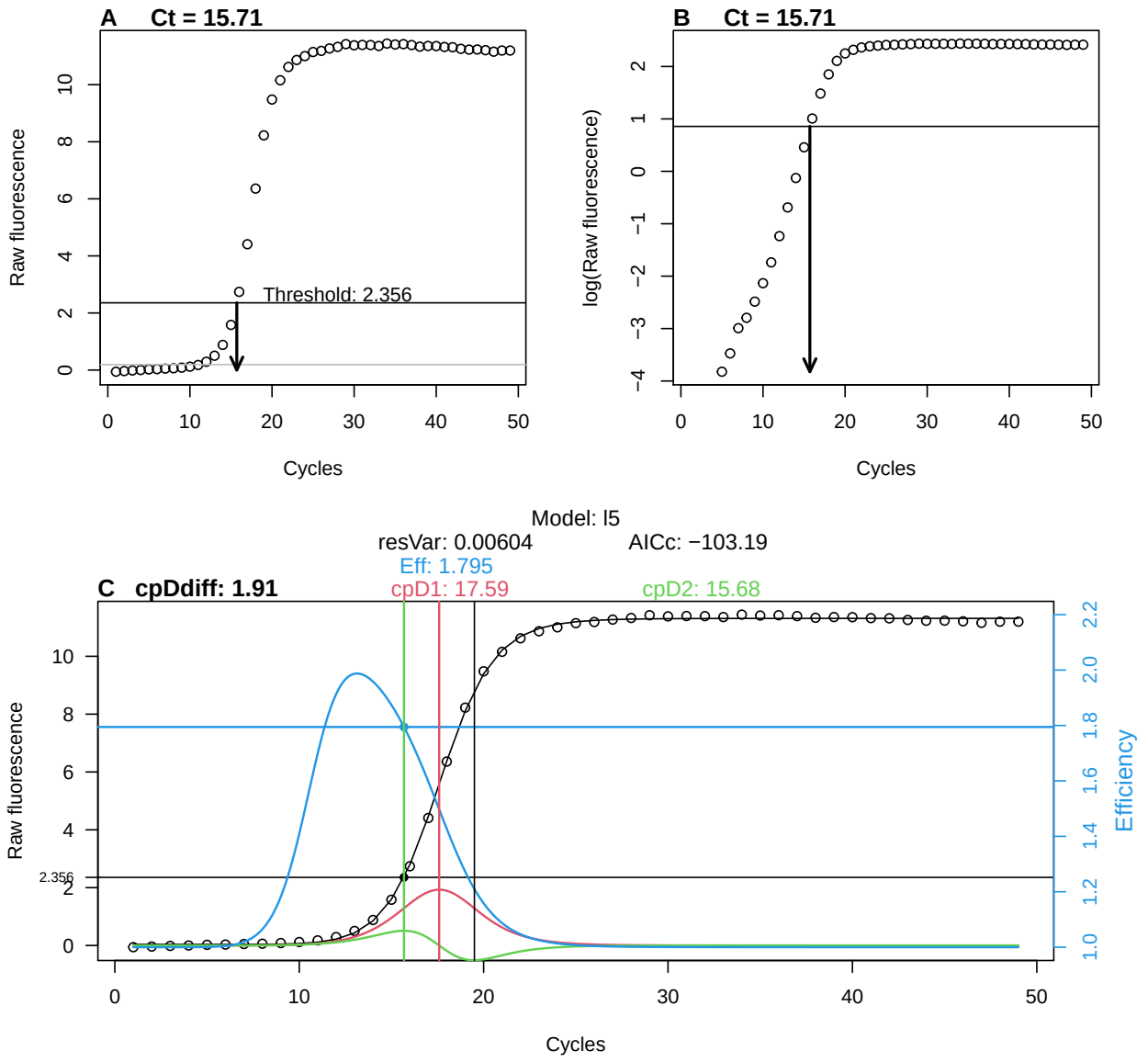


Figure 6: Frequently used methods for the analysis of quantification points. A) The amplification curve is intersected by a gray horizontal line. This is the background signal ($3\sigma$) determined from the *68-95-99.7 rule* from the fluorescence emission of cycles 1 to 10. The black horizontal line is the user-defined threshold (Ct value) in the exponential phase. Based on this, the cycle at which the amplification curve differs significantly from the background is calculated. B) The amplification curve can also be analyzed by fitting a multi-parametric model (black line, five parameters). The red line is the first derivative of the amplification curve with a maximum of 17.59 cycles. The first derivative maximum ('cpD1') is used as a quantification point (Cq value) in some qPCR systems. The green line shows the second derivative of the amplification curve, with a maximum at 15.68 cycles a minimum at 19.5 cycles. The maximum of the second derivative ('cpD2') is used as the Cq value in many systems. The blue line shows the amplification efficiency estimated from the trajectory of the exponential region. The 'Eff' value of 1.795 means that the amplification efficiency is approximately 89%. 'cpDdiff' is the difference between the first and second derivative maximum ($cpDdiff = cpD1 - cpD2$).

## 3.3 Data Analysis Functions of the PCRedux Package

The PCRedux package contains functions for analyzing amplification curves. In the following, these are distinguished into helper functions (subsection 3.6) and analysis functions (subsubsection 3.3.1).

### 3.3.1 Amplification Curve Analysis Functions of the PCRedux package

On the basis of these observations, **concepts** for predictors (*features*) were developed and implemented in algorithms to describe amplification curves. The functions described in the following are aimed for experimental studies. It is important to note that the concepts for the predictors proposed herein emerged by a *critical reasoning* process and *domain knowledge* of the PCRedux package creator. The aim of the package is to propose a set of predictors, functions and data for an independent research.

### 3.3.2 pcrfit_single() and encu()- Functions to Calculate Predictors from an Amplification Curve

The following sections give a concise description of the algorithms used to calculate predictor vectors by the pcrfit_single() function. Based on considerations and experience, the algorithms of the pcrfit_single() function are restricted to ROIs (Figure 5) to calculate specific predictors.

The encu() function is a wrapper for the pcrfit_single() function. encu() can be used to process large records of amplification curve data arranged in columns. The progress of processing is displayed in the form of a progress bar and the estimated run-time. Additionally, encu() allows specifying which monitoring chemistry (e. g., DNA binding dye, sequence specific probes) and which thermo-cycler was used. Ruijter et al. (2014) demonstrated that the monitoring chemistry and the type of input DNA (single stranded, double stranded) are important when analysing qPCR data, because they have an influence on the shape of the amplification curve. For simplicity, the documentation will describe the pcrfit_single() only.

The underlying hypotheses and concepts of the predictors are formulated and supported by *exemplary applications*. Different representative data sets were used to support a concept or predictors. For example, the RAS002 data set represents a typical qPCR. This means that the positive amplification curves start with a flat plateau phase and then transition into the sigmoid shape with a plateau. The negative amplification curves display no significant peculiarities. For both positive and negative amplification curves, there is a shift from the origin. The htPCR data set serves as a problem example in several places, since it contains many observations (amplification curves from high-throughput experiments). Besides, the amplification curves have a high diversity of curve shapes that cannot be uniquely and reproducibly classified even by experienced users. Other data sets are used in the documentation, but these are not discussed in detail.

To underscore the usability of the algorithms and their predictors, 3302 observations (471 negative amplification curves, 2831 positive amplification curves) from the batsch1, boggy, C126EG595, competimer, dil4reps94, guescini1, karlen1, lievens1, reps384, rutledge, testdat, vermeulen1, VIMCFX96_60, stepone_std, RAS002, RAS003, HCU32_aggR and lc96_bACTXY were analyzed with the encu() function and the results (predictors) were combined in the file **data_sample.rda**. Users of this function should independently verify and validate the results of the methods for their own applications.

A new data set called data_sample_subset_balanced has been compiled from the data_sample data set for some applications. Selection criteria included:

- both positive and negative amplification curves had to be included in a similar ratio,
- there should not be a dominating thermal cycler platform,
- the amplification curves should represent typical amplification curves (subjective criterion). The compilation of the data sets batsch1, HCU32_aggR, lc96_bACTXY, RAS002, RAS003 and stepone_std met this requirement satisfactorily.

```
data_sample_subset_balanced <- data_sample[data_sample$dataset %in%
c("batsch1", "boggy", "C126EG595", "HCU32_aggR", "lc96_bACTXY",
  "RAS002", "RAS003", "stepone_std", "testdat"), ]
```

```r
# Dimension of data_sample_subset_balanced
dim(data_sample_subset_balanced) ## Observations predictors
```

```
## [1] 651  62
```

```r
# Show the counts of negative and positive amplification
# curves in a bar plot
# Build a contingency table of the counts at each
# combination of factor levels.

dec_table<- table(data_sample_subset_balanced[["decision"]])
barplot(dec_table, ylab = "Number of Observations", col = c("green", "black"),
        border = "white")
text(c(0.7, 1.9), rep(min(dec_table) *0.9, length(dec_table)),
     c(paste("y = ", dec_table[1]), paste("n = ", dec_table[2])),
     col = c("black", "white"))
mtext("data_sample_subset_balanced", cex = 1, side = 3, adj = 0, font = 2,
      las = 0)
```

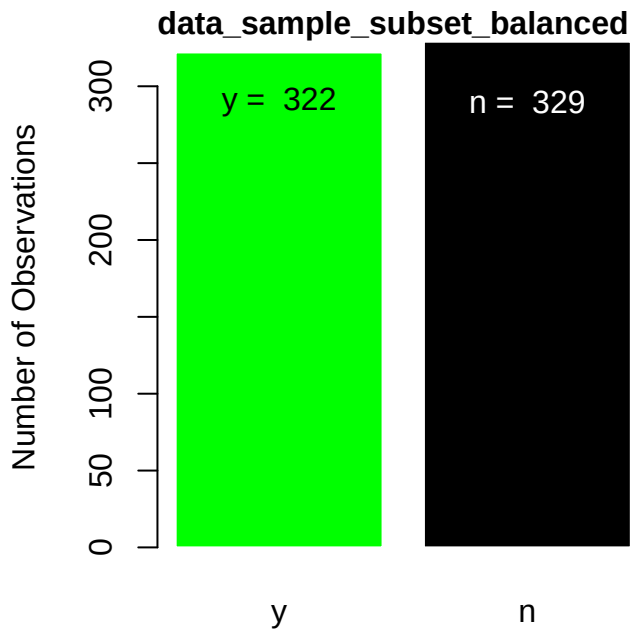


For the comparison of predictors, the data set was enlarged. Selection criteria for the data sets were comparatively less stringent.

```r
data_sample_subset <- data_sample[data_sample$dataset %in% c("stepone_std",
                                                             "RAS002", "RAS003",
                                                             "lc96_bACTXY",
                                                             "C126EG595",
                                                             "dil4reps94",
```

```
                                                    "testdat",
                                                    "boggy"), ]

# Dimension of data_sample_subset
dim(data_sample_subset) ## Observations predictors
```

```
## [1] 979  62
```

```
# Show the counts of negative and positive amplification
# curves in a bar plot
# Build a contingency table of the counts at each
# combination of factor levels.

dec_table<- table(data_sample_subset[["decision"]])
barplot(dec_table, ylab = "Number of Observations", col = c("green", "black"),
        border = "white")
text(c(0.7, 1.9), rep(min(dec_table) *0.9, length(dec_table)),
     c(paste("y = ", dec_table[1]), paste("n = ", dec_table[2])),
     col = c("black", "white"))
mtext("data_sample_subset", cex = 1, side = 3, adj = 0, font = 2,
      las = 0)
```

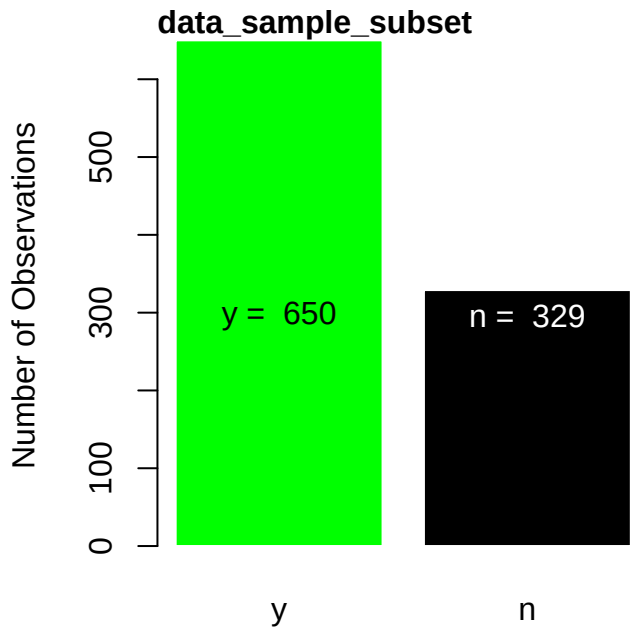


The goal is to demonstrate the basic functionality of the algorithms for predictor calculation. Similar concepts are presented in groups. The algorithms are divided into the following broad categories:

- algorithms that determine slopes, signal levels,
- algorithms that determine turning points and

- algorithms that determine areas.

The algorithms in

- `earlyreg()` (subsubsection 3.3.9),
- `head2tailratio()` (subsubsection 3.3.10),
- `hookreg()`& `hookregNL()` (subsubsection 3.3.11) and
- `mblrr()` (subsubsection 3.3.12),
- `autocorrelation_test()` (subsubsection 3.3.13)

were implemented as standalone functions to make them available for other applications.

The output below shows the predictors and their data type (`num`, numeric; `int`, integer; `Factor`, factor; `logi`, boolean) that were determined with the `pcrfit_single()` function.

```
library(PCRedux)
# Calculate predictor vector of column two from the RAS002 data set.
str(pcrfit_single(RAS002[, 2]))
```

```
## 'data.frame':    1 obs. of  90 variables:
##  $ cpD1                  : num 28.3
##  $ cpD2                  : num 25.6
##  $ cpD2_approx           : num 26
##  $ cpD2_ratio            : num 0.986
##  $ eff                   : num 1.48
##  $ sliwin                : num 1.37
##  $ cpDdiff               : num 2.67
##  $ loglin_slope          : num 118
##  $ cpD2_range            : num 4.62
##  $ top                   : num 25
##  $ f.top                 : num 160
##  $ tdp                   : num 33
##  $ f.tdp                 : num 907
##  $ bg.stop               : num 15
##  $ amp.stop              : num 40
##  $ b_slope               : num -13.6
##  $ b_model_param         : num -13.6
##  $ c_model_param         : num -62.9
##  $ d_model_param         : num 818
##  $ e_model_param         : num 26
##  $ f_model_param         : num 3.17
##  $ f_intercept           : num 3.17
##  $ k1_model_param        : num 10.3
##  $ k2_model_param        : num -0.133
##  $ convInfo_iteratons    : int 13
##  $ qPCRmodel             : Factor w/ 1 level "l7": 1
##  $ qPCRmodelRF           : Factor w/ 1 level "l7": 1
##  $ minRFU                : num -76.5
##  $ maxRFU                : num 1016
##  $ init2                 : num 0.00846
##  $ fluo                  : num 206
##  $ slope_bg              : num 22.6
##  $ intercept_bg          : num -102
##  $ sigma_bg              : num 15.7
##  $ sd_bg                 : num 0.055
##  $ head2tail_ratio       : num -0.0149
##  $ mblrr_slope_pt        : num 20.2
```

```
##  $ mblrr_intercept_bg   : num -38.6
##  $ mblrr_slope_bg       : num 6.96
##  $ mblrr_cor_bg         : num 0.91
##  $ mblrr_intercept_pt   : num 237
##  $ mblrr_cor_pt         : num 0.942
##  $ polyarea             : num 5960
##  $ peaks_ratio          : num 0.0164
##  $ autocorrelation      : num 0.725
##  $ cp_e.agglo           : int 6
##  $ cp_bcp               : int 8
##  $ amptester_shapiro    : num 0
##  $ amptester_lrt        : num 1
##  $ amptester_rgt        : num 1
##  $ amptester_tht        : num 1
##  $ amptester_slt        : num 1
##  $ amptester_polygon    : num 619
##  $ amptester_slope.ratio: num 0
##  $ hookreg_hook         : num 0
##  $ hookreg_hook_slope   : num 0
##  $ hookreg_hook_delta   : num 0
##  $ central_angle        : num 0.999
##  $ number_of_cycles     : int 40
##  $ direction            : num 0
##  $ range                : num 1093
##  $ polyarea_trapz       : num 12363
##  $ cor                  : num 0.898
##  $ res_coef_pcrfit.b    : num -14.1
##  $ res_coef_pcrfit.c    : num 30.8
##  $ res_coef_pcrfit.d    : num 1024
##  $ res_coef_pcrfit.e    : num 28.6
##  $ fitAIC               : num 408
##  $ fitIter              : int 13
##  $ segment_x            : num 0
##  $ segment_U1.x         : num 0
##  $ segment_U2.x         : num 0
##  $ segment_psi1.x       : num 0
##  $ segment_psi2.x       : num 0
##  $ sumdiff              : num 0.95
##  $ poly_1               : num 321
##  $ poly_2               : num 2238
##  $ poly_3               : num 899
##  $ poly_4               : num -32
##  $ window_Win_1         : num 29.8
##  $ window_Win_2         : num 7.73
##  $ window_Win_3         : num 7.17
##  $ window_Win_4         : num 6.64
##  $ window_Win_5         : num 5.1
##  $ window_Win_6         : num 16.6
##  $ window_Win_7         : num 122
##  $ window_Win_8         : num 125
##  $ window_Win_9         : num 34.4
##  $ window_Win_10        : num 10.3
##  $ sd_plateau           : num 0.0387
```

### 3.3.3 Amplification Curve Preprocessing

The `pcrfit_single()` function performs preprocessing steps before each calculation, including checking whether an amplification curve contains missing values. Missing values (NA) are measuring points in a data set where no measured values are available or have been removed arbitrarily. NAs may occur if no measurement has been carried out (e. g., defective detector) or lengths of the vectors differ (number of cycles) between the observations. Such missing values are automatically imputed by spline interpolation as described in Rödiger, Burdukiewicz, and Schierack (2015).

All values of an amplification curve are normalized to their 99% quantile. The normalization is used to equalize the amplitudes differences of amplification curves from thermo-cyclers (sensor technology, software processing) and detection chemistries. To compare amplification curves from different thermo-cyclers, the values should always be scaled systematically using the same method. Although there are other normalization methods (e. g., minimum-maximum normalization, see Rödiger, Burdukiewicz, and Schierack (2015), the normalization by the 99% quantile preserves the information about the level of the background phase. A normalization to the maximum is not used to avoid strong extenuation by outliers. The data in Figure 16D show that the `maxRFU` values after normalization are approximately 1. There is no statistical significant difference between `maxRFU` values of positive and negative amplification curves.

Selected algorithms of the `pcrfit_single()` function use the `CPP()` [`chipPCR`] function to preprocess (e. g., base-lining, smoothing, imputation of missing values) the amplification curves. Further details are given in Rödiger, Burdukiewicz, and Schierack (2015). Until package version 0.2.6-4 was the `visdat_pcrfit()` part of the package. `visdat_pcrfit()` was used for visualizing the content of data from an analysis with the `pcrfit_single()` function. There are other more powerful packages such as `visdat` by Tierney (2017), `assertr` by Fischetti (2019) and `xray` by Seibelt (2017).

During the analysis, several values are determined to describe the amplitude of an amplification curve. The resulting potential predictors are `minRFU` (minimum of the amplification curve, which is determined at the 1% quantile to minimize the influence of outliers), `init2` (the initial template fluorescence from an exponential model) and `fluo` (raw fluorescence value at the second derivative maximum). The `minRFU`, `init2` and `fluo` values differ significantly between negative and positive amplification curves (Figure 16C, E & F).

### 3.3.4 Handling of Missing Predictors

Missing values (NA) can occur if a calculation of a predictor is impossible (e. g., if a logistic function cannot be adapted to noisy raw data). The lack of a predictor is nevertheless an useful information (no predictor calculate $\mapsto$ amplification curves deviate from sigmoid shape). The NAs were left unchanged in the `PCRedux` package up to version 0.2.5-1. Since version 0.2.6 the NAs are replaced by numerical values (e. g., total number of cycles) or factors (e. g., *lNA* for non-fitted model). Under the term "imputation", there are a number of procedures based on statistical methods (e. g., neighboring median, spline interpolation) or on user-defined rules (Williams 2009; Cook and Swayne 2007; Hothorn and Everitt 2014). Rules are mainly used in the functions of `PCRedux` to relieve the user from the decision as to how to deal with missing values. For example, slope parameters of a model are set to zero when it cannot be determined. The disadvantage is that rules do not necessarily concur to real world values.

### 3.3.5 Multi-parametric Models for Amplification Curve Fitting

Both the `pcrfit_single()` function and the `encu()` function use four multi-parametric models based on the findings of Spiess, Feig, and Ritz (2008) and Ritz and Spiess (2008). The `pcrfit_single()` function starts by adjusting a seven-parameter model since this adapts *easier* and more frequent to a data set (Figure 7).

- **l7**:

$$f(x) = c + k1 \cdot x + k2 \cdot x^2 + \frac{d - c}{(1 + exp(b(log(x) - log(e))))^f} \tag{1}$$

From that model, the `pcrfit_single()` function estimates the variables `b_slope` and `c_intercept`, describing the slope and the y-intercept. The number of iterations required to adapt the model is also stored. That value is returned by the `pcrfit_single()` function as `convInfo_iteratons`. The higher the `convInfo_iteratons` value, the more iterations are necessary to converge from the start parameters (Figure 12L). A low `convInfo_iteratons` value is an indicator for

- a sigmoid curve shape or
- close start parameters.

High iterations numbers imply

- noisy amplification curves or
- non-sigmoid amplification curves.

The amplification curve fitting process continues with the four-parameter model (*l4*, Equation 2). This is followed by a model with five parameters (*l5*, Equation 3) and six parameters (*l6*, Equation 4).

- **l4**:

$$f(x) = c + \frac{d-c}{1 + exp(b(log(x) - log(e)))} \tag{2}$$

- **l5**:

$$f(x) = c + \frac{d-c}{(1 + exp(b(log(x) - log(e))))^f} \tag{3}$$

- **l6**:

$$f(x) = c + k \cdot x + \frac{d-c}{(1 + exp(b(log(x) - log(e))))^f} \tag{4}$$

The optimal model is selected on the basis of the Akaike information criterion and used for all further calculations. The `pcrfit_single()` function returns `qPCRmodel` as a factor (*l4*, *l5*, *l6*, *l7*). In case no model could be fitted, an *lNA* is returned.

The model is an indicator of the amplification curve shape. Model with many parameters deviate more from an ideal sigmoid model. For instance, a four-parameter model, unlike the six-parameter model, does not have a linear component. A negative linear slope in the plateau phase is an indicator of a *hook effect* (Burdukiewicz et al. 2018).

### 3.3.6 `winklR()` - A function to calculate the central angle based on the first and the second derivative of an amplification curve data

`winklR()` is a function to calculate the in the trajectory of the first negative and the second negative derivatives maxima and minima (Figure 9) of an amplification curve data from a quantitative PCR experiment. For the determination of the angle, the origin is the maximum of the first derivative. On this basis, the vectors to the approximate minimum and maximum of the second derivatives are determined. The vectors result from the relation of the maximum of the first derivative to the minimum of the second derivative and from the maximum of the first derivative to the maximum of the second derivative. In a simple trigonometric approach, the scalar product of the two vectors is formed first. Then the absolute values are calculated and multiplied by each other. Finally, the value is converted into an angle with the cosine. The assumption is that flat (negative amplification curves) have a large angle and sigmoid (positive amplification curves) have a smaller angle. Another assumption is that this angle is independent of the rotation of the amplification curve. This means that systematic off-sets, such as those caused by incorrect background correction, are of no consequence. The cycles to be analyzed is defined by the user. The output contains the angle and the coordinates of the minima and maxima.

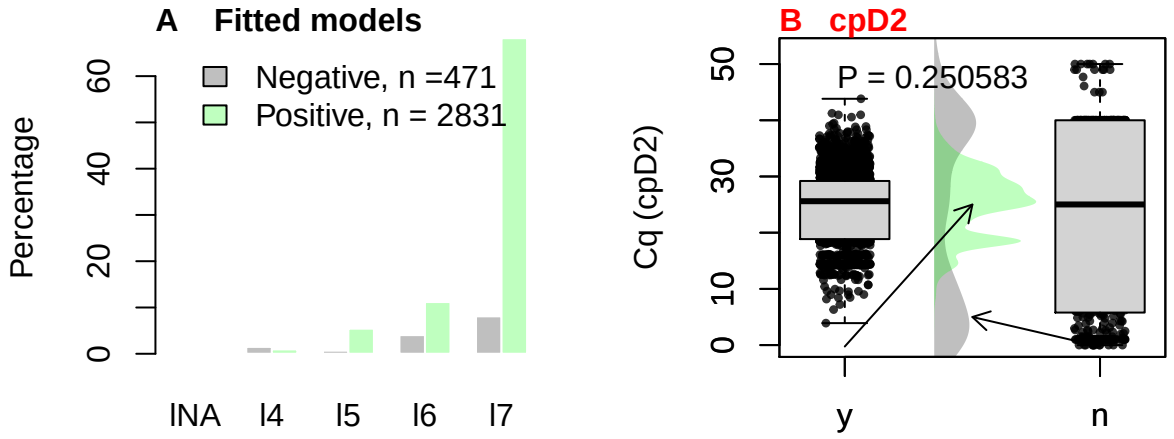


Figure 7: Frequencies of the fitted multiparametric models and Cq values. The amplification curves (n = 3302) of the 'data_sample' data set were analyzed with the encu() function. The amplification curves have been stratified according to their classes (negative: grey, positive: green). A) The optimal multiparametric model was selected for each amplification curve based on the Akaike information criterion. lNA stands for 'no model' and l4 . . . l7 for a model with four to seven parameters. B) All Cq values were calculated from optimal multiparametric models. Cqs of positive amplification curves accumulate in the range between 15 and 30 PCR cycles (50%). For the negative amplification curves, the Cqs are distributed over the entire span of the cycles. Note: The Cqs of the negative amplification curves are false-positive!

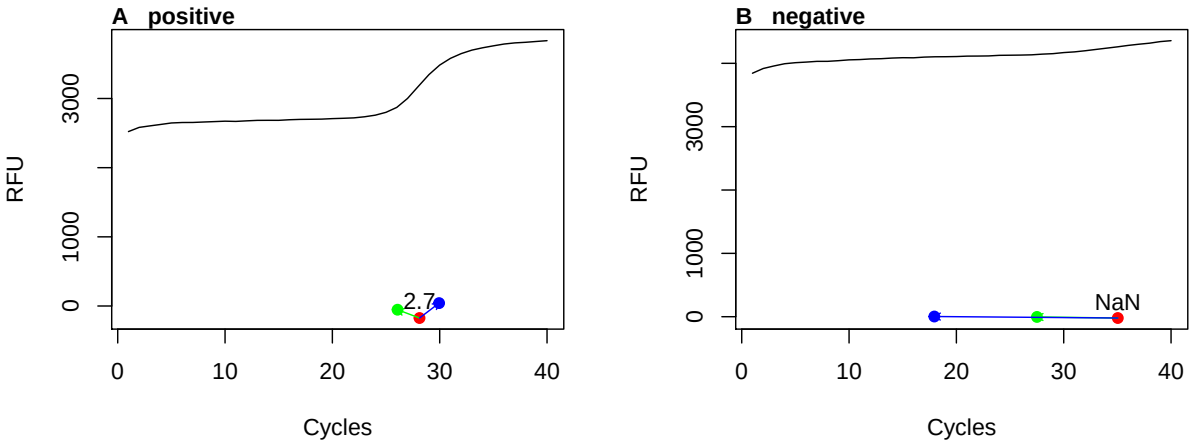


Figure 8: Concept of the winklR() function. Analysis of the amplification curves of the 'RAS002' data set with the winklR() function. Two amplification curves (A: positive, B: negative) were used. The red point shows the origin (first negative derivative maximum) while the green and blue points show the minimum and maximum of the second negative derivative. The angle is calculated from these points. Positive curves have smaller angles than negative curves.

```r
# Calculate the central angles for amplification curves from the RAS002 data set.
library(PCRedux)

# Load the amplification curves from the RAS002 data set.

DATA <- PCRedux::RAS002

# Load the RAS002_decisions data set.
dec <- RAS002_decisions

# Give tabular output of classes
table(dec)
```

```
## dec
##   y   n
##  42 150
```

```r
# Assign colors to the classes (n: black, y: green).

colors <- factor(dec, levels = c("y", "n"),
                 label = c("black", "red"))

# Test for the angles via the winklR() function on the RAS002 data set

res_winklR <- sapply(2L:ncol(DATA), function(i) {
    winklR(DATA[, 1], DATA[, i])$angle
})

# Plot the results
par(mfrow = c(1,2))

# Use a stripchart to show the angles of positive (y)
# and negative (n) amplification curves
stripchart(res_winklR ~ dec, method = "jitter",
           vertical = TRUE, pch = 19, xlab = "class", ylab = "angle")
mtext("A", cex = 1, side = 3, adj = 0, font = 2, las = 0)

# Use a calculates the conditional densities of the angles
# based on the values of y weighted by the boundary
# distribution of y

cdplot(as.factor(dec) ~ res_winklR,
       xlab = "angle", ylab = "decision")
mtext("B", cex = 1, side = 3, adj = 0, font = 2, las = 0)
```

### 3.3.7 Quantification Points, Ratios and Slopes

The `pcrfit_single()` function calculates `cpD1` and `cpD2` and uses them for further analysis. Both the `cpD1` and `cpD2` value are used for describing the amplification reaction quantitatively. For example, low `cpD1` and `cpD2` values ($< 5$ cycles) indicate that the PCR reaction was negative or that the amount of input DNA was to high Figure 7B. Since the `pcrfit_single()` function gives the parameters of all models (subsubsection 3.3.5) they are part of the feature set for completeness (Figure 10). In particular, the results of the five-parameter function and of the seven-parameter function are reported.

Further predictors from the `pcrfit_single()` function are:

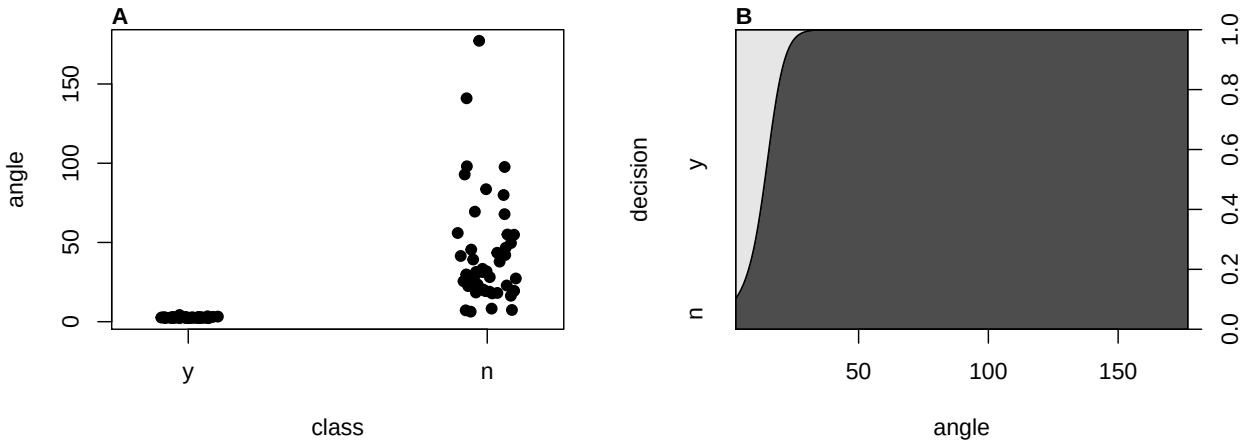


Figure 9: Analysis of the amplification curves of the 'RAS002' data set with the winklR() function. All amplification curves of the data set 'RAS002' were analyzed. Negative amplification curves are shown in red and positive amplification curves in black. The winklR() function was used to analyze all amplification curves. B) The stripchart of the analysis of positive and negative amplification curves shows separation. C) The cdplot calculates the conditional densities of x based on the values of y weighted by the boundary distribution of y. The densities are derived cumulatively via the values of y. The probability that the decision is negative (n) when the angle equals 30 is approximately 100%.

- `eff` is the optimized PCR efficiency found within a sliding window (Figure 6C). A linear model of cycles versus log(Fluorescence) is fit within a sliding window (for details see `sliwin()` [`qpcR`] function). The comparison of positive and negative amplification curves in Figure 12A demonstrates that the classes are significantly different from each other. The `eff` values differ significantly between negative and positive amplification curves (Figure 12A).
- `sliwin` is the PCR efficiency by the 'window-of-linearity' method (Spiess, Feig, and Ritz 2008) (Figure 12B). The `sliwin` values differ significantly between negative and positive amplification curves (Figure 12B).
- `cpDdiff` is the difference between the first (`cpD1`) and the second derivative maximum `cpD2` ($cpDdiff = cpD1 - cpD2$) **from the fitted model** (Figure 6C). If a model can be exactly fitted, the estimates of the difference are reliable. Higher `cpDdiff` values indicate a negative amplification reaction or a very low amplification efficiency. The comparison of positive and negative amplification curves in Figure 12C demonstrates that the classes are significantly different from each other. If the `cpDdiff` value cannot be determined (NA), it is replaced by zero. The `cpDdiff` values differ significantly between negative and positive amplification curves (Figure 12C).
- `cpD2_range` is the absolute value of the difference between the minimum and the maximum of the second derivative maximum ($cpD2\_range = |cpD2m - cpD2|$) from the `diffQ2()` function (**no model fitted**) (Figure 11E). The `cpD2_range` value does not require an adjustment of a multiparametric model. The approximate first and second derivatives are determined using a five-point stencil (Rödiger, Burdukiewicz, and Schierack 2015). The comparison of positive and negative amplification curves in Figure 12E shows that the classes differ significantly from each other. In the event that the `cpD2_range` value cannot be determined (NA), it is replaced by zero. The `cpD2_range` values differ significantly between negative and positive amplification curves (Figure 12E).
- `cpD2_approx` is the approximate second derivative maximum. In most cases the value should be close to the `cpD2`. Deviations indicate noise in the data, negative amplification curves or positive amplification curves that deviate from a typical sigmoid amplification curve.
- `cpD2_ratio` is the ratio between the approximate second derivative maximum `cpD2_approx` and the second derivative maximum `cpD2` ($cpD2_ratio = cpD2/cpD2_approx$). In the event that the `cpD2_ratio`

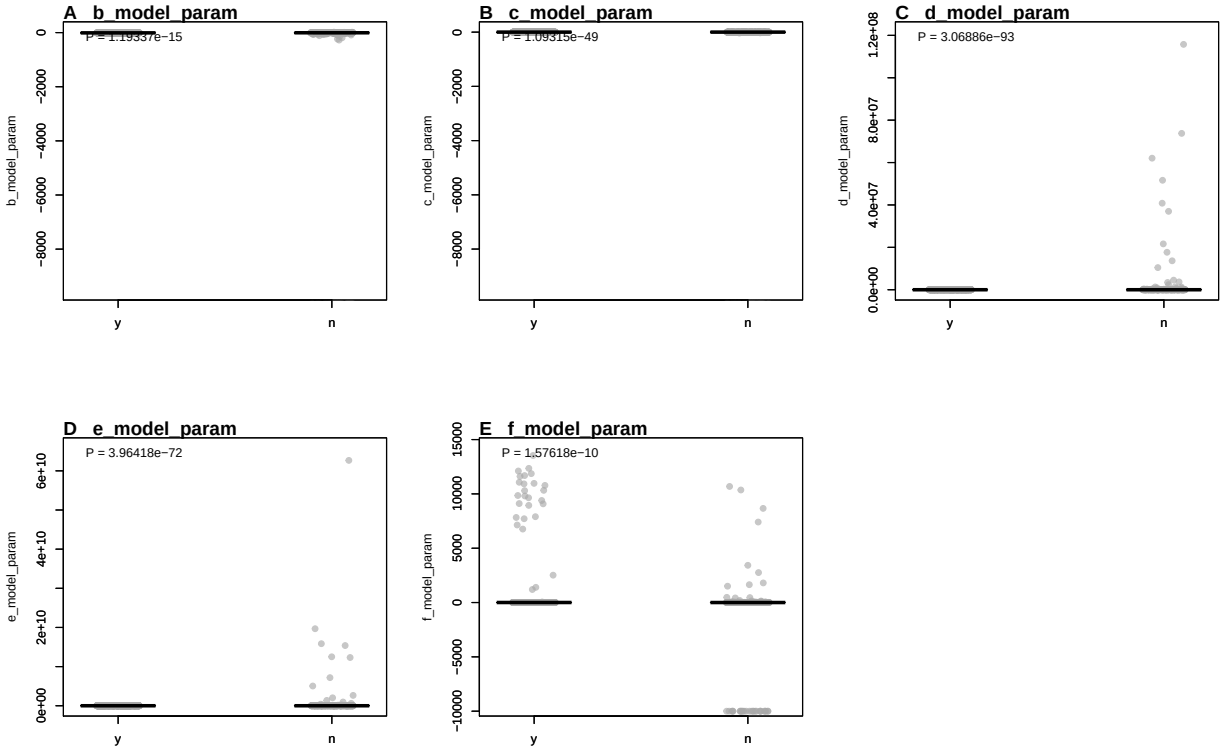


Figure 10: Values of predictors calculated from negative and positive amplification curves. Amplification curve predictors from the 'data_sample_subset' data set were used as they contain positive and negative amplification curves, as well as amplification curves that exhibit a *hook effect* or non-sigmoid shapes. A) 'c_model_param', is the c model parameter of the seven parameter model. B) 'd_model_param', is the d model parameter of the seven parameter model. C) 'e_model_param', is the e model parameter of the seven parameter model. D) 'f_model_param', is the f model parameter of the seven parameter model. The classes were compared using the Wilcoxon Rank Sum Test.

value cannot be determined (NA, Inf), it is replaced by zero. Provided that a model can be exactly fitted and that the function has little noise the ratio between both values should be close to 1. Note: Empirical data suggest that an interval of 0.85 and 1.1 indicates positive amplification curves. These can be set to 1. Values outside this interval indicate non-sigmoidal (e. g., negative) amplification curves. These can be set to 0.

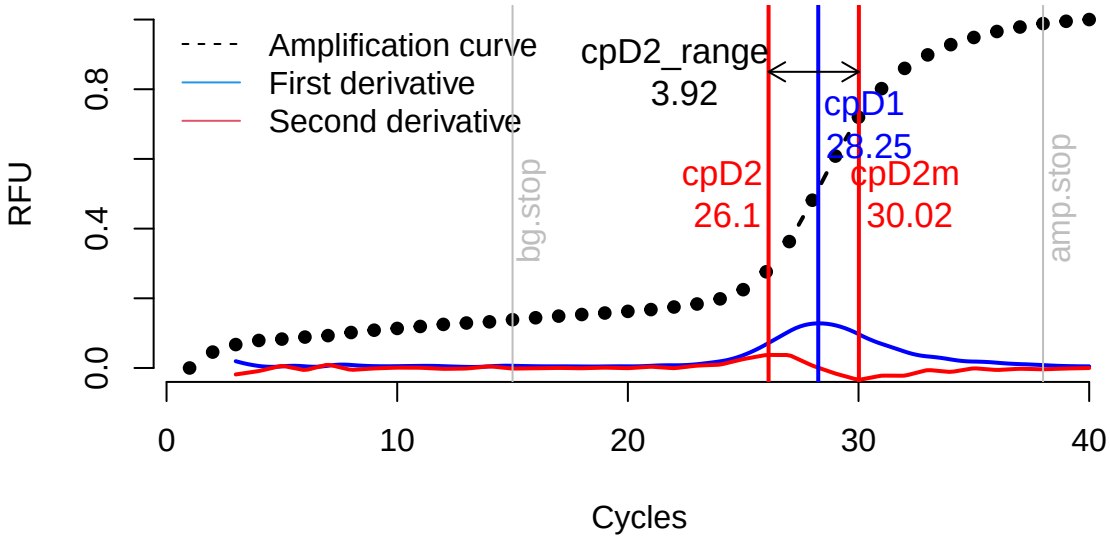


Figure 11: Location of the predictors 'cpD2_range', 'bg.start', 'bg.stop' within an amplification curve. The minimum (cpD2m) and maximum (cpD2) of the second derivative were calculated numerically using the diffQ2() function. This function also returns the maximum of the first derivative (cpD1). The 'cpD2_range' is defined as $cpD2\_range = |cpD2 - cpD2m|$. Large 'cpD2_range' values indicate a low amplification efficiency or a negative amplification reaction. The predictor 'bg.start' is an estimate for the end of the ground phase. 'bg.start' is an approximation for the onset of the plateau phase.

- `bg.stop` is the end of the ground phase and `amp.stop` is the end of the exponential phase estimated by the `bg.max()` [`chipPCR`] function (Rödiger, Burdukiewicz, and Schierack 2015). A graphical presentation of the locations in the amplification curve are shown in Figure 11. The `bg.stop` and `bg.stop` values differ significantly between negative and positive amplification curves (Figure 12J & K).
- `top` is the *takeoff point* as proposed by Tichopad et al. (2003). The `top` is calculated using externally studentized residuals, which tested to be an outlier in terms of the t-distribution. The `top` signifies to first PCR cycle entering the exponential phase. `tdp` is the *takedown point*. This is an implementation in the `pcrfit_single()` function, which uses the rotated $f(x) \mapsto f_1(f(x))$ and flipped $g(x) = -(x)$ amplification curve for calculation. Figure 5A describes the location of `top` and `tdp`. The position (`f.top`, `f.tdp`) on the ordinate is also determined from these points. If an amplification curve is negative or neither `top` nor `tdp` can be calculated, then `top` & `tdp` will be assigned the number of cycles and `f.top` & `f.tdp` the value 1. The distribution of `top`, `tdp`, `f.top` and `f.tdp` is shown in Figure 12F-I. The `top`, `tdp`, `f.top` and `f.tdp` values differ significantly between negative and positive amplification curves. Potentially they enable a qualitative classification of the amplification reaction. An interesting aspect is that the positive `f.top` values are markedly lower than the negative `f.top` values The same applies inversely to the `tdp` values. In this way, amplification curves can be classified according to these

values.

- `peaks_ratio` is based on a sequential chaining of functions. The `diffQ()` [`MBmca`] function determines numerically the first derivative of an amplification curve. This derivative is passed to the `mcaPeaks()` [`MBmca`] function. In the output all minima and all maxima are contained. The ranges are calculated from the minima and maxima. The Lagged Difference is determined from the ranges of the minima and maxima. Finally, the ratio of the differences (maximum/minimum) is calculated. The `peaks_ratio` values differ significantly between negative and positive amplification curves (Figure 23B).
- `loglin_slope` is calculated from the slope determined by a linear model of the data points from the cycle dependent fluorescence at the minimum of the second derivative and maximum of the second derivative (Figure 13), provided that the locations of the minimum of the second derivative and the maximum of the second derivative yield a *suitable* interval. As a precaution, the algorithm checks, for example, whether the distance between the minimum of the second derivative and the maximum of the second derivative is not more than nine PCR cycles. Failing this, the `loglin_slope` value is set to zero (no slope), as in the example of Figure 13. The `loglin_slope` values differ significantly between negative and positive amplification curves (Figure 12D).

The predictor `loglin_slope` is used in the following to test if the slope within this ROI can be used to distinguish positive and negative amplification curves. The hypothesis is that positive amplification curves have a higher `loglin_slope` than negative amplification curves. As shown in Figure 12D, there is a statistically significant difference between positive and negative amplification curves.

The `loglin_slope` values from the `data_sample_subset_balanced` data set (subsubsection 3.3.1) were used to save computing time. A binomial logistic regression (see subsubsection 3.2.1)) was used to analyze the relationship between the `loglin_slope` value and the class (negative, positive). The data set was split into two chunks. This is an important step during such applications. One chunk is for adapting, i.e. training, the model and the other chunk for testing the model. By convention, 70% to 80% of the data is used for training (Walsh, Pollastri, and Tosatto 2015; Kuhn 2008). The binomial logistic regression model was adapted using the `glm()` [`stats`] function by using the parameter `family = binomial(link = 'logit')`. To objectify the splitting, the `sample()` [`stats`] function was used.

```
library(PCRedux)

data <- data_sample_subset_balanced

n_positive <- sum(data[["decision"]] == "y")
n_negative <- sum(data[["decision"]] == "n")

dat <- data.frame(loglin_slope = data[, "loglin_slope"],
                  decision = as.numeric(factor(data$decision,
                                               levels = c("n", "y"),
                                               label = c(0, 1))) - 1)

# Select randomly observations from 70% of the data for training.
# n_train is the number of observations used for training.

n_train <- round(nrow(data) * 0.7)

paste0("Percentage of observations (", n_train, ") = ",
       signif((n_train/nrow(data)*100),3), "%")
```

```
## [1] "Percentage of observations (456) = 70%"
```

```
# index_test is the index of observations to be selected for the training
index_test <- sample(1L:nrow(dat), size = n_train)
```

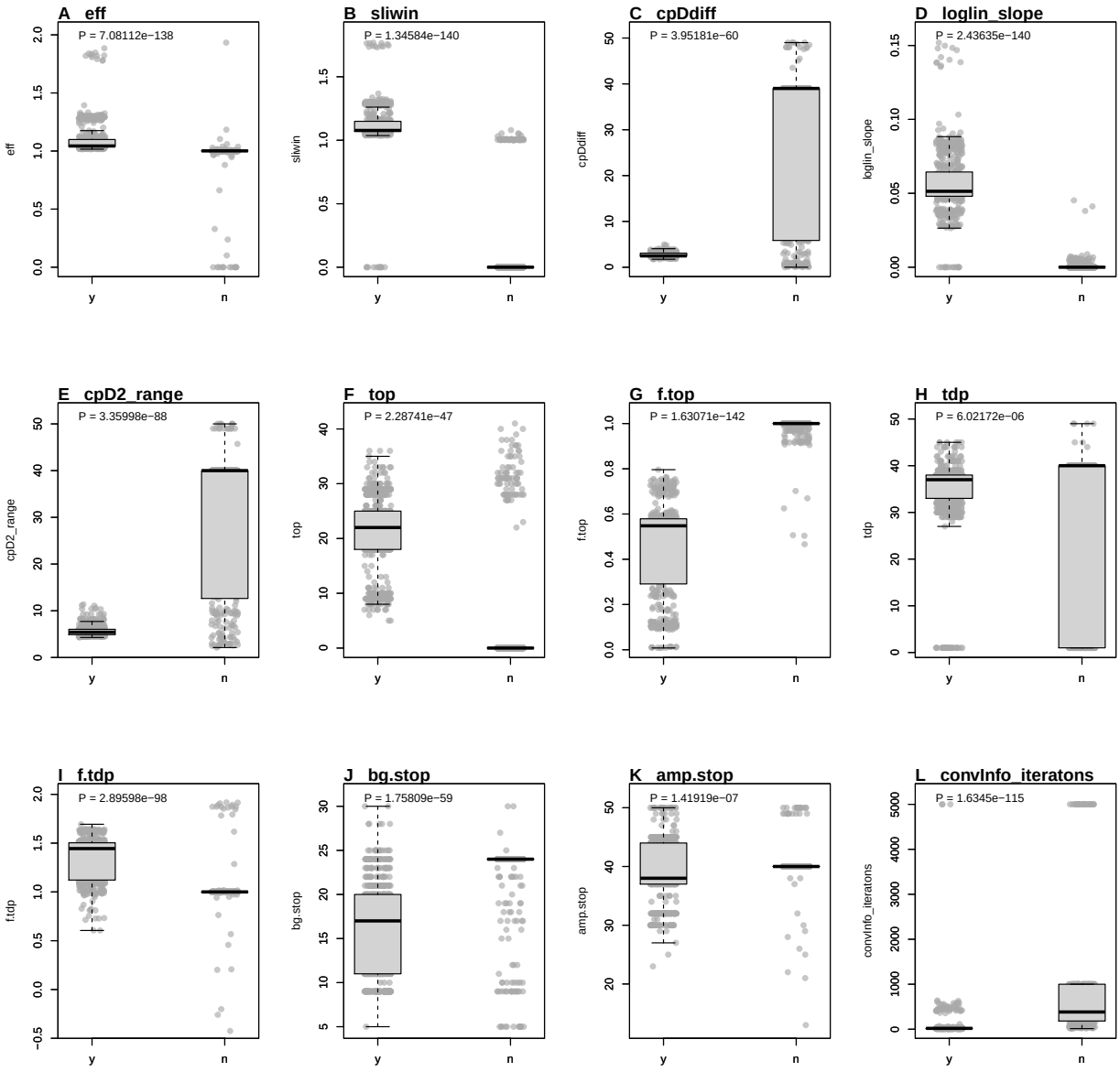


Figure 12: Values of predictors calculated from negative and positive amplification curves. Amplification curve predictors from the 'data_sample_subset' data set were used as they contain positive and negative amplification curves, and amplification curves that exhibit a *hook effect* or non-sigmoid shapes. A) 'eff', optimized PCR efficiency found within a sliding window. B) 'sliwin', PCR efficiency by the 'window-of-linearity' method. C) 'cpDdiff', difference between the Cq values calculated from the first and the second derivative maximum. D) 'loglin_slope', slope from the cycle at the second derivative maximum to the second derivative minimum. E) 'cpD2_range', absolute value of the difference between the minimum and the maximum of the second derivative maximum. F) 'top', takeoff point. G) 'f.top', fluorescence intensity at takeoff point. H) 'tdp', takedown point. I) 'f.tdp', fluorescence intensity at takedown point. J) 'bg.stop', estimated end of the ground phase. K) 'amp.stop', estimated end of the exponential phase. L) 'convInfo_iteratons', number of iterations until convergence.

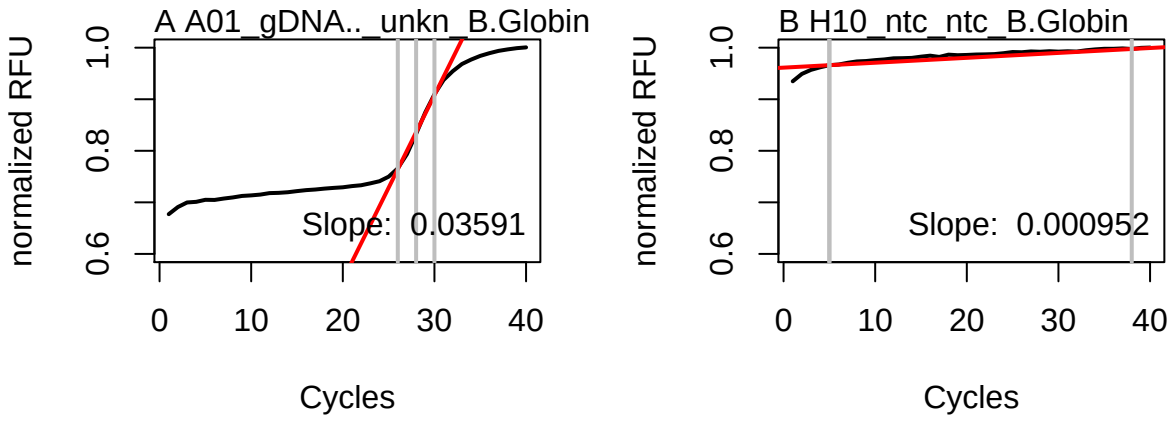


Figure 13: Concept of the 'loglin_slope' predictor. The algorithm determines the fluorescence values of the raw data at the approximate positions of the maximum off the first derivative, the minimum of the second derivative and the maximum of the second derivative, which are in the exponential phase of the amplification curve. The data were taken from the 'RAS002' data set. A linear model is created from these parameter sets and the slope is determined. A) Positive amplification curves have a clearly positive slope. B) Negative amplification curves usually have a low, sometimes negative slope.

```
# index_test is the index of observations to be selected for the testing
index_training <- which(!(1L:nrow(dat) %in% index_test))

# train_data contains the data used for training

train_data <- dat[index_test, ]

# test_data contains the data used for training

test_data <- dat[index_training, ]

# Fit the binomial logistic regression model

model_glm <- glm(decision ~ loglin_slope, family=binomial(link='logit'),
                 data = train_data)

predictions <- ifelse(predict(model_glm,
                              newdata = test_data, type = 'response') > 0.5,
                      1, 0)

res_performeR <- performeR(predictions, test_data[["decision"]])[, c(1:10, 12)]
```

The `summary()` function returns the results of the model fitting. This can be analysed and interpreted.

```
summary(model_glm)
```

```
##
## Call:
```

```
## glm(formula = decision ~ loglin_slope, family = binomial(link = "logit"),
##     data = train_data)
##
## Deviance Residuals:
##     Min       1Q   Median       3Q      Max
## -3.2221  -0.2377  -0.2377   0.0070   2.6760
##
## Coefficients:
##              Estimate Std. Error z value Pr(>|z|)
## (Intercept)   -3.5521     0.3764  -9.437   <2e-16 ***
## loglin_slope 193.2203    22.3144   8.659   <2e-16 ***
## ---
## Signif. codes:  0 '***' 0.001 '**' 0.01 '*' 0.05 '.' 0.1 ' ' 1
##
## (Dispersion parameter for binomial family taken to be 1)
##
##     Null deviance: 632.010  on 455  degrees of freedom
## Residual deviance:  90.206  on 454  degrees of freedom
## AIC: 94.206
##
## Number of Fisher Scoring iterations: 8
```

Based on the results it can be concluded that the parameters `(intercept)` and `loglin_slope` are statistically significant ($P <$ 2e-16). This indicates an association between `loglin_slope` and the probability that an amplification curve is positive.

In order to apply the model to a new data set, further steps are necessary. `predict()` [`stats`] is a generic function for predicting the results of a model fitting function (Figure 14A). All previously split test data is passed to the function argument `newdata`. By setting the `type = 'response'` parameter, the `predict()` function returns probabilities in the form of $P(y = 1|X)$. In the case in hand, it was decided that a decision limit of 0.5 is to be applied. If $P(y = 1|X) < 0.5$ then $y = 0$ (amplification curve negative), otherwise $y = 1$ (amplification curves positive).

```
library(PCRedux)

# Create graphic device for the plot(s)
# Plot train_data (grey points) and the predicted model (blue)
par(mfrow = c(1,2))


plot(train_data$loglin_slope, train_data$decision, pch = 19,
     xlab = "loglin_slope", ylab = "Probability",
     col = adjustcolor("grey", alpha.f = 0.9), cex = 1.5)
mtext("A", cex = 1, side = 3, adj = 0, font = 2, las = 0)
abline(h = 0.5, col = "grey")

curve(predict(model_glm, data.frame(loglin_slope = x), type = "resp"),
      add = TRUE, col = "blue")

# Plot test_data (red)

points(test_data$loglin_slope, test_data$decision, pch = 19,
       col = adjustcolor("red", alpha.f = 0.3))
legend("right", paste("Positive: ", n_positive,
                      "\nNegative: ", n_negative), bty = "n")
```

```r
# Plot the sensitivity, specificity and other measures to describe
# the prediction.

position_bp <- barplot(as.matrix(res_performeR), yaxt = "n",
                       ylab = "Probability", main = "", las = 2,
                       col = adjustcolor("grey", alpha.f = 0.5),
                       border = "white")

par(srt = 90)
text(position_bp, rep(0.8, length(res_performeR)),
     paste(signif(res_performeR, 2)*100, "%"), cex = 0.6)
axis(2, at = c(0, 1), labels = c("0", "1"), las = 2)
abline(h = 0.85, col = "grey")

mtext("B", cex = 1, side = 3, adj = 0, font = 2, las = 0)
```

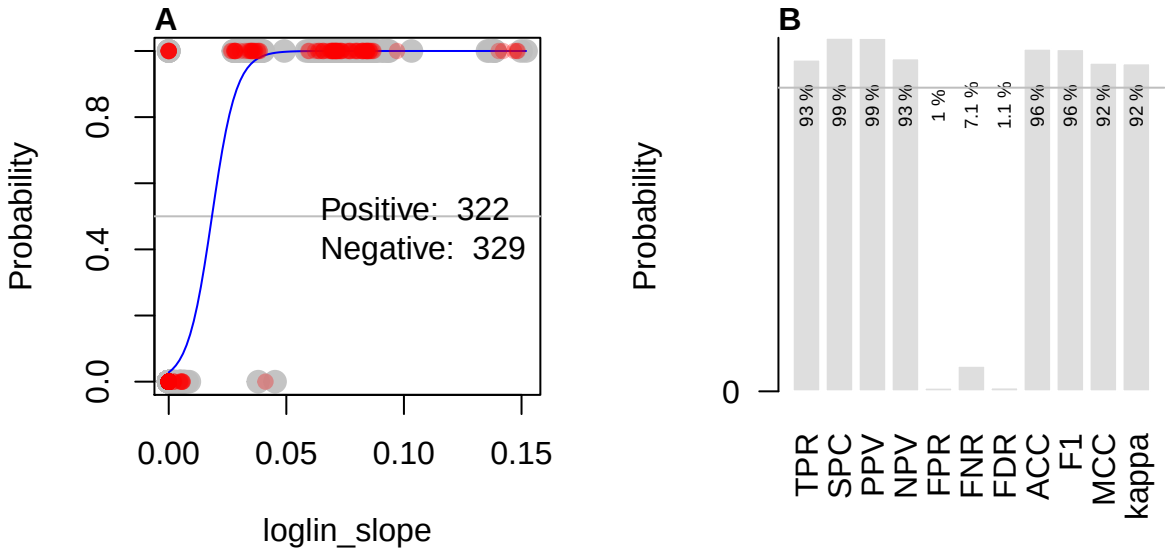


Figure 14: Machine classification by means of binomial logistic regression using the 'loglin_slope' predictor. A) For the calculation of a binomial logistic regression model, the categorical response variable $Y$ (decision with classes: negative and positive) must be converted to a numerical value. With binomial logistic regression, the probability of a categorical response can be estimated using the $X$ predictor variable. In this example, the predictor variable 'loglin_slope' is used. Grey measurement points (70% of the data set) were used for training. Red dots represent the values used for testing. The regression curve of the binomial logistic regression is shown in blue. The grey horizontal line at 0.5 marks the threshold of probability above which it is determined whether an amplification curve is negative or positive. B) The performance indicators were calculated using the performeR() function. Sensitivity, TPR; Specificity, SPC; Precision, PPV; Negative prediction value, NPV; Fall-out, FPR; False negative rate, FNR; False detection rate, FDR; Accuracy, ACC; F1 score, F1; Matthews correlation coefficient, MCC, Cohens kappa (binary classification), kappa ($\kappa$).

Sensitivity, specificity and further parameters for estimating predictions were calculated using the `performeR()` function (subsubsection 3.6.1). The results indicate that the sensitivity and specificity for the test data set provides a good result. However, in this case, they depend heavily on the computer-aided random sampling

of the training data, and the total size of the data set (Figure 14B). Over-fitting and under-fitting and other problems need to be addressed (Walsh, Pollastri, and Tosatto 2015).

To proof the results, further methods such as Likelihood Ratio Test, McFadden's $R^2$, k-fold cross-validation, Receiver Operating Characteristic (ROC) analysis and model interpretation should be used (Arlot and Celisse 2010; McFadden 1974; Sing et al. 2005).

- `sd_bg` is the standard deviation from the first PCR cycle to the takeoff point (Figure 5A). Manufacturers of thermo-cyclers use different sensors and data processing algorithms. The same applies to the detection chemistry used in experiments subsubsection 3.2.2. The signal variation in the ground phase differs between the different systems (Figure 3D). If no takeoff point can be determined from an amplification curve, the value for `sd_bg` is calculated from the first to the eighth PCR cycle. The results for the predictor `sd_bg` were broken down by the thermo-cycler and the output of the amplification reaction (negative, positive). It can be seen that the signal variation between the thermo-cyclers seems to be different. There is also a difference between negative and positive amplification curves Figure 15. The `sd_bg` values differ significantly between negative and positive amplification curves (Figure 16J).

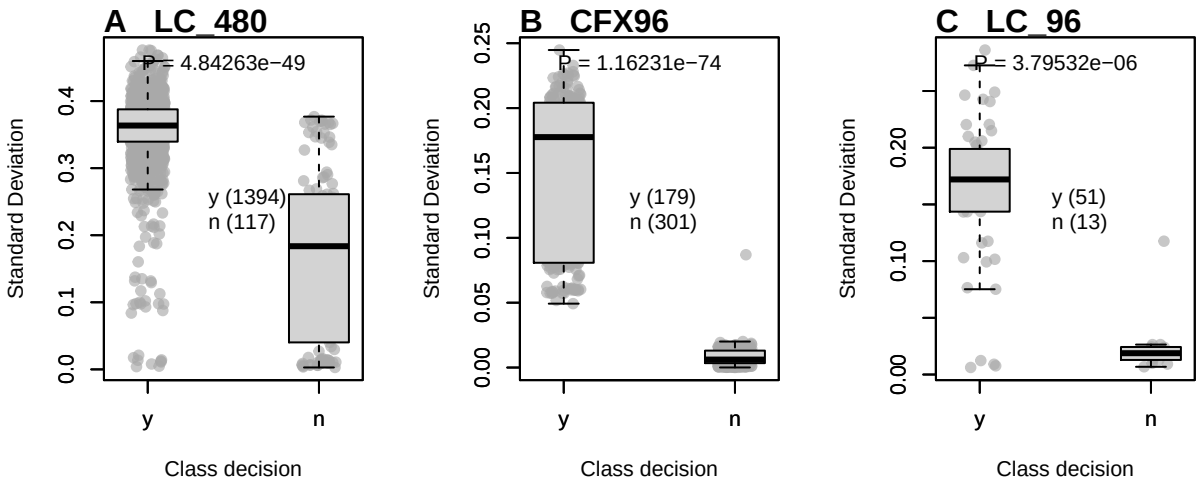


Figure 15: Standard deviation in the ground phase of various qPCR devices. The 'sd_bg' predictor was used to determine if the standard deviation between thermo-cyclers and between positive and negative amplification curves was different. The standard deviation was determined from the fluorescence values from the first cycle to the takeoff point. If the takeoff point could not be determined, the standard deviation from the first cycle to the eighth cycle was calculated. The Mann-Whitney test was used to compare the medians of the two populations (y, positive; n, negative). The differences were significant for A) LC_480 (Roche), B) CFX96 (Bio-Rad) and C) LC96 (Roche).

### 3.3.8 Integration of the `amptester()` function in `PCRedux`

`amptester_polygon` is another method to calculate the area under an amplification curve. `amptester_polygon`[7] is part of the `amptester()` [`chipPCR`] package (Rödiger, Burdukiewicz, and Schierack 2015). In contrast to the implementation in `amptester()`, `amptester_polygon` has values normalized to the total number of cycles, thereby allowing comparable predictions (Figure 23Ds).

[7] This predictor is determined from the points in an amplification curve (like a polygon, in particular non-convex polygons) in a 'clockwise' order. The sum over the edges result in a positive value if the amplification curve is 'clockwise' and is negative if the curve is 'counter-clockwise'.

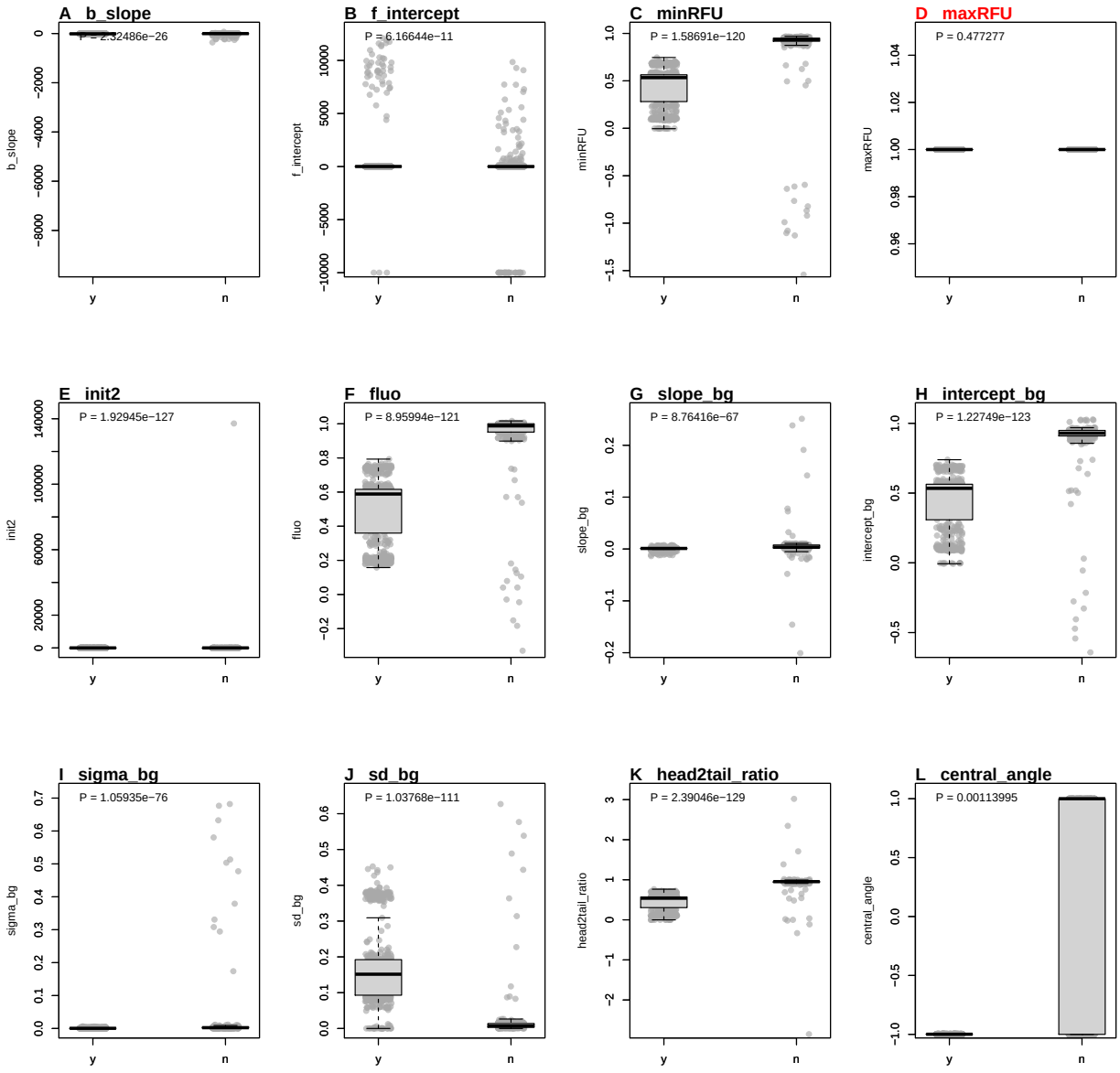


Figure 16: Values of predictors calculated from negative and positive amplification curves. Amplification curve predictors from the 'data_sample_subset' data set were used as they contain positive and negative amplification curves, as well as amplification curves that exhibit a *hook effect* or non-sigmoid shapes. A) 'eff', optimized PCR efficiency in a sliding window. B) 'sliwin', PCR efficiency according to the window-of-linearity method. C) 'cpDdiff', difference between the Cq values calculated from the first and the second derivative maximum. D) 'loglin_slope', slope from cycle at second derivative maximum to second derivative minimum. E) 'cpD2_range', absolute difference between the minimum and maximum of the second derivative. F) 'top', takeoff point. G) 'f.top', fluorescence intensity at takeoff point. H) 'tdp', takedown point. I) 'f.tdp', fluorescence intensity at the takedown point. J) 'bg.stop', estimated end of the ground phase. K) 'amp.stop', estimated end of the exponential phase. L) 'convInfo_iteratons', number of iterations until convergence when fitting a multiparametric model. The classes were compared using the Wilcoxon Rank Sum Test.

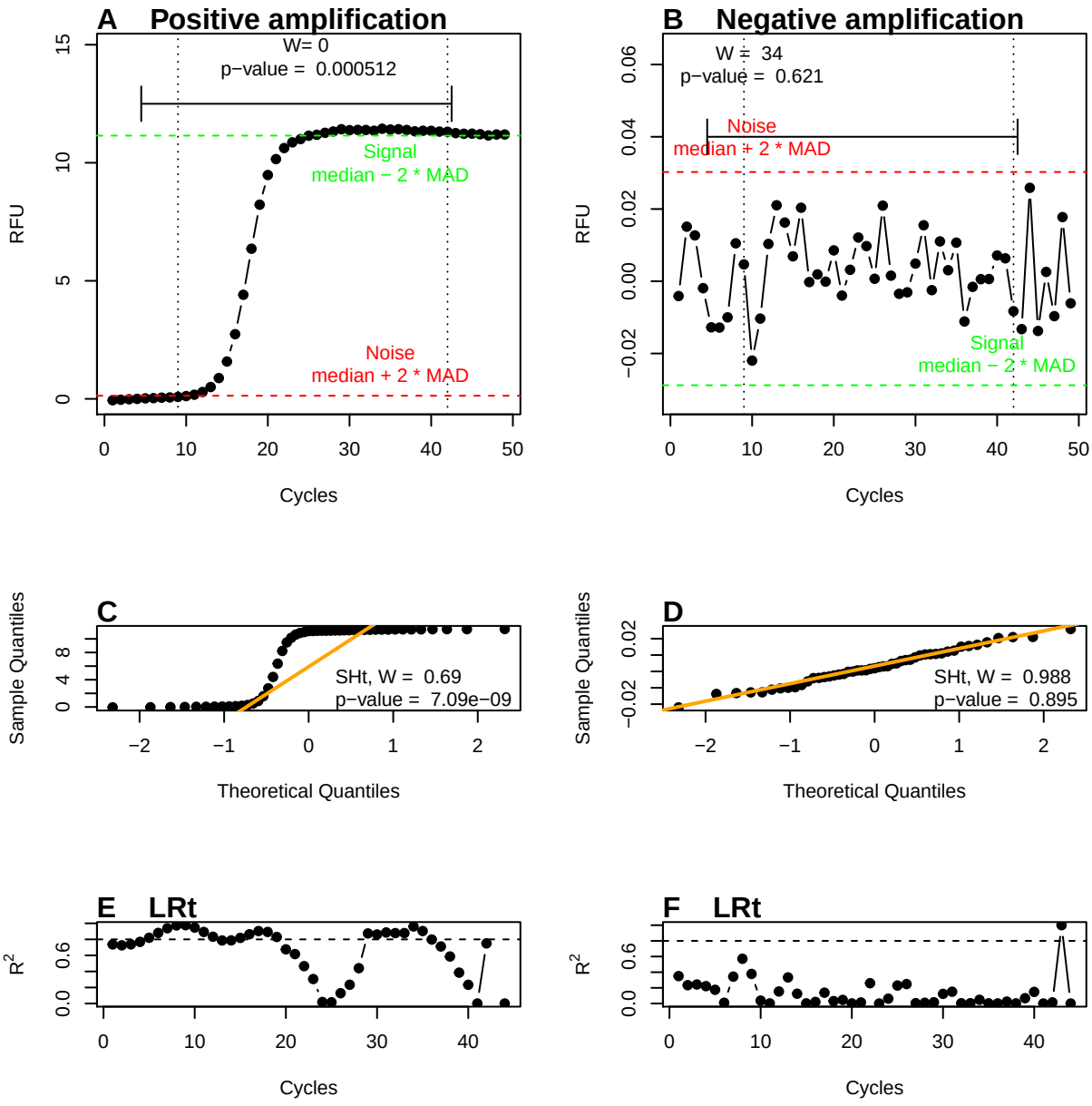


Figure 17: Analysis of amplification curves with the "amptester()" function. A & B) The threshold test (THt) is based on the Wilcoxon ranksum test and compares 20% of the fluorescence values of the ground phase with 15% of the plateau phase. In the example, a significant difference ($p = 0.000512$) was found for the positive amplification curve. However, this did not apply to the negative amplification curve ($p = 0.621$). C & D) A Q-Q diagram is used to graphically compare two probability distributions. In this study the probability distribution of the amplification curve was compared with a theoretical normal distribution. The orange line is the theoretically normal quantil-quantile plot that passes through the probabilities of the first and third quartiles. The Shapiro-Wilk test (SHt) of normality checks whether the underlying measurement data of the amplification curve is significantly normal distributed. Since the p-value of $7.09e^{-9}$ of the positive amplification curve is $\alpha \leq 5e^{-4}$, the null hypothesis is rejected. However, this does not apply to the negative amplification curve ($p = 0.895$). E & F) The linear regression test (LRt) calculates the coefficient of determination ($R^2$) using an ordinary least square regression where all measured values are integrated into the model in a cycle-dependent manner. Experience shows that the non-linear part of an amplification curve has a $R^2$ smaller than 0.8, which is also shown in the example.

### 3.3.9 `earlyreg()` - A Function to Calculate the Slope and Intercept in the Ground Phase of an Amplification Curve

The signal height and the slope in the first cycles (1 - 10) of amplification curves are potentially useful because some qPCR systems calibrate themselves by fluorescence intensity of the first cycles. This is noticeable as strong signal changes which appear spontaneously between the first and second cycle (e. g., Figure 1B). Furthermore, the signal level can be used to determine which background signal is present and whether the ground phase already has a slope. Moreover, characteristics of the detection probe system are noticeable (see subsubsection 3.2.4). From the slope, it may be deduced whether amplification has already started (see subsubsection 3.2.4).

Consequently, the `earlyreg()` function was developed. This function uses an ordinary least squares linear regression within a limited number of cycles. As ROI, the first 10 cycles were defined. This restriction is based on the developers experience, suggesting that during the first ten cycles only a significant increase in signal strength can be measured within few qPCRs. However, `earlyreg()` does not ignore the first cycle, as many thermo-cyclers use this cycle for sensor calibration. Extreme values are therefore included. As standard, the next nine amplitude values are used for the linear regression. The number of cycles can also be adjusted via the parameter `range`. Since all amplification curves are normalized to the 99%-percentile, comparability between the background signals and the slopes is ensured. The output of the `earlyreg()` function is:

- `slope_bg`, which is the slope of the ordinary least squares linear regression model,
- `intercept_bg`, which is the intercept of the linear model and
- `sigma_bg`, which is the square root of the estimated variance of the random error.

The `slope_bg`, `intercept_bg` and `sigma_bg` values differ significantly between negative and positive amplification curves (Figure 16G-I).

The following example illustrates possible usage of `earlyreg()`. For that purpose, amplification curves from the `C127EGHP` data set were analyzed (Figure 18A). In figure Figure 18A the amplification curves for all cycles are shown. Next, the `earlyreg()` function was used to determine the `slope_bg`, `intercept_bg` and `sigma_bg` in the range of the first ten PCR cycles. The results were used in a cluster analysis using k-means clustering, demonstrating that the slope seems to be an indicator of differences between the amplification curves. The first 8 cycles were colored according to their cluster (Figure 18B). After cluster analysis, the same could also be observed (Figure 18D-F). Hence, it can be postulated that the slope in the background phase is useful for the amplification curve classification.

```
library(PCRedux)

# box_cox() function for the Box-Cox transformation of data

box_cox <- function(x, lambda = 1, offset = 0) {
    if (lambda == 0) {
        log(x + offset)
    } else
    {
        ((x + offset)^lambda - 1)/lambda
    }
}

# Load the C127EGHP data set
data <- chipPCR::C127EGHP[, -1]

# Normalize each amplification curve to their 0.99 percentile and use the
# earlyreg() function to determine the slope and intercept of the first
# cycles 'user_range'

user_range <- 8
```

```r
res_earlyreg <- do.call(rbind, lapply(2L:ncol(data), function(i) {
  earlyreg(x = data[, 1], y = data[, i], range = user_range, normalize = TRUE)
})) %>% box_cox(.)

# Label the observation with their names
rownames(res_earlyreg) <- substr(colnames(data)[-1], 1, 10)

# Show the first five lines of the res_earlyreg data matrix

head(res_earlyreg)
```

```
##      intercept      slope      sigma
## EG1 -0.9996982 -1.0000257 -0.9994170
## EG2 -0.9999187 -0.9999724 -0.9994349
## EG3 -1.0001748 -0.9999236 -0.9995357
## EG4 -1.0000410 -0.9999487 -0.9994961
## EG5 -1.0001467 -0.9999259 -0.9995627
## EG6 -1.0003437 -0.9998825 -0.9995230
```

```r
# Perform k-means clustering on the res_earlyreg data matrix
cl <- kmeans(res_earlyreg, centers = 2)

# Plot the results
# Use x_roi (cycles) and rfu_range (RFU values) to limit the
# range for the detailed plot of first cycles.

x_roi <- 1:(user_range + 1)
rfu_range <- range(data[x_roi, -1])

# Create graphic device for the plot(s)
layout(matrix(c(1, 2, 1, 2, 3, 3), 3, 2, byrow = TRUE))

# Plot of raw amplification curves

matplot(
    data[, 1], data[, -1], ylim = range(data[, -1]), pch = 19, lty = 1,
        type = "l", xlab = "Cycles", ylab = "RFU", main = "", col = "grey"
)
mtext("A", cex = 1, side = 3, adj = 0, font = 2)
abline(v = c(1,user_range))
text(3, range(data[, -1])[2], "ROI")

# Detailed plot of the first cycles and the clusters according
# to the k-means clustering
# Define some user colors (blue: EvaGreen, orange: Hydrolysis probes)
colors <- c(
    adjustcolor("blue", alpha.f = 0.5),
            adjustcolor("orange", alpha.f = 0.8)
)

matplot(NA, NA, xlim = range(x_roi), ylim = rfu_range, xlab = "Cycles",
        ylab = "RFU", main = "")

for(i in 1L:length(unique(cl$cluster))) {
```

```
cl_id <- which(cl[["cluster"]] == i) + 1
par(new=TRUE)
matplot(data[x_roi, 1], xlab = "", ylab = "", xaxt = "n", yaxt = "n",
        data[x_roi, cl_id], ylim = rfu_range, pch = 19, lty = 1, type = "l",
        col = colors[i])
}


mtext("B", cex = 1, side = 3, adj = 0, font = 2)
abline(v = c(1,user_range))
text(3, rfu_range[2], "ROI")
legend("bottomleft", c("Cluster 1", "Cluster 2"), pch = 15, cex = 1.2,
       col = colors, bty = "n")

# Overview of clusters and corresponding detection chemistry

eghp <- rep(0.7, length(cl$cluster))
names(eghp) <- names(cl$cluster)

barplot(eghp, las = 2, col = colors[cl[["cluster"]]],
        border = "white", xlab = "", ylab = "",
        yaxt = "n", ylim = c(0,2.2), cex.axis = 0.7)
mtext("C", cex = 1, side = 3, adj = 0, font = 2)
legend("topleft", c("Cluster 1", "Cluster 2"), pch = 15, col = colors,
       bty = "n", box.col =  "white", cex = 0.9)
arrows(0.5, 2, 38, 2, angle = 90, code = 3)
arrows(39, 2, 76.5, 2, angle = 90, code = 3)
text(c(18.75, 57.5), c(1.6, 1.6), c("EvaGreen", "Hydrolysis probes"))
```

#### 3.3.10 `head2tailratio()` - A Function to Calculate the Ratio of the Head and the Tail of a Quantitative PCR Amplification Curve

The ratios from the ground and plateau phase can be used to search for patterns in amplification curves. Positive amplification curves have different slopes and intercepts at the start (head, background region) and the end (tail, plateau region) of the amplification curve. Hence, these regions are potentially useful to extract a predictor for amplification curve classification. Negative amplification curves (no slope) are assumed to have a ratio of about 1. In contrast, positive amplification curves should have a ratio of less than 1.

The $n$-dimensional space of all predictor variables $X_{1,2...n}$ is also called feature space. In the present study the feature space was extended by domain knowledge using known features. The `head2tailratio()`-function is an example for this. Here the feature $X_3 \equiv head2tail\_ratio$ could be calculated by determining the ratio of the $X_1 \equiv$ *fluorescence intensity in the head region* and $X_2 \equiv$ *fluorescence intensity in the tail region* of a quantitative PCR amplification curve ($X_3 = \frac{X_1}{X_2}$). As ROI, the areas in the ground phase (head) and plateau phases (tail) are used (Figure 5A). For the calculation, the median from the first six data points of the amplification curve and the median from the last six data points are used. The determination of six data points in both regions was made on the basis of *empirical experience*. As a rule, no significant increase in amplification signals can be measured in the first six cycles and in the last six cycles (where the amplification curve usually transitions into the plateau). This assumption is sometimes violated (e. g., *hook effect*) and might lead to false estimates.

```
library(PCRedux)

# Load the RAS002 amplification curve data set and assign it to the object data
```

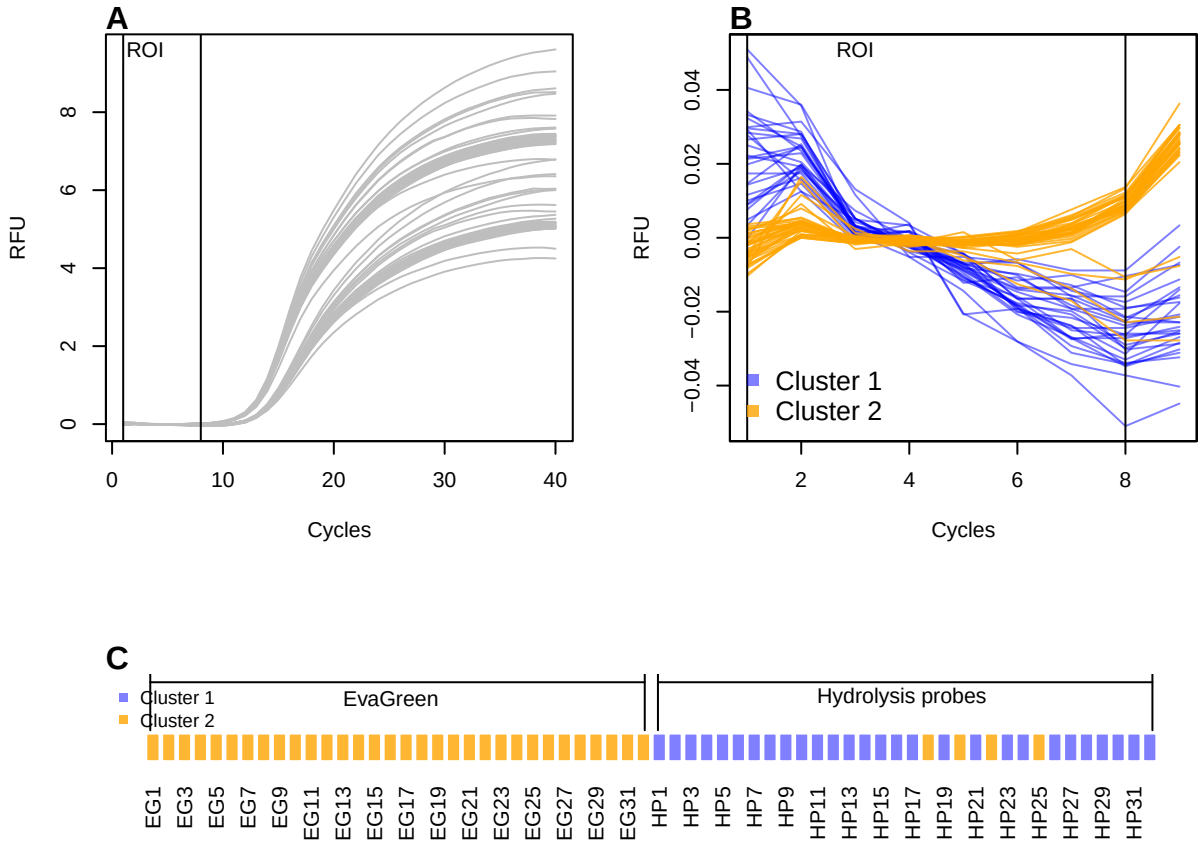


Figure 18: Analysis of the ground phase with the earlyreg() function and the 'C127EGHP' data set (n = 64 amplification curves). This data set consists of 32 samples, which were simultaneously monitored with the intercalator EvaGreen or hydrolysis probes. A) All amplification curves possess slightly different slopes and intercepts in the first cycles of the ground phase (ROI: Cycles 1 to 8). Both the slope and the intercept of each amplification curve were used for cluster analysis (k-means, Hartigan-Wong algorithm, number of centers $k = 2$). B) The amplification curves were assigned to five clusters, depending on their slope and their intersection (red, black). C) Finally, the clusters were associated to the detection chemistries (EvaGreen (EG) or hydrolysis probes (HP)).

```
data <- RAS002

# Load the RAS002 decision data set and assign it to the object data_decisions
data_decisions <- RAS002_decisions

# Calculate the head2tailratio of all amplification curves

res_head2tailratio <- lapply(2L:ncol(data), function(i) {
  head2tailratio(
    y = data[, i], normalize = TRUE, slope_normalizer = TRUE,
    verbose = TRUE
  )
})

# Fetch all values of the head2tailratio analysis for a later comparison
# by a boxplot.

res <- sapply(1L:length(res_head2tailratio), function(i)
  res_head2tailratio[[i]]$head_tail_ratio)

data_normalized <- cbind(
  data[, 1],
  sapply(2L:ncol(data), function(i) {
    data[, i] / quantile(data[, i], 0.99)
  })
)

# Assign colors to the classes (n: black, y: green).
colors <- as.character(factor(
  data_decisions, levels = c("y", "n"),
  labels = c(
      adjustcolor("green", alpha.f = 0.5), adjustcolor("black", alpha.f = 0.5))
))

res_wilcox.test <- stats::wilcox.test(res ~ data_decisions)
```

The amplification curves in Figure 19 show a signal increase within the first three cycles, and those in Figure 5C have a negative slope in the tail. The median is used to minimize the influence of outliers.

```
# Plot the results of the analysis
#
# Position and plot parameters
h <- max(na.omit(res))
h_text <- rep(h * 0.976, 2)

# Create a graphic device for the plot(s)
layout(matrix(c(1,1,2), 1, 3, byrow = TRUE))

matplot(
  data_normalized[, 1], data_normalized[, -1],
  xlab = "Cycles", ylab = "normalized RFU", main = "",
  type = "l", lty = 1, lwd = 2, col = colors
)
for (i in 1L:(ncol(data_normalized) - 1)) {
```

```
  points(
    res_head2tailratio[[i]]$x_roi, res_head2tailratio[[i]]$y_roi,
    col = colors[i], pch = 19, cex = 1.5
  )
  abline(res_head2tailratio[[i]]$fit, col = colors[i], lwd = 2)
}
mtext("A", cex = 1, side = 3, adj = 0, font = 2)

# Boxplot of the head2tail ratios of the positive and negative
# amplification curves.

boxplot(res ~ data_decisions, col = unique(colors), ylab = "Head to Tail Ratio")

lines(c(1, 2), rep(h * 0.945, 2))
text(1.5, h_text, paste0("P = ", signif(res_wilcox.test[["p.value"]])),
     cex = 1)

mtext("B", cex = 1, side = 3, adj = 0, font = 2)
```

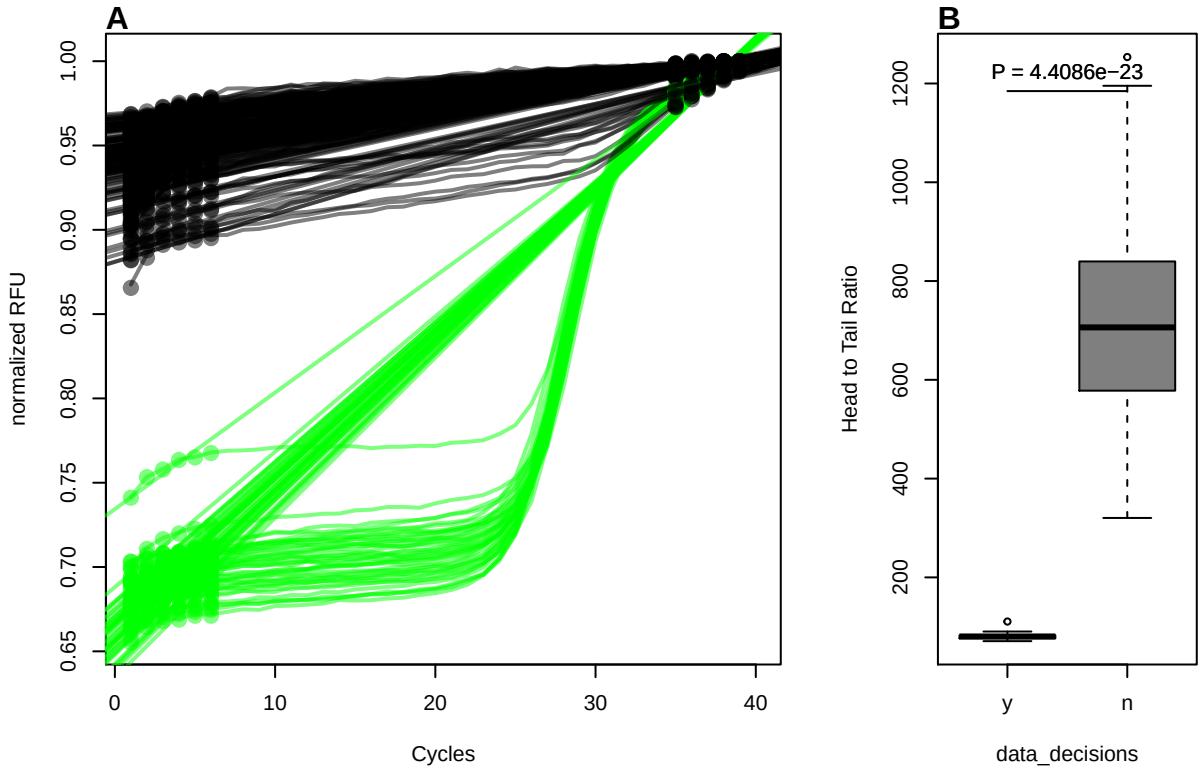


Figure 19: Ratio between the head and the tail of a quantitative PCR amplification curve. A) Plot of quantile normalized amplification curves from the 'RAS002' data set. Data points used in the head and tail are highlighted by circles. The intervals for the Robust Linear Regression are automatically selected using the 25% and 75% quantiles. Therefore, not all data points are used in the regression model. The straight line is the regression line from the robust linear model. The slopes of the positive and negative amplification curves differ. B) Boxplot for the comparison of the *head/tail* ratio. Positive amplification curves have a lower ratio than negative curves. The difference between the classes is significant.

In subsubsection 3.2.4 and in Figure 1, it was shown that negative amplification curves may have a slope with a positive or negative sign. There is no consent in the literature and among peers how to deal with this during the processing. One solution is to include the slope as factor in the ratio calculation. The `head2tailratio()` function uses a linear model that calculates the slope between the ground and plateau phases. If the slope of the model is significant, then the ratio from the head and tail is normalized to this slope. This requires setting the `slope_normalizer` parameter in the `head2tailratio()` function. By default, this parameter is not set.

The `head2tail_ratio` values differ significantly between negative and positive amplification curves (Figure 16K).

### 3.3.11 `hookreg()` and `hookregNL()` - Functions to Detect Hook Effect-like Curvatures

`hookreg()` and `hookregNL()` are functions to detect amplification curves bearing a *hook effect* (Barratt and Mackay 2002) or negative slope at the end of the amplification curve. Both functions calculate the slope and intercept of an amplification curve data. The assumption is that a strong negative slope at the end of an amplification curve is indicative for a *hook effect*. `hookreg()` and `hookregNL()` are part of a peer-reviewed publication (Burdukiewicz et al. 2018). For this reason, the functions will not be discussed here.

### 3.3.12 `mblrr()` - A Function to Perform the Quantile-filter Based Local Robust Regression

`mblrr()` is a function to perform the **m**edian **b**ased **l**ocal **r**obust **r**egression (mblrr) from a quantitative PCR experiment. In detail, this function attempts to break the amplification curve in two ROIs (head (~background) and tail (~plateau)). As opposed to the `earlyreg()` function, the `mblrr()` function does not use a fixed interval. Instead, the `mblrr()` function dynamically determines cut points for each amplification curve. It was defined that:

- the 25% quantile is the value for which 25% of all values are smaller than this value.
- the 75% quantile is the value for which 75% of all values are greater than this value.

Subsequent, a robust linear regression analysis (`lmrob()`) is preformed individually on both regions of the amplification curve. The rationale behind this analysis is that the slope and intercept of an amplification curve differ in the background and plateau region. This is also shown by the simulations in Figure 3A-C. In the example shown below, the observations "P01.W19", "P06.W35", "P33.W66", "P65.W90", "P71.W23" and "P87.W01" were arbitrarily selected for demonstration purposes Figure 20. Another example is shown in Figure 29A. Those amplification curves have a slight negative trend in the base-line region and a positive trend in the plateau region.

The correlation coefficient[8] is a measure to quantify the dependence on variables (e. g., number of cycles, signal height). The correlation coefficient is always between -1 and 1, with a value close to -1 describing a strong-negative dependency and close to 1 describing a strong-positive dependency; if the value is 0, there is no dependency between the variables. The most frequently used correlation coefficient to describe a linear dependency is the Pearson correlation coefficient $r$. The correlation coefficient can be used as a predictor. Similar data structures have similar correlation coefficients. However, variables that are not strongly correlated can also be important for modeling.

```
library(PCRedux)

# Select four amplification curves from the RAS002 data set
amplification_curves <- c(2, 3, 4, 5, 44, 45)
data <- RAS002[, c(1, amplification_curves)]

# Load the decision_res_htPCR.csv data set from a csv file.
filename <- system.file("decision_res_RAS002.csv", package = "PCRedux")
decision_res <- read.csv(filename)
```

[8] Product moment correlation coefficient (Pearson)

```r
# Overview of the amplicon curve classifications
res_decision <- decision_res[amplification_curves - 1, -c(3,4)]

res_decision
```

```
##                       RAS002 test.result.1 conformity
## 1  A01_gDNA.._unkn_B.Globin             y       TRUE
## 2     A01_gDNA.._unkn_HPRT1             n       TRUE
## 3  A02_gDNA.._unkn_B.Globin             y       TRUE
## 4     A02_gDNA.._unkn_HPRT1             n       TRUE
## 43 B10_gDNA.._unkn_B.Globin             n       TRUE
## 44    B10_gDNA.._unkn_HPRT1             n       TRUE
```

```r
# Plot the regions and the linear regression line in the
# amplification curve plot

colors <- c(
            adjustcolor("blue", alpha.f = 0.5),
            adjustcolor("orange", alpha.f = 0.8)
           )

# Create a graphic device for the plot(s)
par(mfrow = c(3, 2))

for (i in 2L:ncol(data)) {
  x <- data[, 1]
  y_tmp <- data[, i] / quantile(data[, i], 0.99)
  res_q25 <- y_tmp < quantile(y_tmp, 0.25)
  res_q75 <- y_tmp > quantile(y_tmp, 0.75)
  res_q25_lm <- try(
    suppressWarnings(lmrob(y_tmp[res_q25] ~ x[res_q25])),
    silent = TRUE
  )
  res_q75_lm <- try(
    suppressWarnings(lmrob(y_tmp[res_q75] ~ x[res_q75])),
    silent = TRUE
  )

  plot(x, y_tmp, xlab = "Cycles", ylab = "RFU (normalized)",
    main = "", type = "b", pch = 19)

  mtext(paste0(LETTERS[i - 1], "   ", colnames(data)[i]), cex = 1,
        side = 3, adj = 0, font = 2)
  legend("topleft", paste0(ifelse(res_decision[i - 1, 2] == "n",
                                  "negative", "positive")),
         bty = "n")
  abline(res_q25_lm, col = colors[1])
  points(x[res_q25], y_tmp[res_q25], cex = 2.5, col = colors[1])
  abline(res_q75_lm, col = colors[2])
  points(x[res_q75], y_tmp[res_q75], cex = 2.5, col = colors[2])
}
```

Finally, the results of the analysis were printed in a tabular format.

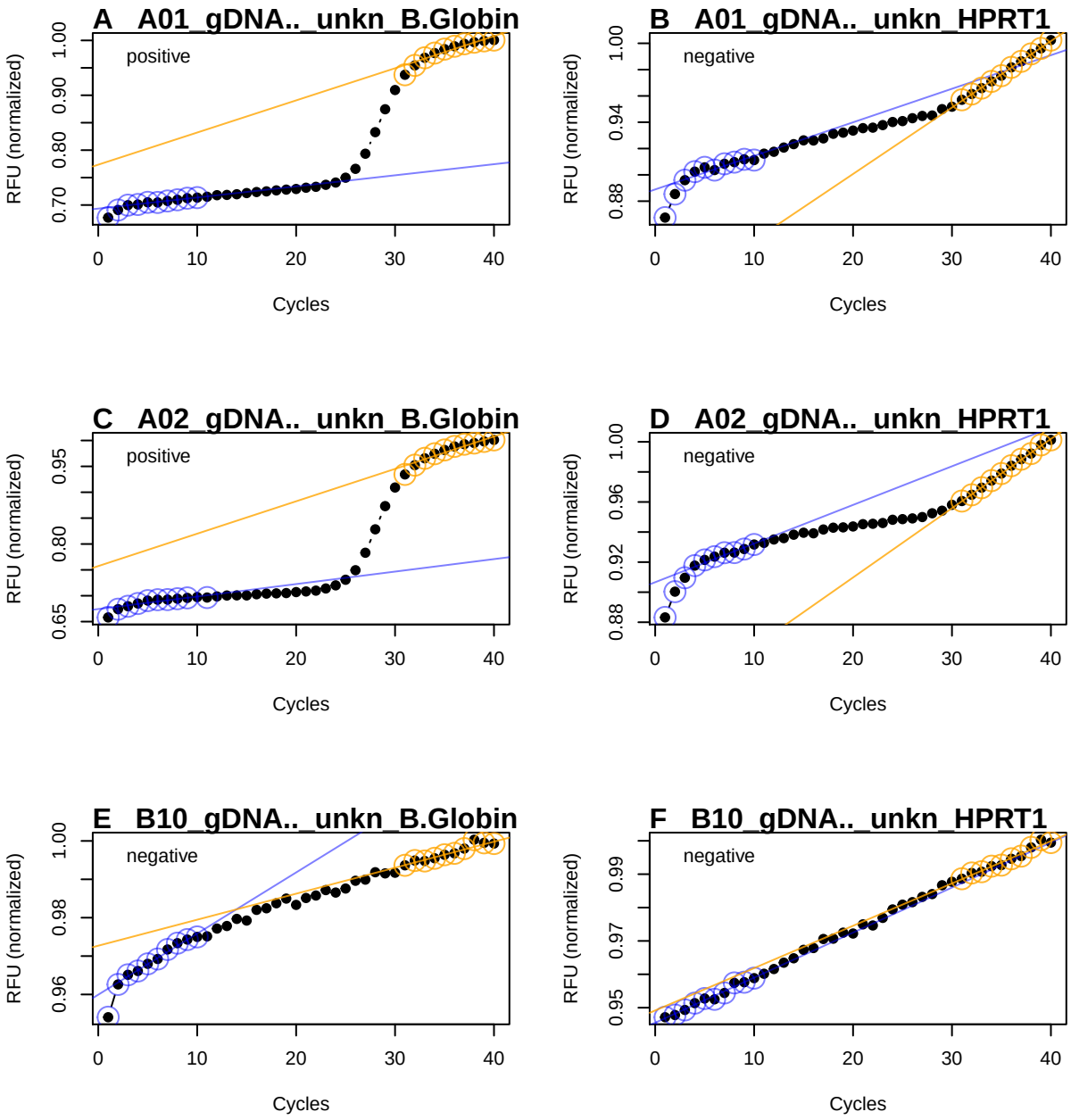


Figure 20: Robust local regression to analyze amplification curves. The amplification curves were arbitrarily selected from the 'RAS002' data set. In the qPCR setup, the target genes beta globin (B. globin) and HPRT1 were simultaneously measured in a PCR cavity using two specific hydrolysis probes (duplex qPCR). Both positive (A, C, E) and negative (B, D, F) amplification curves were used. The amplification curves are normalized to the 99% quantile. The differences in slopes and intercepts (blue and orange lines and dots). The mblrr() function is presumably useful for data sets which are accompanied by noise and artifacts.

```r
# Load the xtable library for an appealing table output
library(xtable)

# Analyze the data via the mblrr() function

res_mblrr <- do.call(cbind, lapply(2L:ncol(data), function(i) {
  suppressMessages(mblrr(
    x = data[, 1], y = data[, i],
    normalize = TRUE
  )) %>% data.frame()
}))
colnames(res_mblrr) <- colnames(data)[-1]

# Transform the data for a tabular output and assign the results to the object
# output_res_mblrr.

output_res_mblrr <- res_mblrr %>% t()

# The output variable names of the mblrr() function are rather long. For better
# readability the variable names were changed to "nBG" (intercept of the head
# region), "mBG" (slope of the head region), "rBG" (Pearson correlation of head
# region), "nTP" (intercept of the tail region), "mTP" (slope of tail region),
# "rBG" (Pearson correlation of the tail region)

colnames(output_res_mblrr) <- c(
  "nBG", "mBG", "rBG",
  "nTP", "mTP", "rTP"
)

print(xtable(
  output_res_mblrr, caption = "Selected results of predictors from the mblrr()
             function. nBG, intercept of head region; mBG, slope of head region;
             rBG, Pearson correlation of head region; nTP, intercept of tail
             region; mTP, slope of tail region; rBG, Pearson correlation of
             tail region",
  label = "tablemblrrintroduction"
), comment = FALSE, caption.placement = "top")
```

Table 1: Selected results of predictors from the mblrr() function. nBG, intercept of head region; mBG, slope of head region; rBG, Pearson correlation of head region; nTP, intercept of tail region; mTP, slope of tail region; rBG, Pearson correlation of tail region

| | nBG | mBG | rBG | nTP | mTP | rTP |
|---|---|---|---|---|---|---|
| A01_gDNA.._unkn_B.Globin | 0.69 | 0.00 | 0.91 | 0.77 | 0.01 | 0.94 |
| A01_gDNA.._unkn_HPRT1 | 0.89 | 0.00 | 0.87 | 0.80 | 0.01 | 1.00 |
| A02_gDNA.._unkn_B.Globin | 0.67 | 0.00 | 0.88 | 0.76 | 0.01 | 0.95 |
| A02_gDNA.._unkn_HPRT1 | 0.91 | 0.00 | 0.90 | 0.82 | 0.00 | 1.00 |
| B10_gDNA.._unkn_B.Globin | 0.96 | 0.00 | 0.95 | 0.97 | 0.00 | 0.96 |
| B10_gDNA.._unkn_HPRT1 | 0.95 | 0.00 | 0.99 | 0.95 | 0.00 | 0.98 |

In another example, the results from the `mblrr()` function were combined with human classifications (positive, negative) to apply them in an analysis with Fast and Frugal Trees (FFTrees). FFTrees belong to class of simple decision rules. DT's are a classic approach to machine learning (Quinlan 1986). Here relatively simple algorithms and simple tree structures are used to create a model. A general introduction to decision trees

is given in (Quinlan 1986; Luan, Schooler, and Gigerenzer 2011). In many situations, FFTrees make fast decisions based on a few predictors (N = 1 - 5). In this example six predictors were used for the analysis.

The `FFTrees` package (Phillips et al. 2017) provides an implementation for the `R` statistical computing language. All that is needed for the present example are:

- the data assessed by the `mblrr()` function,
- the classification of the amplification curve data by a human,
- and a standard formula, which looks like $outcome \sim var1 + var2 + \ldots$ along with the data arguments. The function `FFTrees()` returns a fast and frugal tree object. This rich object contains the underlying trees and many classification statistics (similar to subsubsection 3.6.1). In the following example, the `RAS002` data set was used.

```
# Load the xtable library for an appealing table output
library(FFTrees)
library(PCRedux)

# The RAS002 amplification curves were analyzed with the mblrr() function
# to save computing time and the.results of this analysis are stored in the
# `data_sample` data set.

data <- data_sample[data_sample$dataset == "RAS002", c("mblrr_intercept_bg",
                                                       "mblrr_slope_bg",
                                                       "mblrr_cor_bg",
                                                       "mblrr_intercept_pt",
                                                       "mblrr_slope_pt",
                                                       "mblrr_cor_pt")]

# The output variable names of the mblrr() function are rather long. For better
# readability the variable names were changed to "nBG" (intercept of head
# region), "mBG" (slope of head region), "rBG" (Pearson correlation of head
# region), "nTP" (intercept of tail region), "mTP" (slope of tail region),
# "rBG" (Pearson correlation of tail region).


res_mblrr <- data.frame(
    class = as.numeric(as.character(factor(RAS002_decisions,
                                           levels = c("y", "n"),
                                           label = c(1, 0)))),
  data
)

res_mblrr$class <- as.logical(res_mblrr$class)

colnames(res_mblrr) <- c("class", "nBG", "mBG", "rBG", "nTP", "mTP", "rTP")

res_mblrr.fft <- suppressMessages(
            FFTrees(formula = class ~., data = res_mblrr)
            )
```

Figure 21 shows the Fast and Frugal Trees by using the predictors nBG (intercept of head region), mBG (slope of head region), rBG (Pearson correlation of head region), nTP (intercept of tail region), mTP (slope of tail region), and rBG (Pearson correlation of tail region).

`R` offers several packages like `party` (Hothorn, Hornik, and Zeileis 2006), `rpart` (Therneau, Atkinson, and Ripley 2017) and `Rattle` (Williams 2009) for creating and visualizing decision trees.

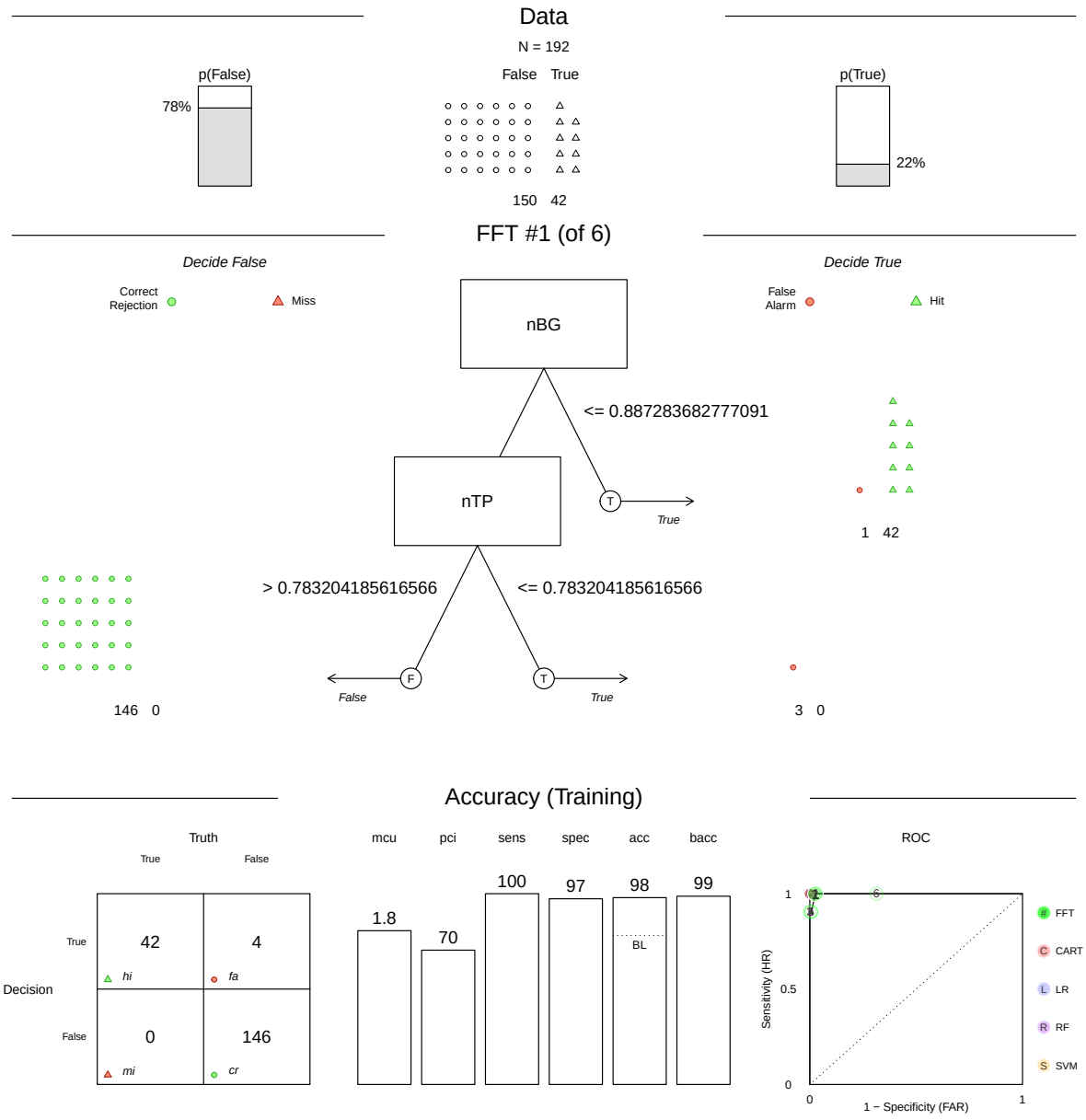


Figure 21: Visualization of decisions in Fast and Frugal Trees after data analysis of amplification curves via the mblrr() function. **Top row** 'Data') Overview of the data set, stating the total number of observations (N = 192) and percentage of positive (22%) and negative (78%) amplification curves. **Middle row** 'FFT #1 (of 6)') Decision Tree with the number of observations classified at each level of the tree. For the analysis, six predictors (nBG, intercept of head region; mBG, slope of head region; rBG, Pearson correlation of head region; nTP, intercept of tail region; mTP, slope of tail region; rBG, Pearson correlation of tail region) have been used for the analysis. After two tree levels (nBG, nTP), the decision tree is created, where all positive amplification curves (N = 40) are correctly classified. Two observations are classified as false-negative in the negative amplification curves. **Lower row** 'Performance') The FFTrees() [FFTrees] function determines several performance statistics. For the training data, there is a classification table on the left side showing the relationship between tree 'decision' and the 'truth'. The correct rejection ('Cor Rej') and 'Hit' are the right decisions. 'Miss' and false alarm ('False Al') are wrong decisions. The centre shows the cumulative tree performance in terms of mean of used cues ('mcu'), Percent of ignored cues ('pci'), sensitivity ('sens'), specificity ('spec'), accuracy ('acc') and weighted Accuracy ('wacc'). The receiver operating characteristic (ROC) curve on the right-hand side compares the performance of all trees in the FFTrees object. The system also displays the performance of the fast frugal trees ('#', green), CART ('C', red), logistical regression ('L', blue), random forest ('R', violet) and the support vector machine ('S', yellow).

### 3.3.13 `autocorrelation_test()` - A Function to Detect Positive Amplification Curves

Autocorrelation analysis is a technique that is used in the field of time series analysis. It can be used to reveal regularly occurring patterns in one-dimensional data (Spiess et al. 2016). Autocorrelation measures the correlation of a signal $f(t)$ with itself shifted by some time delay $f(t - \tau)$.

The `autocorrelation_test()` function coerces the amplification curve data to an object of class "zoo" (`zoo` package) as indexed totally ordered observations. Then follows the computation of a lagged version of the amplification curve data. The shifting of the amplification curve data is based on the number of observations (number of cycles 'c') with the following $\tau$.

| Number of Cycles (c) | $\tau$ |
|---|---|
| $c \leq 35$ | 8 |
| $35 > c \leq 40$ | 10 |
| $40 < c \leq 45$ | 12 |
| $c > 45$ | 14 |

This is followed by a significance test for correlation between paired observations (original & lagged amplification curve data). The hypothesis is that paired observations of positive amplification curves exhibit significant correlation (`stats::cor.test`, significance level is 0.01) in contrast to negative amplification curves (noise). The application of the `autocorrelation_test()` function is shown in the following example.

In addition, the decisions file `decision_res_RAS002.csv` from the user was analyzed for the most frequent decision (modus) using the `decision_modus()` function (subsubsection 3.5.3).

```
# Test for autocorrelation in amplification curve data. The amplification
# curve data from the `htPCR` data set was used.
library(PCRedux)

# Load the decision_res_htPCR.csv data set from a csv file.
filename <- system.file("decision_res_htPCR.csv", package = "PCRedux")
decision_res_htPCR <- read.csv(filename)

# Select only amplification curves (obs) were all
# classifications were in concordance ("conformity == TRUE" ).
# This subset of the htPCR data set contains the classes
# n: negative
# a: ambiguous
# p: positive

obs_number <- which(decision_res_htPCR[["conformity"]] == TRUE)
dec <- unlist(decision_res_htPCR[obs_number, "test.result.1"])

# Give tabular output of classes
table(dec)
```

```
## dec
##   a   n   y
##   1 202 279
```

```
# Since the number of ambiguous is low (n = 2), they were re-assigned to the
# class negative

dec[dec == "a"] <- "n"
```

```r
table(dec)
```

```
## dec
##   n   y
## 203 279
```

```r
# Load only the amplification curves from the htPCR data set that were
# uniquely assigned to one class (e.g., eight out of eight positive).

data <- qpcR::htPCR[, c(1, obs_number + 1)]

# Assign colors to the classes (n: black, y: green).

colors <- factor(dec, levels = c("y", "n"), label = c("black", "green"))


# Test for autocorrelation in the subset of the htPCR data set

res_ac <- sapply(2:ncol(data), function(i) {
    autocorrelation_test(data[, i])
})


# Plot curve data as overview
# Names of the observations
# Create a graphic device for the plot(s)

layout(matrix(c(1, 2, 3, 1, 4, 4), 2, 3, byrow = TRUE))
matplot(
    data[, 1], data[, -1], xlab = "Cycles", ylab = "RFU",
    main = "", type = "l", lty = 1,
    col = colors, lwd = 2
)
legend("topleft", c("positive", "negative"), pch = 19, col = c(1, 2), bty = "n")
mtext("A    RAS002 data set", cex = 1, side = 3, adj = 0, font = 2)


# Convert the n.s. (not significant) in 0 and others to 1.
# Combine the results of the aromatic autocorrelation_test as variable "ac",
# the human classified values as variable "hc" in a new data frame (res_ac_hc).

cutoff <- 0.85

res_ac_hc <- as.matrix(data.frame(
    ac = ifelse(res_ac > cutoff, 1, 0),
                        hc = ifelse(dec == "y", 0, 1)
))
res_performeR <- performeR(s = res_ac_hc[, "ac"], r = res_ac_hc[, "hc"])


plot(density(res_ac), xlab = "Autocorrelation", ylab = "Density", main = "")
rug(res_ac)

abline(v = cutoff)
```

```
mtext("B", cex = 1, side = 3, adj = 0, font = 2, las = 0)


cdplot(res_ac, as.factor(dec), xlab = "Autocorrelation", ylab = "Class decision")

mtext("C", cex = 1, side = 3, adj = 0, font = 2, las = 0)

position_bp <- barplot(
    as.matrix(res_performeR[, c(1:10, 12)]), yaxt = "n", ylab = "",
        main = "Performance of autocorrelation_test",
        col = adjustcolor("grey", alpha.f = 0.5), border = "white"
)
text(position_bp, rep(0.8, length(res_performeR[, c(1:10, 12)])),
     paste(signif(res_performeR[, c(1:10, 12)], 2)*100, "%"))
axis(2, at = c(0, 1), labels = c("0", "1"), las = 2)
mtext("D", cex = 1, side = 3, adj = 0, font = 2, las = 0)
```

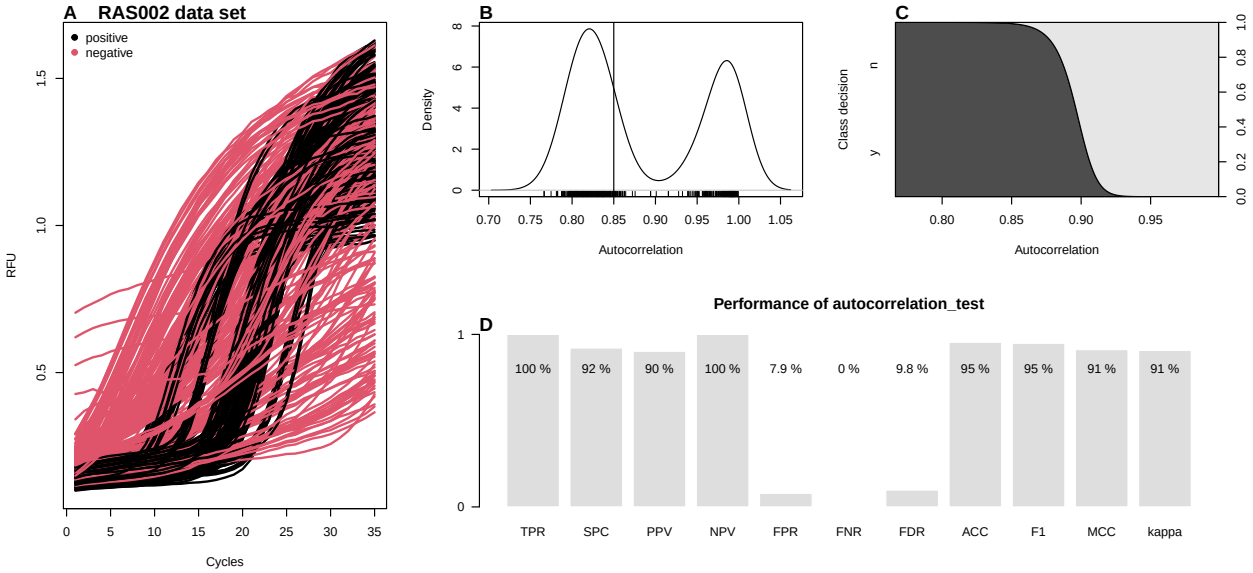


Figure 22: Autocorrelation analysis of the amplification curves of the 'RAS002' data set. A) Display of all amplification curves of the data set 'RAS002'. Negative amplification curves are shown in red and positive amplification curves in black. The autocorrelation_test() function was used to analyze all amplification curves. B) The density diagram of the autocorrelation of positive and negative amplification curves shows a bimodal distribution. C) The cdplot calculates the conditional densities of x based on the values of y weighted by the boundary distribution of y. The densities are derived cumulatively via the values of y. The probability that the decision is negative (n) when autocorrelation equals 0.85 is approximately 100%. D) Performance analysis using the performeR() function (see subsubsection 3.6.1 for details).

As shown in this example, the `autocorrelation_test()` function is able to distinguish between positive and negative amplification curves. Negative amplification curves were in all cases non-significant. In contrast, the coefficients of correlation for positive amplification curves ranged between 0.766 and 0.999 at a significance level of 0.01 and a lag of 3.

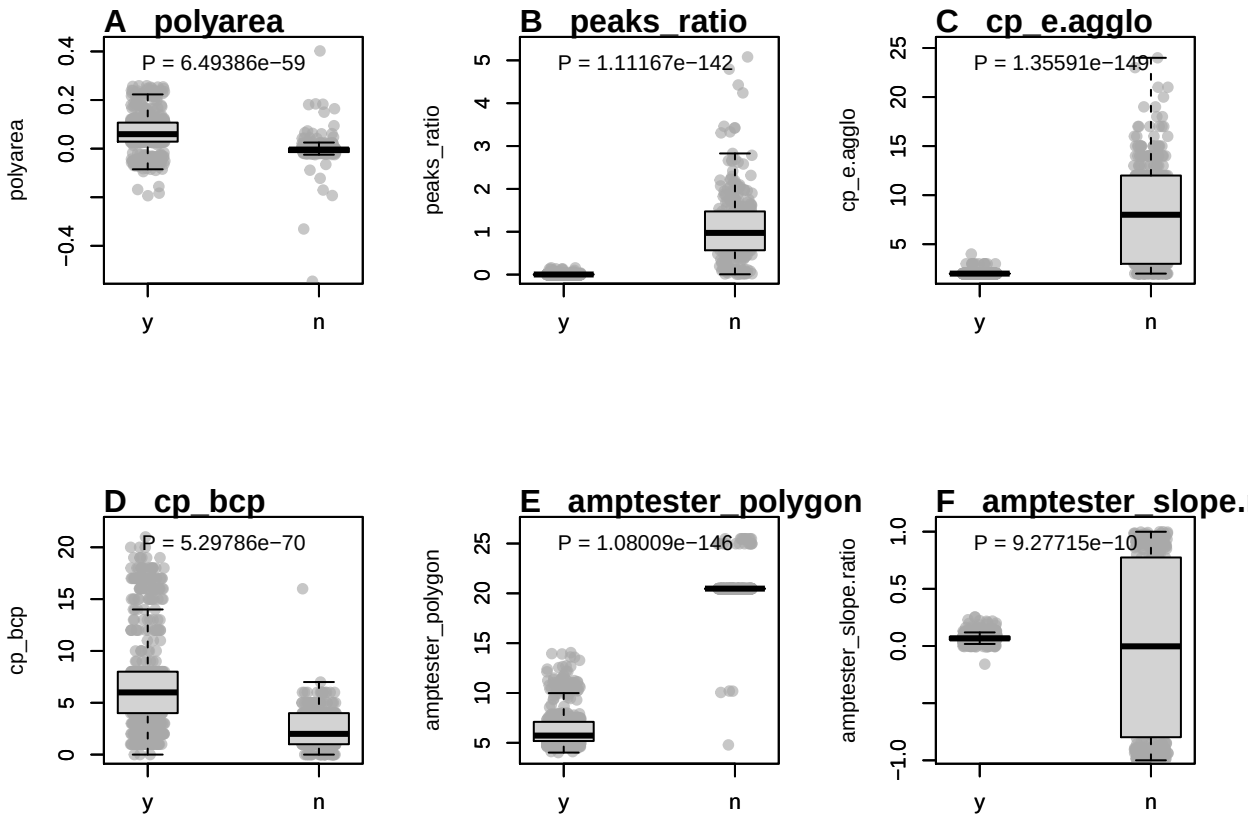


Figure 23: Values of predictors calculated from negative and positive amplification curves. Amplification curves predictors from the 'data_sample_subset' data set were used as they contain positive and negative amplification curves and amplification curves that exhibit a *hook effect* or non-sigmoid shapes. A) 'polyarea', is the area under the amplification curve determined by the Gauss polygon area formula. B) 'peaks_ratio', is the ratio of the local minima and the local maxima. C) 'cp_e.agglo', makes use of energy agglomerative clustering. Positive amplification curves have fewer change points than negative amplification curves. These two change point analyzes generally separate positive and negative amplification curves. D) 'cp_bcp', analyzes change points by a Bayesian approach. Positive amplification curves appear to contain more change points than negative amplification curves. Nevertheless, there is an overlap between the positive and negative amplification curves in both methods. This can lead to false-positive or false-negative classifications. E) 'amptester_polygon' is the cycle normalized order of a polygon. F) 'amptester_slope.ratio' is the slope (linear model) of the raw fluorescence values at the approximate first derivate maximum, second derivative minimum and second derivative maximum.

### 3.3.14 Frequentist and Bayesian Change Point Analysis

Change point analysis (CPA) encompasses methods to identify or estimate single or multiple locations of distributional changes in a series of data points indexed in time order. A change herein refers to a statistical property. CPA is used for example in econometrics and bioinformatics (Killick and Eckley 2014; Erdman, Emerson, and others 2007). Several change point algorithms exist, such as the binary segmentation algorithm (Scott and Knott 1974). In change point analysis one assumes independent ordered observations $x_1, x_2, \ldots, x_n \in \mathbb{R}^d$ (N. A. James and Matteson 2013). In the case of qPCR, this is simply the cycle-dependent fluorescence, used to create $k$ homogeneous subsets of unknown size (Erdman, Emerson, and others 2007). While frequentist methods make an estimation of the parameter at the location (e. g., mean) of the change points at specific points, change point analysis using Bayesian method produces a probability for the occurrence

of a change point at certain points. For the analysis of the amplification curves, it was hypothesized that the number of change points differs between positive (sigmoidal) and negative (noise) amplification curves.

The `pcrfit_single()` function uses two independent approaches for change point analysis. These are the `bcp()` [`bcp`] (Erdman, Emerson, and others 2007) and the `e.agglo()` [`ecp`] function (N. A. James and Matteson 2013). The `e.agglo()` function performs a non-parametric change point analysis based on agglomerative hierarchical estimation and is useful to "detect changes within the marginal distributions" (N. A. James and Matteson 2013). Measurements from the qPCR systems typically show noise that has rapidly changing components. Differentiators amplify these rapidly changing noise components (Rödiger, Böhm, and Schimke 2013). Therefore, the first derivation of the amplification curve was used for both change point analyzes. It was assumed for the change point analysis of amplification curves, that this leads to larger differences between positive and negative amplification curves. An example is shown on Figure 24. In contrast, the `bcp()` [`bcp`] function performs a change point analysis based on a Bayesian approach. This method can detect changes in the mean of independent Gaussian observations. As a result, the analysis returns the posterior probability of a change point at each $x_i$. An example is shown on Figure 24. Both the change point analysis methods provide additional information to distinguish positive and negative amplification curves Figure 23E & F).

#### 3.3.15 Frequentist Approaches to Test the Class of an Amplification Reaction and Application of the `amptester()` Predictors

A part of `pcrfit_single()` is the `amptester()` [`chipPCR`] function, which contains tests to determine whether an amplification curve is positive or negative. The input values for the function differ due to the different preprocessing steps in the `pcrfit_single()` function. Therefore, the concepts of the tests are briefly described below.

- The first test, designated as SHt, is based on this Shapiro-Wilk test of normality. This relatively simple procedure can be used to check whether the underlying population of a sample (amplification curve) is significantly ($\alpha \leq 5e-04$) normal distributed. The name of the output of the `pcrfit_single()` function is `amptester_shapiro`.
- The second test is the *Resids growth test* (RGt), which tests if the fluorescence values in linear phase are stable. Whenever no amplification occurs, fluorescence values quickly deviate from linear model. Their standardized residuals will be strongly correlated with their value. For real amplification curves, the situation is much more stable. Noise (meaning deviations from linear model) in background do not correlate strongly with the changes in fluorescence. The decision is based on the threshold value (here 0.5). The output is binary coded (negative = 0, positive = 1). The output name of the `pcrfit_single()` function is `amptester_rgt`.
- The third test is the *Linear Regression test* (LRt). This test determines the coefficient of determination ($R^2$) by an ordinary least squares linear (OLS) regression. The $R^2$ are determined from a run of $\sim 15\%$ range of the data. If a sequence of more than six $R^2$s larger than 0.8 is found, a nonlinear signal is plausible. This is somewhat counter-intuitive, because $R^2$ of nonlinear data should be low. The output is binary coded (negative = 0, positive = 1). The output name of the `pcrfit_single()` function is `amptester_lrt`.
- The fourth test is called *Threshold test* (THt), based on the Wilcoxon rank sum test. As a simple rule the first 20% (head) and the last 15% (tail) of an amplification curve are used as input data. From this, a one-sided Wilcoxon rank sum tests of the head versus the tail is performed ($\alpha \leq 1e-02$). The output is binary coded (negative = 0, positive = 1). The output name of the `pcrfit_single()` function is `amptester_tht`.
- The fifth test is called *Signal level test* (SLt). The test compares the signals of the head and the tail by a robust "sigma" rule (median + 2 * MAD) and the comparison of the head/tail ratio. If the returned value is less than 1.25 (25 percent), then the amplification curve is likely negative. The output is binary coded (negative = 0, positive = 1). The output name of the `pcrfit_single()` function is `amptester_slt`.
- The sixth test is called *Polygon test* (pco). The pco test determines if the points in an amplification curve (like a polygon) are in a "clockwise" order. The sum over the edges result in a positive value if the

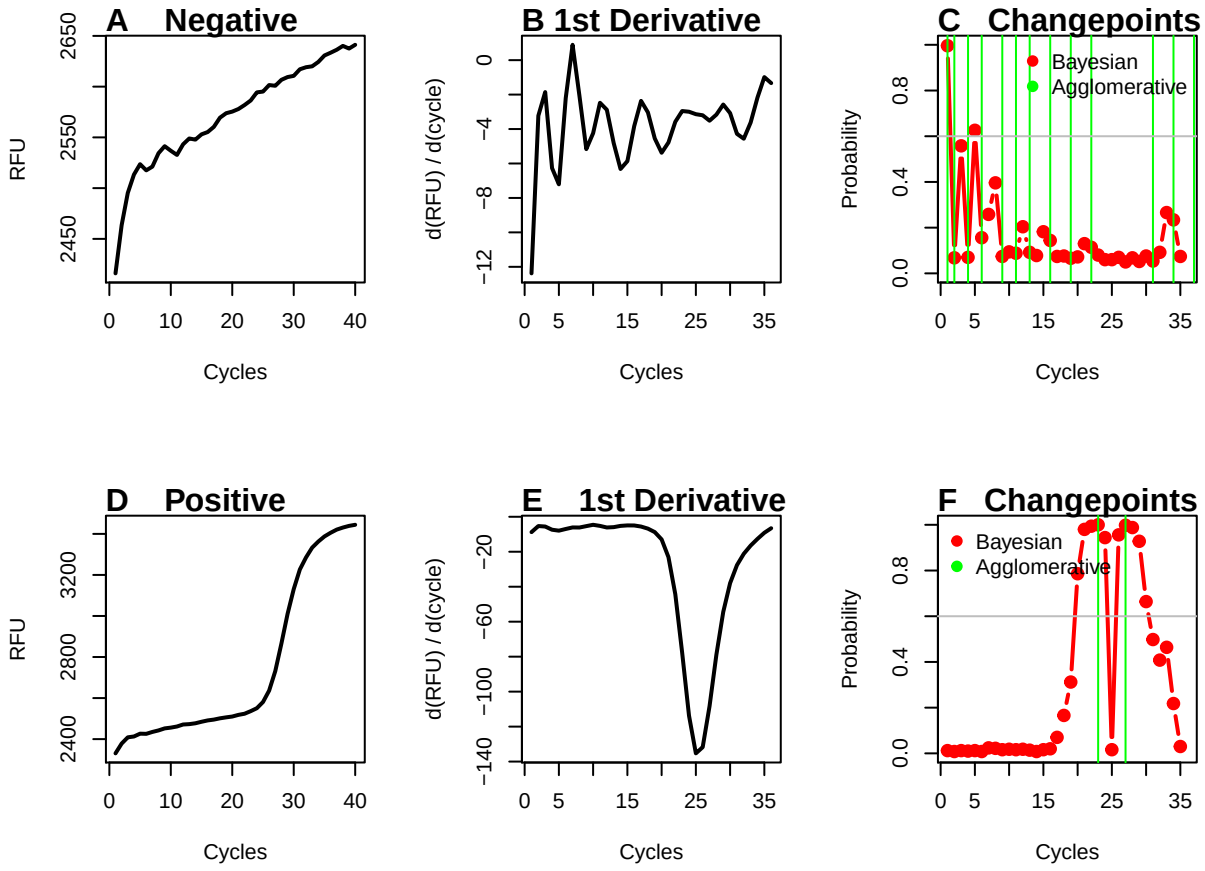


Figure 24: Bayesian and energy agglomerative change point analysis on negative and positive amplification curves. An analysis of a negative and a positive amplification curve from the 'RAS002' data set was performed using the pcrfit_single() function. In this process, the amplification curves were analyzed for change points using Bayesian change point analysis and energy agglomerative clustering. A) The negative amplification curve has a base signal of approximately 2450 RFU and only a small signal increase to 2650 RFU. There is a clear indication of the signal variation (noise). B) The first negative derivative amplifies the noise so that some peaks are visible. C) The change point analysis shows changes in energy agglomerative clustering at several positions (green vertical line). The Bayesian change point analysis rarely exceeds a probability of 0.6 (grey vert line). D) The positive amplification curve has a lower base signal ($\sim$ 2450 RFU) and increases up to the 40th cycle ($\sim$ 3400 RFU). A sigmoid shape of the curve is visible. E) The first negative derivation of the positive amplification curve shows a distinctive peak with a minimum at cycle 25. F) The change point analysis in energy agglomerative clustering shows changes (green vertical line) only at two positions. The Bayesian change point analysis shows a probability higher than 0.6 (grey horizontal line) at several positions.

amplification curve is "clockwise" and is negative if the curve is counter-clockwise. Experience states that noise is positive and "true" amplification curves are "highly" negative. In contrast to the implementation in the `amptester()` function, the result is normalized by a division to the number of PCR cycles. The output is numeric. The output name of the `pcrfit_single()` function is `amptester_polygon`.

- The seventh test is the *Slope Ratio test* (SlR). This test uses the approximated first derivative maximum, the second derivative minimum and the second derivative maximum of the amplification curve. Next, the raw fluorescence at the approximated second derivative minimum and the second derivative maximum are taken from the original data set. The fluorescence intensities are normalized to the maximum fluorescence of this data and then employed in a linear regression, using the estimated slope. The output is numeric and the output name of the `pcrfit_single()` function is `amptester_slope.ratio`.

Random Forest is an enhancement of decision tree algorithms. Random Forest uses $n$ random data subsets, by creating an ensemble consisting of $n$ small decision trees. Each decision tree contains a biased classifier. Only classes that provide reliable prediction to the outcome are then selected for classification. Compared to a single tree classifier, Random Forests display a high robustness against noise, outliers and over-fitting (Williams 2009; Breiman 2001).

In the following example, the `randomForest()` [`randomForest`] function (Liaw and Wiener 2002) was used for classification. In classification problems, one tries to predict a discrete number of values, in this case a binary classification. The aim of this **proof-of-concept** *in silico* experiment was to find the most important predictors for the classification of positive and negative amplification curves. As response vector ($y$) (in `R` type vector) the `decision` served with its possible finite classes labeled as "positive" and "negative".

- `amptester_shapiro`,
- `amptester_lrt`,
- `amptester_rgt`,
- `amptester_tht`,
- `amptester_slt`,
- `amptester_polygon` and
- `amptester_slope.ratio` served as a matrix of predictors describing the model to be adapted. The `data_sample_subset_balanced` data set (subsubsection 3.3.2) was used for the analysis to save computing time. The `data_sample_subset_balanced` data set contains similar proportions of observations (positive and negative amplification curves.

```
library(randomForest)
library(PCRedux)
set.seed(1999)

# Dimensions of the data_sample_subset_balanced object
dim(data_sample_subset_balanced)
```

```
## [1] 651  62
```

```
# Show proportions of positive and negative amplification curves in
# data_sample_subset_balanced

table(data_sample_subset_balanced[["decision"]])
```

```
##
##   y   n
## 322 329
```

```
data <- as.matrix(cbind(data_sample_subset_balanced[, c("amptester_shapiro",
                            "amptester_lrt",
                            "amptester_rgt",
                            "amptester_tht",
                            "amptester_slt",
```

```
                          "amptester_polygon",
                          "amptester_slope.ratio")],
                 decision = as.numeric(
                     factor(data_sample_subset_balanced$decision,
                                          levels = c("n", "y"),
                                          label = c(0, 1))) - 1)
                )


# Summary of data

summary(data)
```

```
##  amptester_shapiro amptester_lrt    amptester_rgt    amptester_tht
##  Min.   :0.0000    Min.   :0.0000   Min.   :0.0000   Min.   :0.0000
##  1st Qu.:0.0000    1st Qu.:1.0000   1st Qu.:1.0000   1st Qu.:1.0000
##  Median :0.0000    Median :1.0000   Median :1.0000   Median :1.0000
##  Mean   :0.4117    Mean   :0.9785   Mean   :0.9462   Mean   :0.9708
##  3rd Qu.:1.0000    3rd Qu.:1.0000   3rd Qu.:1.0000   3rd Qu.:1.0000
##  Max.   :1.0000    Max.   :1.0000   Max.   :1.0000   Max.   :1.0000
##  amptester_slt    amptester_polygon amptester_slope.ratio    decision
##  Min.   :0.0000   Min.   : 4.018    Min.   :-0.999888     Min.   :0.0000
##  1st Qu.:0.0000   1st Qu.: 5.505    1st Qu.:-0.008099     1st Qu.:0.0000
##  Median :1.0000   Median :14.053    Median : 0.050291     Median :0.0000
##  Mean   :0.5008   Mean   :13.765    Mean   : 0.034182     Mean   :0.4946
##  3rd Qu.:1.0000   3rd Qu.:20.475    3rd Qu.: 0.128971     3rd Qu.:1.0000
##  Max.   :1.0000   Max.   :25.480    Max.   : 0.999209     Max.   :1.0000
```

```
# Select randomly 70% of the observations data for training (-> n_train).
# n_train is the number of observations used for training.

# First determine the number of observations that would cover 70% of all data.

n_train <- round(nrow(data) * 0.7)
paste0("Percentage of observations (n = ", n_train, ") -> ",
       signif((n_train/nrow(data)*100), 3), "%")
```

```
## [1] "Percentage of observations (n = 456) -> 70%"
```

```
# index_test is the index of observations to be selected for the testing
index_test <- sample(1L:nrow(data), size = n_train)

# index_test is the index of observations to be selected for the training
index_training <- which(!(1L:nrow(data) %in% index_test))


# The randomForest() function was used to train a forest of 200 trees.
# Convert decision into factor, since randomForest() uses type="regression",
# instead of type="classification" by default. Each tree is trained on 63.2 %
# of the training data. Each observation is drawn at random with replacement
# from the original data.
# The predictor variables are drawn at random out of the feature space
# "amptester_shapiro", "amptester_lrt", "amptester_rgt", "amptester_tht",
# "amptester_slt", "amptester_polygon" and "amptester_slope.ratio".
```

```
model_rf <- randomForest(as.factor(decision) ~ ., data = data,
                         subset = index_training,
                         ntree = 200, importance = TRUE)

# The prediction accuracy of the random forest is summarized
model_rf
```

```
##
## Call:
##  randomForest(formula = as.factor(decision) ~ ., data = data,      ntree = 200, importance = TRUE, su
##                Type of random forest: classification
##                      Number of trees: 200
## No. of variables tried at each split: 2
##
##         OOB estimate of  error rate: 0.51%
## Confusion matrix:
##    0  1 class.error
## 0 96  1  0.01030928
## 1  0 98  0.00000000
```

The number of variables randomly selected at each split is *mtry* = 2 (as starter, the square root of total number of all predictors is used). The out-of-bag (OOB) error (= misclassification rate) is 0.516%. To fine tune a random forest model, the number of *ntree* values must be varied and plotted against the OOB rate. It is recommended selecting a mtry value with minimum OOB error, which was not done in this example.

```
# Determine variable importance
res_importance <- importance(model_rf)

print(xtable::xtable(res_importance, caption = "Results of the random forest
classification.",
label = "randomforstresults"
), comment = FALSE, caption.placement = "top")
```

Table 3: Results of the random forest classification.

| | 0 | 1 | MeanDecreaseAccuracy | MeanDecreaseGini |
|---|---|---|---|---|
| amptester_shapiro | 1.72 | 7.85 | 7.80 | 14.84 |
| amptester_lrt | 0.00 | 3.67 | 3.63 | 0.28 |
| amptester_rgt | 1.90 | -1.00 | 1.88 | 0.07 |
| amptester_tht | 1.85 | 3.61 | 4.02 | 0.57 |
| amptester_slt | 10.98 | 12.93 | 12.64 | 34.49 |
| amptester_polygon | 11.76 | 13.73 | 13.65 | 36.18 |
| amptester_slope.ratio | 1.13 | 5.56 | 5.40 | 7.79 |

The variables *MeanDecreaseAccuracy* and *MeanDecreaseGini* are used to determine the importance of the variables for a classification from a `Random Forest` model. MeanDecreaseAccuracy tells how much removing each variable reduces the accuracy of the model. Mean Decrease Gini tells how important a variable is based on the Gini impurity index used for the calculation of splits in trees. The higher the values, the more significant they are.

```
# Create a graphic device for the plot(s)
par(mfrow = c(1,3))

# Plot the properties if the Random Forest model
```

```
plot(model_rf, main = "", las = 2)
mtext("A", cex = 1, side = 3, adj = 0, font = 2, las = 0)

rownames(res_importance) <- substr(rownames(res_importance), 11, 22)

# Show the predictors sorted by their importance using MeanDecreaseAccuracy
# and MeanDecreaseGini

barplot(t(as.matrix(sort(res_importance[, "MeanDecreaseAccuracy"]))),
        ylab = "MeanDecreaseAccuracy",
        ylim = c(0, max(res_importance[, "MeanDecreaseAccuracy"]) + 5),
        main = "", las = 2, col = adjustcolor("grey", alpha.f = 0.5),
        border = "white")
mtext("B", cex = 1, side = 3, adj = 0, font = 2, las = 0)

barplot(t(as.matrix(sort(res_importance[, "MeanDecreaseGini"]))),
        ylab = "MeanDecreaseGini",
        ylim = c(0, max(res_importance[, "MeanDecreaseGini"]) + 10),
        main = "", las = 2, col = adjustcolor("grey", alpha.f = 0.5),
        border = "white")
mtext("C", cex = 1, side = 3, adj = 0, font = 2, las = 0)
```

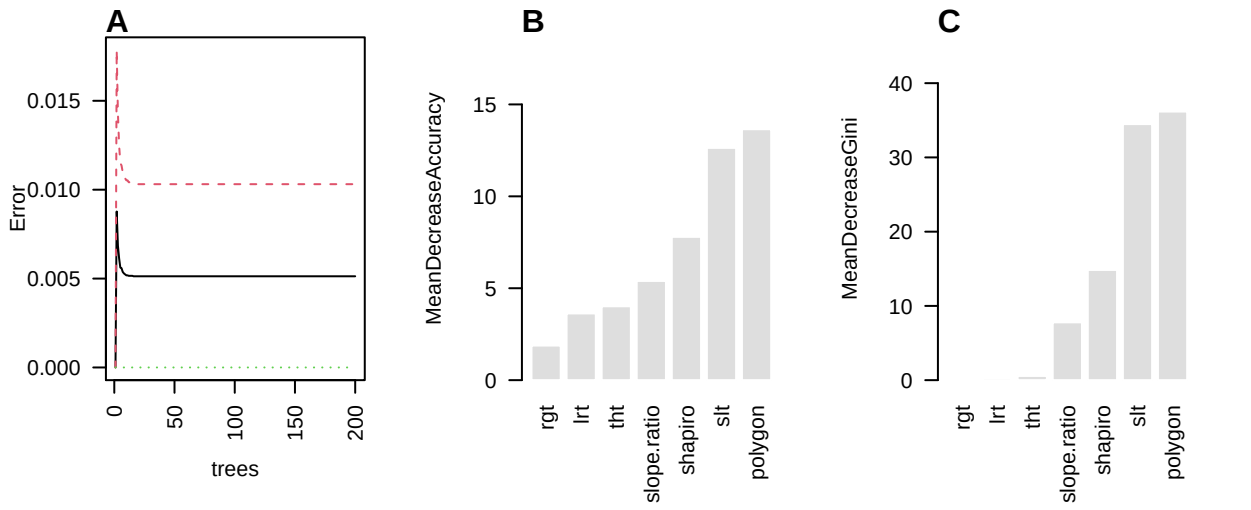


Figure 25: The predictors 'amptester_lrt' (lrt), 'amptester_rgt' (rgt), 'amptester_tht' (tht), 'amptester_slt' (slt), 'amptester_polygon'(polygon) and 'amptester_slope.ratio' (slope.ratio) were used for classification using random forest. A) This plot shows the error depending on the number of trees. The error decreases as more and more trees are added and averaged. B). Mean Decrease Accuracy shown how much the model accuracy decreases if a variable is dropped. C) Mean Decrease Gini shows the importance of a variable based on the Gini impurity index used for the calculation of splits in trees.

The top two important predictors are `polygon` (MeanDecreaseAccuracy = 13.65, MeanDecreaseGini = 36.18) and `slt` (MeanDecreaseAccuracy = 12.64, MeanDecreaseGini = 34.49).

## 3.4 Classified Amplification Curve Datasets

Amplification curves from different sources (e. g., detection chemistries, thermo-cyclers) were manually classified with the `humanrater()` function (subsubsection 3.5.1) or with the `tReem()` function (subsubsection 3.5.2). Raw amplification curve data were exported as comma separated values or in the Real-time PCR Data Markup Language (RDML) format via the `RDML` package. RDML is human readable data exchange format for qPCR experiments. A detailed description can be found in Rödiger et al. (2017). The following code section describes the import of an RDML file from the `PCRedux` package. The RDML file contains amplification curve data of a duplex qPCR (HPV 16 & HPV 18) performed in the CFX96 (Bio-Rad).

At least the following datasets with a dichotomous decision (positive, negative) are included.

- decision_res_batsch1.csv
- decision_res_batsch2.csv
- decision_res_batsch3.csv
- decision_res_batsch4.csv
- decision_res_batsch5.csv
- decision_res_boggy.csv
- decision_res_C126EG595.csv
- decision_res_C127EGHP.csv
- decision_res_C316.amp.csv
- decision_res_C317.amp.csv
- decision_res_C60.amp.csv
- decision_res_CD74.csv
- decision_res_competimer.csv
- decision_res_dil4reps94.csv
- decision_res_guescini1.csv
- decision_res_guescini2.csv
- decision_res_HCU32_aggR.csv
- decision_res_htPCR.csv
- decision_res_karlen1.csv
- decision_res_karlen2.csv
- decision_res_karlen3.csv
- decision_res_lc96_bACTXY.csv
- decision_res_lievens1.csv
- decision_res_lievens2.csv
- decision_res_lievens3.csv
- decision_res_RAS002.csv
- decision_res_RAS003.csv
- decision_res_reps2.csv
- decision_res_reps384.csv
- decision_res_reps3.csv
- decision_res_reps.csv
- decision_res_rutledge.csv
- decision_res_stepone_std.csv
- decision_res_testdat.csv
- decision_res_vermeulen1.csv
- decision_res_vermeulen2.csv
- decision_res_VIMCFX96_60.csv

```
library(RDML)
# Load the RDML package and use its functions to import the amplification curve
#  data
library(RDML)
filename <- system.file("RAS002.rdml", package = "PCRedux")
raw_data <- RDML$new(filename = filename)
```

The following example shows the export of the `RAS002.rdml` file from the RDML format to the csv format.

```
# Export the RDML data from the PCRedux package as the objects RAS002 and RAS003.
library(RDML)
library(PCRedux)

RAS002 <- data.frame(RDML$new(paste0(
    path.package("PCRedux"), "/", "RAS002.rdml"))$GetFDData()
    )

# The obbject RAS002 can be stored in the working directory as CSV file with
# the name RAS002_amp.csv.
write.csv(RAS002, "RAS002_amp.csv", row.names = FALSE)
```

| RDML data file | Device | Target gene | Detection chemistry |
|---|---|---|---|
| RAS002.rdml | CFX96 | HPV16, HPV18, HPRT1 | TaqMan |
| RAS003.rdml | CFX96 | HPV16, HPV18, HPRT1 | TaqMan |
| hookreg.rdml | Bio-Rad | various | TaqMan, DNA binding dyes |

## 3.5 Technologies for Amplification Curve Classification and Classified Amplification Curves

Many machine learning concepts exist. One method is supervised machine learning, where the goal is to derive a property from user-defined (classified) training data. Categories such as negative, ambiguous or positive are assigned depending on the form of the amplification curve. An extensive literature research showed that there are no openly accessible classified amplification curve data sets. Open Data is meant in the sense that data are freely available, free of charge, free to use and that data can be republished, without restrictions from copyright, patents or other mechanisms of control (Kitchin 2014).

Therefore, a large number of records with amplification curves and their classification (negative, ambiguous, positive) were added to the `PCRedux` package.

For the amplification curves in Table 5, a dichotomous classification was performed (roughly sigmoid or negative amplification reaction with a flat curve shape). Consequently, this does not rule out

- if an unspecific amplification product has been synthesized,
- if a contamination has been amplified or
- if only primer-dimers have been amplified.

To answer this question, other methods such as agarose gel electrophoresis need to be used.

### 3.5.1 Manual Amplification Curve Classification

For machine learning and method validation, it was important to classify the amplification curves individually. In Rödiger, Burdukiewicz, and Schierack (2015), the `humanrater()` [`chipPCR`] function was described. This function was developed to help the user during the classification of amplification curves and melting curves. The user has to define classes, which get assigned to an amplification curve after an expert has entered the class in input mask.

> By convention, class labels were specified as e. g., negative ("n"), ambiguous ("a"), positive ("y") in the `PCRedux` package.

All amplification curve data sets listed in Table 5 were classified in interactive, semi-blinded sessions. `humanrater()` [`chipPCR`] was set to randomly select individual amplification curves. All data sets were manually classified at least three times. The `htPCR` data set (Figure 4B) was classified eight times in total (see Figure 26). Most of the amplification curves are neither unequivocal classifiable as positive or negative.

Table 5: Classified amplification curve data sets. Decision data sets in `PCRedux`: table with results of manual classification as comma separated values. qPCR data set: name of original amplification curve data set. Package: name of the `R` package containing the amplification curves. Device: is the device used to measure the amplification reaction. `Note: The original data sets contain information about the detection chemistry used within the corresponding qPCR experiments.` AB, Applied Biosystems.

| Decision Datasets in PCRedux | qPCR Dataset | Package | Device |
|---|---|---|---|
| decision_res_RAS002.csv | RAS002.rdml | `PCRedux` | CFX96, Bio-Rad |
| decision_res_RAS003.csv | RAS003.rdml | `PCRedux` | CFX96, Bio-Rad |
| decision_res_batsch1.csv | batsch1 | `qpcR` | Light Cycler 1.0, Roche |
| decision_res_batsch2.csv | batsch2 | `qpcR` | Light Cycler 1.0, Roche |
| decision_res_batsch3.csv | batsch3 | `qpcR` | Light Cycler 1.0, Roche |
| decision_res_batsch4.csv | batsch4 | `qpcR` | Light Cycler 1.0, Roche |
| decision_res_batsch5.csv | batsch5 | `qpcR` | Light Cycler 1.0, Roche |
| decision_res_lc96_bACTXY.csv | lc96_bACTXY.rdml | `RDML` | Light Cycler 1.0, Roche |
| decision_res_boggy.csv | boggy | `qpcR` | Light Cycler 96, Roche |
| decision_res_C126EG595.csv | C126EG595 | `chipPCR` | Chromo4, Bio-Rad |
| decision_res_C127EGHP.csv | C127EGHP | `chipPCR` | iQ5, Bio-Rad |
| decision_res_C316.amp.csv | C316.amp | `chipPCR` | iQ5, Bio-Rad |
| decision_res_C317.amp.csv | C317.amp | `chipPCR` | iQ5, Bio-Rad |
| decision_res_C60.amp.csv | C60.amp | `chipPCR` | iQ5, Bio-Rad |
| decision_res_CD74.csv | CD74 | `chipPCR` | iQ5, Bio-Rad |
| decision_res_competimer.csv | competimer | `qpcR` | Light Cycler 480, Roche |
| decision_res_dil4reps94.csv | dil4reps94 | `qpcR` | CFX384, Bio-Rad |
| decision_res_guescini1.csv | guescini1 | `qpcR` | Light Cycler 480, Roche |
| decision_res_guescini2.csv | guescini2 | `qpcR` | Light Cycler 480, Roche |
| decision_res_htPCR.csv | htPCR | `qpcR` | Biomark HD, Fluidigm |
| decision_HCU32_aggR.csv | HCU32_aggR.csv | `PCRedux` | VideoScan |
| decision_res_karlen1.csv | karlen1 | `qpcR` | ABI Prism 7700, AB |
| decision_res_karlen2.csv | karlen2 | `qpcR` | ABI Prism 7700, AB |
| decision_res_karlen3.csv | karlen3 | `qpcR` | ABI Prism 7700, AB |
| decision_res_lievens1.csv | lievens1 | `qpcR` | ABI7300, ABI |
| decision_res_lievens2.csv | lievens2 | `qpcR` | ABI7300, ABI |
| decision_res_lievens3.csv | lievens3 | `qpcR` | ABI7300, ABI |
| decision_res_reps.csv | reps | `qpcR` | MXPro3000P, Stratagene |
| decision_res_reps2.csv | reps2 | `qpcR` | MXPro3000P, Stratagene |
| decision_res_reps3.csv | reps3 | `qpcR` | MXPro3000P, Stratagene |
| decision_res_reps384.csv | reps384 | `qpcR` | CFX384, Bio-Rad |
| decision_res_rutledge.csv | rutledge | `qpcR` | Opticon 2, MJ Research |
| decision_res_stepone_std.csv | stepone_std | `RDML` | StepOne, AB |
| decision_res_testdat.csv | testdat | `qpcR` | Light Cycler 1.0, Roche |
| decision_res_vermeulen1.csv | vermeulen1 | `qpcR` | Light Cycler 480, Roche |
| decision_res_vermeulen2.csv | vermeulen2 | `qpcR` | Light Cycler 480, Roche |
| decision_res_VIMCFX96_60.csv | VIMCFX96_60 | `chipPCR` | CFX96, Bio-Rad |
| decision_res_kbqPCR | kbqPCR | `PCRedux` | CFX96, Bio-Rad |

```
# Suppress messages and load the packages for reading the data of the classified
# amplification curves.
library(PCRedux)

# Load the decision_res_htPCR.csv data set from a csv file.
filename <- system.file("decision_res_htPCR.csv", package = "PCRedux")
decision_res_htPCR <- read.csv(filename)

# Create graphic device for the plot(s)
par(mfrow = c(2, 4))
for (i in 2L:9) {
    data_tmp <- table(as.factor(decision_res_htPCR[, i]))

    barplot(data_tmp, col = adjustcolor("grey", alpha.f = 0.5),
            xlab = "Class", ylab = "Counts", border = "white")
    text(c(0.7, 1.9, 3.1), rep(quantile(data_tmp, 0.25), 3),
         data_tmp, srt = 90)
    mtext(LETTERS[i - 1], cex = 1, side = 3, adj = 0, font = 2)
}
```

This approach is well suited and has been applied to classify a variety of amplification curves during the development of the `PCRedux` package. From experience this is time-consuming and tiring for large data sets, especially when the amplification curves are similar in shape. A high similarity between amplification curves exists, for example, in replicates and negative controls.

### 3.5.2 `tReem()` - A Function for Shape-based Group-wise Classification of Amplification Curves

The similarity of amplification curves can be used to form groups of similar shapes. The amplification curves in the groups can then be classified in bulk. In this way, a higher throughput can be achieved, a concept yet not described for the analysis of qPCR data in the literature.

The `tReem()` function was developed to perform a *shape-based group classification*. To use the `tReem()` function, the first column must contain the qPCR cycles and all subsequent columns must contain the amplification curves. Two measures of similarity are used within the `tReem()` function.

- In the first measure (default), the Pearson *correlation coefficients* ($r$) are determined in pairs for all combinations of the amplification curves. The correlation coefficient is a statistical measure to describe the strength of the correlation between two or more variables. The correlation coefficient $r$ is regarded as distance between the amplification curves. $r$ is a dimensionless value and only takes values between -1 and 1. If $r = -1$, there is a maximum reciprocal relationship. If $r = 0$ there is no correlation between the two variables. If $r = 1$, there is a maximum rectified correlation.
- In the second measure, the *Hausdorff distance* is used to determine the similarity between amplification curves. The Hausdorff distance is "the maximum of the distances from a point in any of the sets to the nearest point in the other set" (Rote 1991; Herrera et al. 2016). The amplification curves are converted within the `tReem()` function using the `qPCR2data()` function.

Both methods process the distances in the same steps. This involves the calculation of the distance matrix using the Euclidean distances of all distance measures to determine the distance between the lines of the data matrix.

This is used to perform a hierarchical cluster analysis. In the last step, the cluster is divided into groups based on a user-defined $k$ value. For example, two groups are created for $k = 2$. If the amplification curves shapes are highly diverse, a larger $k$ should be used. After a chain of processing steps presents the `tReem()` function a series of plots with grouped of amplification curves. The corresponding classes can then be assigned to the groups of amplification curves by the user using an input mask.

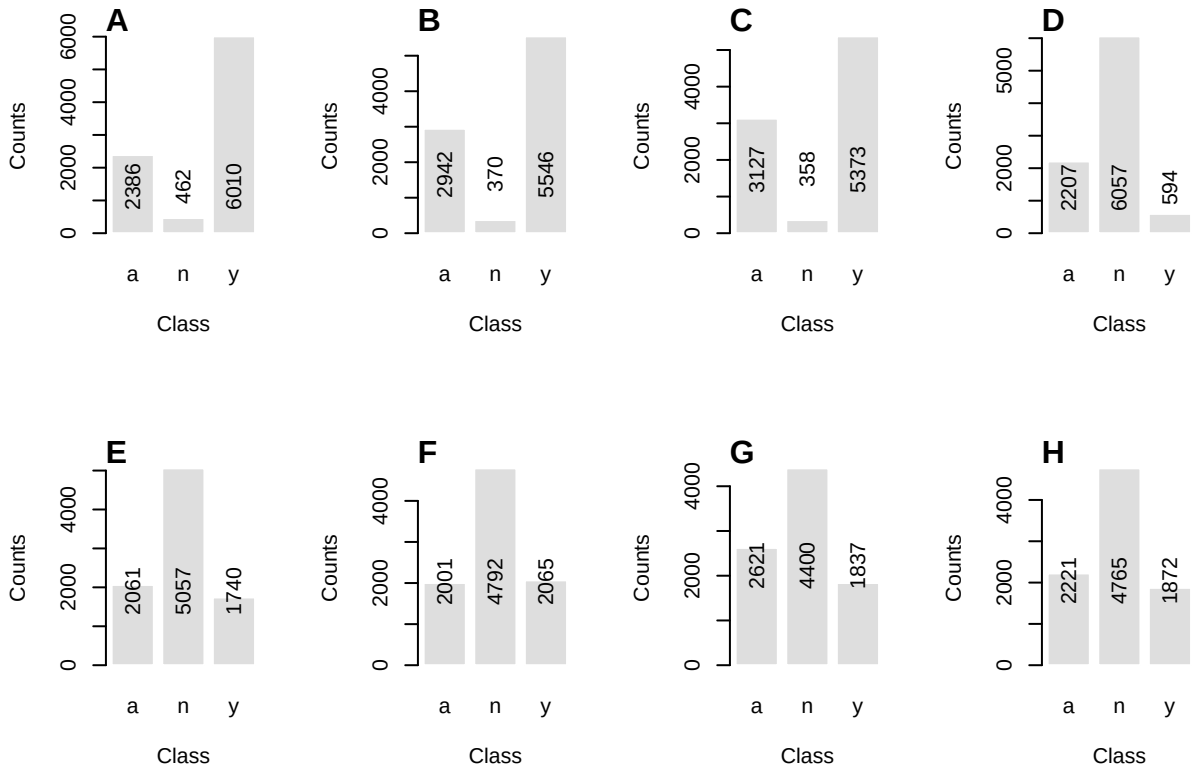


Figure 26: Variations in the classification of amplification curves. A prerequisite for the development of machine-learning models is the availability of manually classified amplification curves. Amplification curves (n = 8858) from the 'htPCR' data set have been classified by one user eight times at different points over time (classes: ambiguous (a), positive (y) or negative (n)). During this process, the amplification curves were presented in random order. The example shows that different (subjective) class mappings may occur for the same data set. While only a few amplification curves were classified as negative in the first three classification cycles (A-C), their proportion increased almost tenfold in later classification cycles (D-H).

Grouping the amplification curves with the Pearson correlation coefficient as a distance measure is usually faster than the Hausdorff distance. The Hausdorff distance is an approximation of a shape metrics to define similarity measures between shapes. (Charpiat, Faugeras, and Keriven 2003).

```
# Classify amplification curve data by correlation coefficients (r)
data <- qpcR::testdat

classification_result <- tReem(data[, 1:15], k = 3)
classification_result
```

### 3.5.3 `decision_modus()` - A Function to Get a Decision (Modus) from a Vector of Classes

For the systematic statistical analysis of classification data sets, the `decision_modus()` function has been developed. This allows the most common decision (mode) to be determined. The mode is useful to consolidate large collections of different decisions into a single (most frequent) decision.

> Observed:$a$, $a$, $a$, $a$, $a$, $n$, $n$, $n$ $\rightarrow$ frequencies 5 x $a$, 3 x $n$ $\rightarrow$ mode: $a$. Since the class names are known, they only have to be interpreted by the user (e. g., "a",$n$,"y" -> "ambivalent","negative","positive").

A manual classification was performed out for the `htPCR` data set (for an example plot Figure 4B) with the `humanrater()` function. The classification of each amplification curve was performed eight times at different time points since many of the amplification curves did not resemble optimal curvatures (e. g., Figure 1). It is likely that the amplification curve (P06.W47, Figure 1) is considered as ambiguous or even positive (positive $\leftrightarrow$ ambivalent) by the users.

Table 6 shows from a total of 8858 amplification curves the first 25 lines classified as negative (*conformity=TRUE*) and the first 25 lines classified as positive. Since in total, the curves were classified eight times (`test.result.1` ... `test.result.8`) a whole of 70864 amplification curves was analysed. In this classification experiment the amplification curves have been classified differently in 94.6% of the cases (e. g., line 1 "P01. W01").

The `decision_modus()` function was applied to the record `decision_res_htPCR.csv` with all classification rounds (columns 2 to 9) and the mode was determined for each amplitude curve Figure 27.

```
# Use decision_modus() to go through each row of all classifications done by
# a human.

# Determine the number of observations where all classifications were
# the same (conformity == TRUE).
conformity <- decision_res_htPCR[["conformity"]]

# List all classifications.
dec <- lapply(1L:nrow(decision_res_htPCR), function(i) {
    decision_modus(decision_res_htPCR[i, 2:9])[1]
}) %>% unlist()

# Show statistic of the decisions
summary(dec)
```

```
##    Min. 1st Qu.  Median    Mean 3rd Qu.    Max.    NA's
##   1.000   1.000   2.000   1.779   2.000   3.000    1179
```

Another usage mode of `decision_modus()` is to set the parameter as `max_freq=FALSE`. This option specifies the number of all classifications.

```
library(PCRedux)
# Decisions for observation P01.W06
```

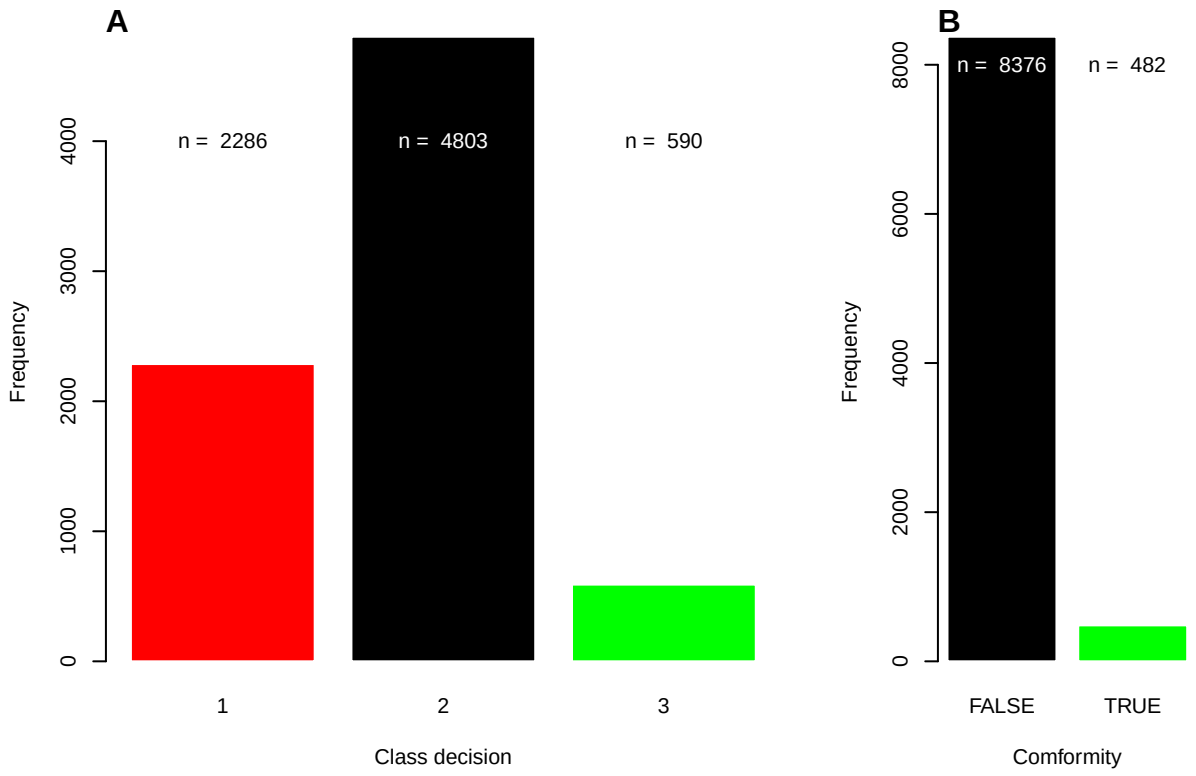


Figure 27: Frequency of amplification curve classes and conformity in the ‘htPCR‘ data set. The ‘htPCR‘ data set was classified by hand eight times. Due to the unusual amplification curve shape and input errors during classification, many amplification curves were classified differently. A) Frequency of negative (black), ambiguous (red) and positive (green) amplification curves in the ‘htPCR‘ data set. The combined number of ambiguous and negative amplification curves appears to be higher, than the number of positive amplification curves. B) The number of observations where all classification cycles made the same decision (conformity == TRUE) accounts for only 5% of the total number of observations. TRUE, all classes of the amplification curve matched. FALSE, at least one in eight observations had a different class.

Table 6: Results of the ‘htPCR‘ data set classification. All amplification curves of the ‘htPCR‘ data set were classified as ‘negative‘, ‘ambiguous‘ and ‘positive‘ by individuals in eight analysis cycles (‘test.result.1‘ ... ‘test.result.8‘). If an amplification curve was always classified with the same class, the last column (‘conformity‘) shows ‘TRUE‘. As an example, the table shows 25 amplification curves with consistent classes and 25 amplification curves with differing classes (‘conformity = FALSE‘).

| htPCR | test.result.1 | test.result.2 | test.result.3 | test.result.4 | test.result.5 | test.result.6 | test.result.7 | test.result.8 | conformity |
|---|---|---|---|---|---|---|---|---|---|
| P01.W01 | y | a | a | n | n | n | a | n | FALSE |
| P01.W02 | a | y | a | n | n | n | n | n | FALSE |
| P01.W03 | y | a | a | n | n | n | n | n | FALSE |
| P01.W04 | y | a | a | n | n | n | n | n | FALSE |
| P01.W05 | y | a | a | n | n | n | a | n | FALSE |
| P01.W06 | a | a | a | n | n | n | n | n | FALSE |
| P01.W07 | a | a | a | n | n | n | n | n | FALSE |
| P01.W08 | y | a | a | n | n | n | n | n | FALSE |
| P01.W09 | y | a | a | n | n | n | n | n | FALSE |
| P01.W10 | n | a | a | n | n | n | n | n | FALSE |
| P01.W11 | y | y | a | y | y | y | a | y | FALSE |
| P01.W12 | a | a | a | n | n | n | n | n | FALSE |
| P01.W13 | y | a | y | n | n | n | n | n | FALSE |
| P01.W14 | y | a | y | n | n | n | n | n | FALSE |
| P01.W15 | y | a | y | n | n | n | n | n | FALSE |
| P01.W16 | y | a | a | n | n | n | n | n | FALSE |
| P01.W17 | y | a | a | n | n | n | n | n | FALSE |
| P01.W18 | a | a | a | n | n | n | n | n | FALSE |
| P01.W19 | y | a | a | n | n | n | a | n | FALSE |
| P01.W20 | y | a | a | y | a | a | y | a | FALSE |
| P01.W21 | a | a | a | n | n | n | n | n | FALSE |
| P01.W22 | y | a | a | n | n | n | n | n | FALSE |
| P01.W23 | y | a | a | n | n | n | n | n | FALSE |
| P01.W24 | y | a | a | n | n | n | a | n | FALSE |
| P01.W25 | y | a | a | n | n | n | n | n | FALSE |
| P01.W58 | n | n | n | n | n | n | n | n | TRUE |
| P02.W09 | y | y | y | y | y | y | y | y | TRUE |
| P02.W19 | y | y | y | y | y | y | y | y | TRUE |
| P02.W31 | y | y | y | y | y | y | y | y | TRUE |
| P02.W41 | y | y | y | y | y | y | y | y | TRUE |
| P02.W72 | y | y | y | y | y | y | y | y | TRUE |
| P02.W81 | y | y | y | y | y | y | y | y | TRUE |
| P02.W84 | n | n | n | n | n | n | n | n | TRUE |
| P03.W09 | y | y | y | y | y | y | y | y | TRUE |
| P03.W21 | y | y | y | y | y | y | y | y | TRUE |
| P03.W22 | y | y | y | y | y | y | y | y | TRUE |
| P03.W31 | y | y | y | y | y | y | y | y | TRUE |
| P03.W32 | y | y | y | y | y | y | y | y | TRUE |
| P03.W39 | y | y | y | y | y | y | y | y | TRUE |
| P03.W56 | y | y | y | y | y | y | y | y | TRUE |
| P03.W59 | y | y | y | y | y | y | y | y | TRUE |
| P03.W68 | y | y | y | y | y | y | y | y | TRUE |
| P03.W72 | y | y | y | y | y | y | y | y | TRUE |
| P03.W73 | y | y | y | y | y | y | y | y | TRUE |
| P04.W19 | y | y | y | y | y | y | y | y | TRUE |
| P04.W31 | y | y | y | y | y | y | y | y | TRUE |
| P04.W66 | y | y | y | y | y | y | y | y | TRUE |
| P04.W81 | y | y | y | y | y | y | y | y | TRUE |
| P04.W91 | y | y | y | y | y | y | y | y | TRUE |
| P05.W20 | y | y | y | y | y | y | y | y | TRUE |

```
res_dec_P01.W06 <- decision_modus(decision_res_htPCR[
which(decision_res_htPCR[["htPCR"]] == "P01.W06"),
                                    2L:9
], max_freq = FALSE)
print(res_dec_P01.W06)
```

```
##   variable freq
## 1        a    3
## 2        n    5
```

The amplification curve `P01. W06` was classified as a=3 times and as n=5 times. Therefore, the decision would turn `negative`.

### 3.5.4 PCRedux-app

`PCRedux-app` is a web server, based on the shiny technology (Chang et al. 2019) wrapped around the `encu()` function (subsubsection 3.3.2). An user can upload qPCR data and download obtained amplification curve features.

There are different ways to use the function.

- Through `RScript` (Scripting Front-End for R):

  - Enter the command `Rscript -e 'PCRedux::run_PCRedux()'` in a console and copy the pasted URL in a browser.
- Through Graphical User Interfaces:
  - The function can be started directly in `RStudio` or `RKWard` by:

```
# run the Shiny app
PCRedux::run_PCRedux()
```

Table 7: Measures for performance analysis for binary classification. TP, true positive; FP, false positive; TN, true negative; FN, false negative

| Measure | Formula |
|---|---|
| Sensitivity - TPR, true positive rate | $TPR = \frac{TP}{TP+FN}$ |
| Specificity - SPC, true negative rate | $SPC = \frac{TN}{TN+FP}$ |
| Precision - PPV, positive predictive value | $PPV = \frac{TP}{TP+FP}$ |
| Negative predictive value - NPV | $NPV = \frac{TN}{TN+FN}$ |
| Fall-out, FPR, false positive rate | $FPR = \frac{FP}{FP+TN} = 1 - SPC$ |
| False negative rate - FNR | $FNR = \frac{FN}{TN+FN} = 1 - TPR$ |
| False discovery rate - FDR | $FDR = \frac{FP}{TP+FP} = 1 - PPV$ |
| Accuracy - ACC | $ACC = \frac{(TP+TN)}{(TP+FP+FN+TN)}$ |
| F1 score - F1 | $F1 = \frac{2TP}{(2TP+FP+FN)}$ |
| Matthews correlation coefficient - MCC | $MCC = \frac{(TP*TN-FP*FN)}{\sqrt{(TP+FP)*(TP+FN)*(TN+FP)*(TN+FN)}}$ |
| Likelihood ratio positive - LRp | $LRp = \frac{TPR}{1-SPC}$ |
| Cohen"s kappa (binary classification) | $\kappa = \frac{p_0-p_c}{1-p_0}$ |

## 3.6 Helper Functions of the `PCRedux` Package

### 3.6.1 `performeR()` - Performance Analysis for Binary Classification

Statistical modeling and machine learning are powerful but expose a risk to the user by introducing an unexpected bias. This may lead to an overestimation of the performance. The assessment of the performance by sensitivity and specificity is fundamental to characterize a classifier or screening test (G. James et al. 2013). Sensitivity is the percentage of true decisions that are identified and specificity is the percentage of negative decisions that are correctly identified (Table 7). An example for the application of the `performeR()` function is shown in subsubsection 3.3.13.

### 3.6.2 `qPCR2fdata()` - A Helper Function to Convert Amplification Curve Data to the `fdata` Format

`qPCR2fdata()` is a helper function to convert amplification curve data to the functional `fdata` class (Febrero-Bande and Oviedo de la Fuente 2012). The `fdata` format is used for functional data analysis to determine the similarity measures between amplification curves shapes by the Hausdorff distance. Similarity herein refers to the difference in spatial location of two *objects* (e. g., amplification curves). Objects with a close distance are presumably more similar. For single objects (e. g., points) one can use a vector distance, such as the Euclidean distance (Herrera et al. 2016).

The `qPCR2fdata()` function takes a `data.frame` containing the amplification cycles (first column) and the fluorescence amplitudes (subsequent columns) as input.

Noise and missing values may affect the analysis adversely. Therefore, an instance of the `CPP()` [`chipPCR`] function (Rödiger, Burdukiewicz, and Schierack 2015) was integrated in `qPCR2fdata()`. If *preprocess=TRUE* in `qPCR2fdata()`, then all curves are smoothed (Savitzky-Golay smoother), missing values are imputed and outliers in the ground phase get removed as described in Rödiger, Burdukiewicz, and Schierack (2015).

The following example illustrates a hierarchical cluster analysis of the `testdat` data set. The amplification curves of the `testdat` data set remained as raw data or were preprocessed (smoothed). Subsequent, the amplification curves were converted by the `qPCR2fdata()`. The converted data were subjected to cluster analysis (Hausdorff distance). This method uses the elements of a proximity matrix to generate a dendrogram. The dendrogram can then be used to further analyze the clusters. There are methods to determine the number of clusters automatically $k$ (Cook and Swayne 2007). However, for simplicity, the number of clusters was determined visually.

```
# Calculate the Hausdorff distance of the amplification curves
# cluster the curves.
# Load additional packages for data and pipes.
library(fda.usc)

data <- qpcR::testdat

# Convert the qPCR data set to the fdata format
# Use unprocessed data from the testdat data set
res_fdata <- qPCR2fdata(data)

# Extract column names and create rainbow color to label the data
columnames <- data[-1] %>% colnames(.)
colors <- rainbow(length(columnames), alpha = 0.5)

# Calculate the Hausdorff distance (fda.usc) package and plot the distances
# as clustered data.

res_fdata_hclust <- metric.hausdorff(res_fdata)
res_hclust <- hclust(as.dist(res_fdata_hclust))
```

The distance based on the Hausdorff metric was already calculated in the next steps involving the `cutree()` [`stats`] function to split the dendrogram into smaller junks. *A priori* it was defined that two classes (*positive* & *negative*) are expected. Therefore, the *group* parameter was set to $k$=2 in the `cutree()`.

```
# Cluster of the unprocessed amplification curves
res_cutree <- cutree(res_hclust, k = 2)
res_cutree <- factor(res_cutree)
levels(res_cutree) <- list(y = "1", n = "2")
```

The dendrogram shows that

- the observations are correctly assigned to a cluster of positive or negative amplification curves and that
- the shift of the Cq (late increase of the fluorescence) is reflected in the positive cluster (Figure 28).

```
# Plot the converted qPCR data
# Create graphic device for the plot(s)
par(mfrow = c(1, 2))

plot(res_fdata, xlab = "Cycles", ylab = "RFU", main = "", type = "l",
        lty = 1, lwd = 2, col = colors
)
legend(
    "topleft", paste0(as.character(columnames), ": ", res_cutree),
       pch = 19, col = colors, bty = "n", ncol = 2, cex = 0.7
)
mtext("A", cex = 1, side = 3, adj = 0, font = 2)

plot(res_hclust, main = "", xlab = "", sub="")
text(c(5.5,18), rep(6.5,2), c("negative", "positive"),
     col = c("black", "green"), cex = 0.9, srt = 90)
mtext("B", cex = 1, side = 3, adj = 0, font = 2)
```

This workflow can be used to cluster amplification curve data according to similar shape. Classification tasks can be preformed in batches of amplification curves. The calculation of the distances is a computation expensive step dependent on the number of amplification curves.

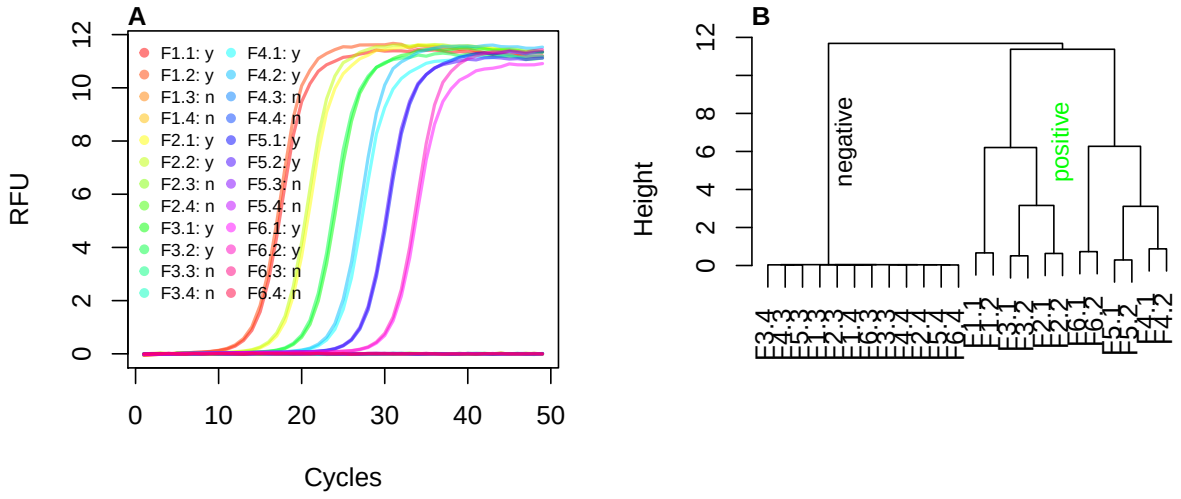


Figure 28: Shape-based clustering of amplification curves. A) The clustering of the amplification curves of the 'testdat' data set (A) was based on the Hausdorff distance. B) The amplification curves were converted with the qPCR2fdata() function, and the Hausdorff distance of the curves was determined by cluster analysis. There were no errors in distinguishing between negative (n) and positive (y) amplification curves.

The following example illustrates the usage for the `HCU32_aggR.csv` data set from the VideoScan platform with 32 heating and cooling units (equivalent of 32 PCR vessels). In this experiment, the bacterial gene *aggR* from *E. coli* was amplified in 32 replicate qPCR reactions. Details of the experiment are described in the manual of the `PCRedux` package. The ambition was to test if the 32 amplification curves of the qPCR reaction are identical. As before, the data were processed with the `qPCR2fdata()` function and compared by the Hausdorff distance. Ideally, the amplification curves form only few clusters.

```
# Calculate slope and intercept on positive amplification curve data from the
# VideoScan 32 cavity real-time PCR device.
# Use the fda.usc package for functional data analysis
library(fda.usc)

# Load the qPCR data from the HCU32_aggR.csv data set
# Convert the qPCR data set to the fdata format

filename <- system.file("HCU32_aggR.csv", package = "PCRedux")
data_32HCU <- read.csv(filename)

res_fdata <- qPCR2fdata(data_32HCU)
# Extract column names and create rainbow color to label the data
columnames <- data_32HCU[-1] %>% colnames(.)
colors <- rainbow(length(columnames), alpha = 0.55)
```

In advance the Cq values were calculated by the following code:

```
# Load the qpcR package to calculate the Cq values by the second derivative
# maximum method.
library(qpcR)
```

```
res_Cq <- sapply(2L:ncol(data_32HCU), function(i) {
    efficiency(pcrfit(data_32HCU, cyc = 1, fluo = i, model = l6))
})

data.frame(
    obs = colnames(data_32HCU)[-1],
           Cq = unlist(res_Cq["cpD2", ]), eff = unlist(res_Cq["eff", ])
)

#        Results
#
# obs    Cq      eff
# 1      A1 14.89 1.092963
# 2      B1 15.68 1.110480
# 3      C1 15.63 1.111474
# ...
# 30     F4 15.71 1.109634
# 31     G4 15.70 1.110373
# 32     H4 15.73 1.117827
```

Next, the amplification curves (Figure 29A), the differences between base-line region and plateau region (Figure 29B), the correlation between the Cq value and amplification efficiency (Figure 29C) and the clusters based on the Hausdorff distance were taken into account.

Some amplification curves (Figure 29A) had stronger noise, and all curves exhibited a negative non-linear trend and shift in the ground phase. The comparison of the ground phase and the plateau phase showed a difference between the 32 amplification curves. The observations `E1`, `F1` and `H1` were most close in the ground and plateau phase. The comparison of Cq values and amplification efficiency showed that most amplification curves are similar. However, there are also amplification curves that show a greater deviation from the median of all Cq values (Figure 29C). The cluster analysis confirmed the shape similarity (Figure 29D).

```
# Use the fda.usc package for functional data analysis
library(fda.usc)

# To save computing time, the Cq values and amplification efficiencies were
# calculated beforehand and transferred as a hard copy here.

calculated_Cqs <- c(
    14.89, 15.68, 15.63, 15.5, 15.54, 15.37, 15.78, 15.24, 15.94,
    15.88, 15.91, 15.77, 15.78, 15.74, 15.84, 15.78, 15.64, 15.61,
    15.66, 15.63, 15.77, 15.71, 15.7, 15.79, 15.8, 15.72, 15.7, 15.82,
    15.62, 15.71, 15.7, 15.73
)

calculated_effs <- c(
    1.09296326515231, 1.11047987547324, 1.11147389307153, 1.10308929700635,
    1.10012176315852, 1.09136717687619, 1.11871308210321, 1.08006168654712,
    1.09500422011318, 1.1078777171126, 1.11269436700649, 1.10628580163733,
    1.1082009954558, 1.11069683827291, 1.11074914659374, 1.10722949813473,
    1.10754282514113, 1.10098387264025, 1.1107026749644, 1.11599641663658,
    1.11388510347017, 1.11398547396991, 1.09410798249025, 1.12422338092929,
    1.11977386646464, 1.11212436173214, 1.12145338871426, 1.12180879952503,
    1.1080276005651, 1.10963449004393, 1.11037302758388, 1.11782689816295
)
```

```
# Plot the converted qPCR data
# Create graphic device for the plot(s)

layout(matrix(c(1, 2, 3, 4, 4, 4), 2, 3, byrow = TRUE))


plot(res_fdata, xlab = "Cycles", ylab = "RFU", main = "HCU32_aggR", type = "l",
         lty = 1, lwd = 2, col = colors)

legend("topleft", as.character(columnames), pch = 19, col = colors,
       bty = "n", ncol = 4)
mtext("A", cex = 1, side = 3, adj = 0, font = 2)

# Plot the background and plateau phase.

boxplot(
    data_32HCU[, -1] - apply(data_32HCU[, -1], 2, min),
        col = colors, las = 2, main = "Signal to noise ratio",
        xlab = "Sample", ylab = "RFU"
)
mtext("B", cex = 1, side = 3, adj = 0, font = 2)

# Plot the Cqs and the amplification efficiencies.
# Determine the median of the Cq values and label all Cqs, which a less 0.1 Cqs
# of the median or more then 0.1 Cqs of the median Cq.

plot(
    calculated_Cqs, calculated_effs, xlab = "Cq (SDM)",
     ylab = "eff", main = "Cq vs. Amplification Efficiency",
     type = "p", pch = 19, lty = 1, lwd = 2, col = colors
)

median_Cq <- median(calculated_Cqs)
abline(v = median_Cq)

text(median_Cq + 0.01, 1.085, expression(paste(tilde(x))))
labeled <- c(
    which(calculated_Cqs < median_Cq - 0.1),
             which(calculated_Cqs > median_Cq + 0.1)
)

text(
    calculated_Cqs[labeled], calculated_effs[labeled],
     as.character(columnames)[labeled]
)
mtext("C", cex = 1, side = 3, adj = 0, font = 2)

# Calculate the Hausdorff distance using the fda.usc package and cluster the
# the distances.

res_fdata_hclust <- metric.hausdorff(res_fdata)
cluster <- hclust(as.dist(res_fdata_hclust))
```

```
# plot the distances as clustered data and label the leafs with the Cq values
# and colored dots.

plot(cluster, main = "Clusters of the amplification\n
curves as calculated by the Hausdorff distance", xlab = "", sub="")
mtext("D", cex = 1, side = 3, adj = 0, font = 2)
```

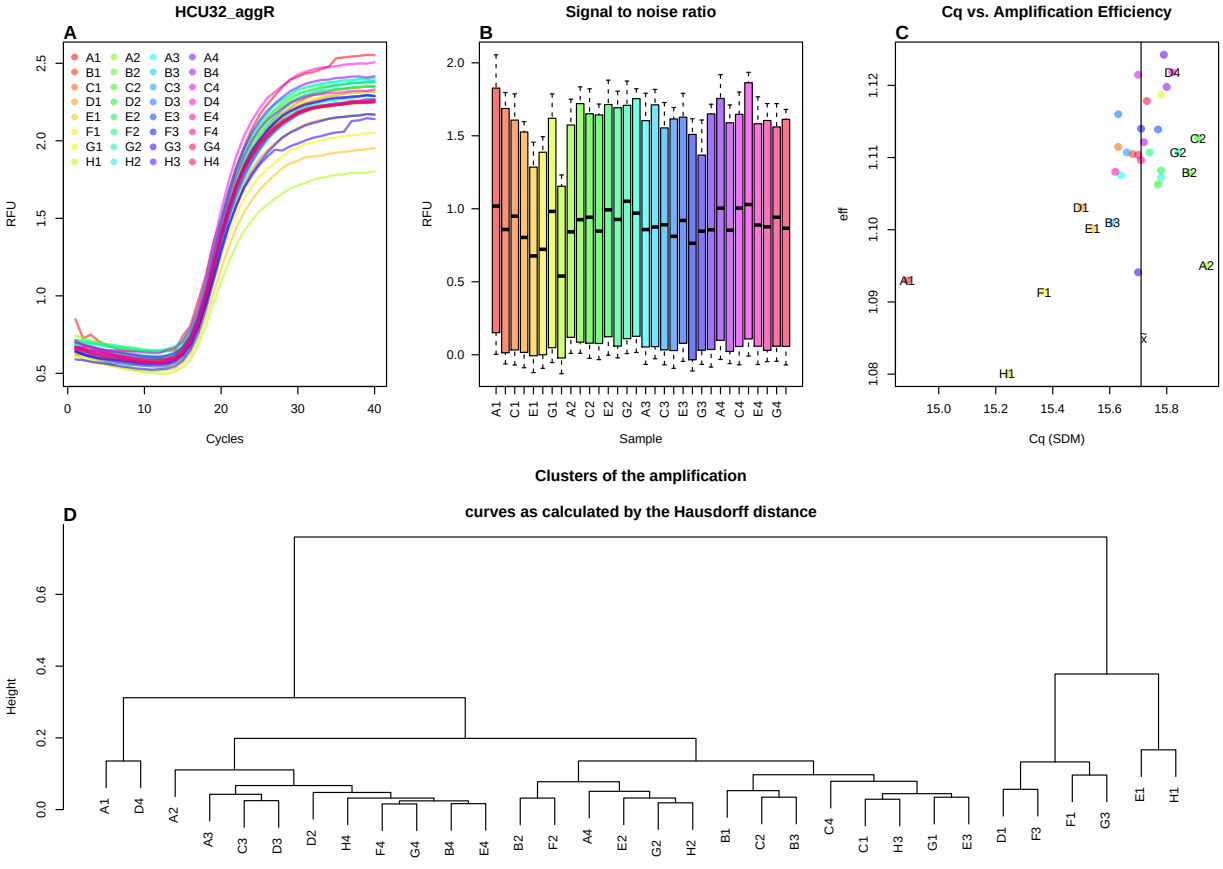


Figure 29: Clustering and variation analysis of amplification curves. The amplification curves of the 32HCU were processed with the qPCR2fdata() function and then processed by cluster analysis (Hausdorff distance). A) Amplification curves were plotted from the raw data. B) Overall, signal-to-noise ratios of the amplification curves between all cavities were similar. C) The Cq values and amplification efficiency were calculated using the efficiency(pcrfit()) [qpcR] function. The median Cq is shown as a vertical line. Cqs greater or less than 0. 1 of Cq $\tilde{x}$ are marked with observation labels. D) The cluster analysis showed no specific pattern with respect to the amplification curve signals. It appears that the observations D1, E1, F1, F3, G3 and H1 differ most from the other amplification curves.

The analysis gives an overview on the variation of the amplification curve data.

# 4 Case study for the application of the PCRedux package

In this case study we used 400 amplification curves from the *kbqPCR* dataset from and assign them to the object *curves*. Before we start we need to load additional libraries (some from CRAN, some from github.com).

```
library(qpcR)
library(PCRedux)

library(dplyr)
library(forcats)
library(reshape2)

library(mlr)
library(ranger)

library(ggplot2)

if("devtools" %in% rownames(installed.packages()) == FALSE) {
  library(devtools)
}

if("gbm" %in% rownames(installed.packages()) == FALSE) {
  install.packages("gbm")
}

if("patchwork" %in% rownames(installed.packages())) {
  library(patchwork)
} else {
  devtools::install_github("thomasp85/patchwork")
  "patchwork" %in% rownames(installed.packages())
  library(patchwork)
}
```

For the example qPCR data from a real experiment with a CFX96 (Bio-Rad) were used. It is an allelic specific PCR with TaqMan probes (FAM, HEX, ROX, Cy5, Cy5-5) (experimental details are described in Romaniuk et al. (2019). Original pcrd and rdml files are here: https://github.com/kablag/AScall/tree/master/examples

```
# Determine the Number of amplification curves
curves <- ncol(kbqPCR)

paste("Number of amplification curves:", curves - 1)
```

```
## [1] "Number of amplification curves: 400"
```

The decision of the classes (negative, ambiguous, positive) were taken from the `decision_res_kbqPCR.rda` of the *PCRedux* package.

```
dec <- unlist(lapply(1L:(curves -1), function(i) {
  decision_modus(decision_res_kbqPCR[i, 2:8])
}))

class <- c(y = sum(dec == "y"), a = sum(dec == "a"), n = sum(dec == "n"))

# Plot the classes
barplot(table(dec), col = c("green", "red", "grey"),
        main = "Frequency of Classes assed by a Human")
legend("topright", c("y: positive", "n: negtive", "a: ambigous"))
```

```
text(c(1:3), rep(150,3), class[c(1,3,2)])
```

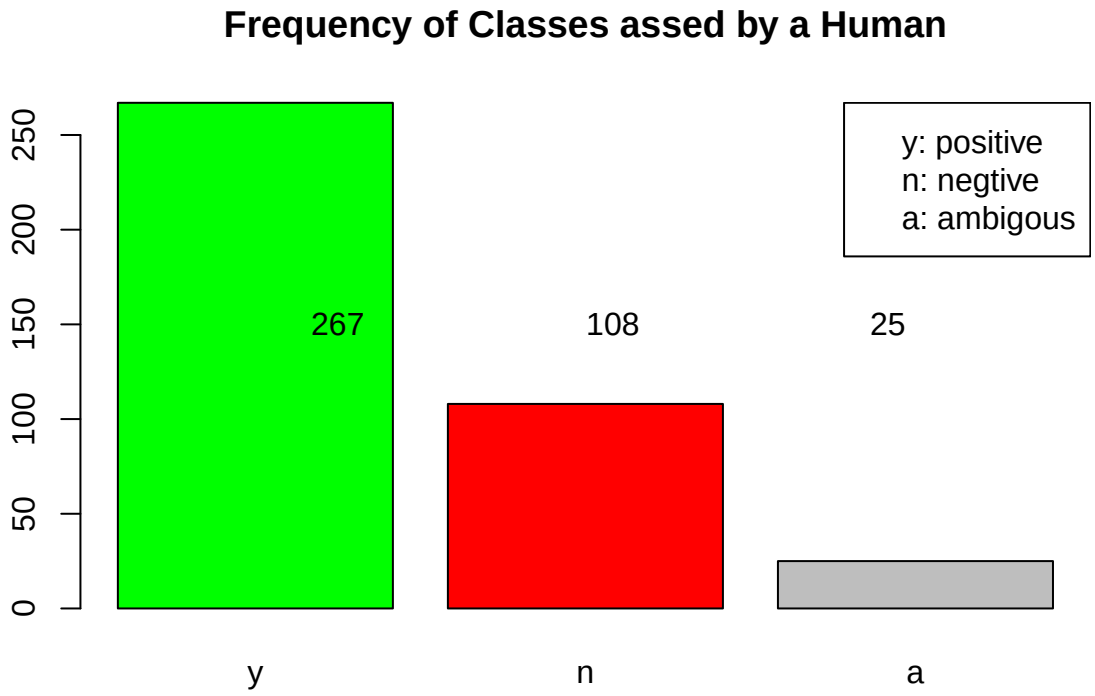


## 4.1 Visualizng qPCR curves separated as positive, negative and ambigous Amplification Curves

As a definition for a positive amplification curve, it is assumed that it has a sigmoid shape and a good signal-to-noise ratio. An ambiguous amplification curve has a signal that is above the noise level but has no sigmoid form. In this example, the ambiguous amplification curves are almost linear and do not show a plateau. Negative amplification curves do not achieve a high signal and do not show a sigmoid curve.

```
p1_pos <- data.frame(kbqPCR[, c(1L, which(dec == "y") + 1)]) %>%
  melt(id.vars = "cyc") %>%
  ggplot(aes(x = cyc, y = value, color = variable)) +
  geom_line() +
  theme_bw() +
  xlab("Cycle") +
  ylab("Raw RFU") +
  ggtitle(paste0("A) positive, ", "n = ", class[1])) + #qPCR curves
  theme(legend.position = "none")

# Positive Curves
p1_pos
```

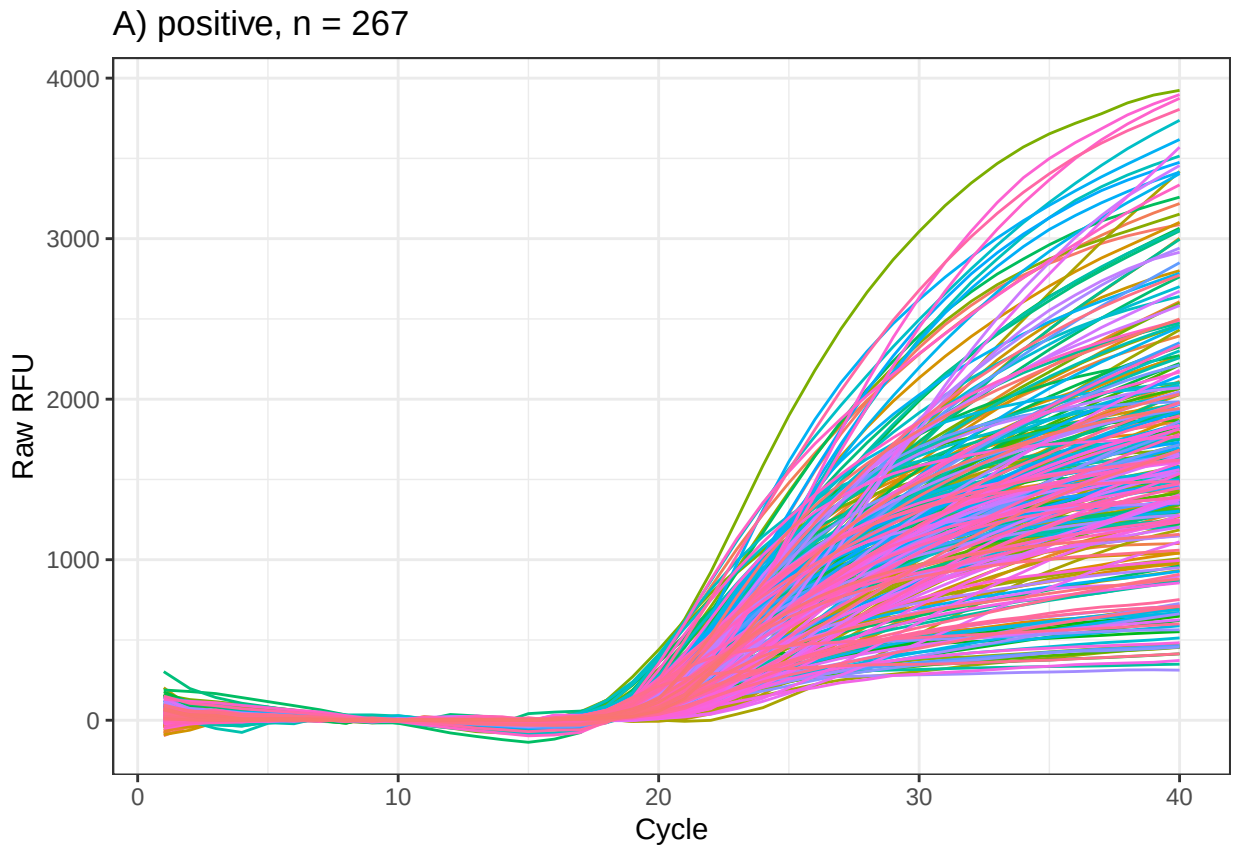


```
p1_neg <- data.frame(kbqPCR[, c(1L, which(dec == "n") + 1)]) %>%
  melt(id.vars = "cyc") %>%
  ggplot(aes(x = cyc, y = value, color = variable)) +
  geom_line() +
  theme_bw() +
  xlab("Cycle") +
  ylab("Raw RFU") +
  ggtitle(paste0("negative, ", "n = ", class[3])) + #qPCR curves
  theme(legend.position = "none")

# Negative Curves
p1_neg
```

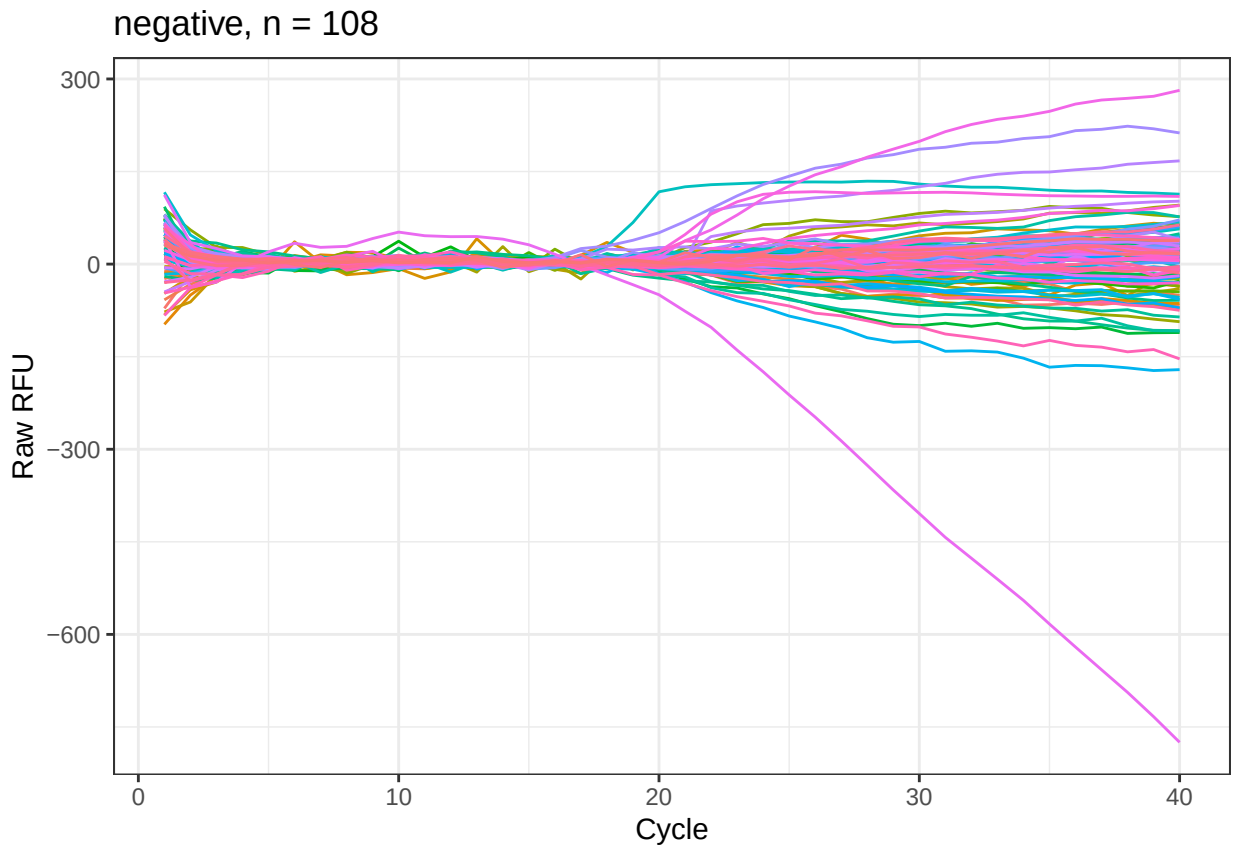


```
p1_amb <- data.frame(kbqPCR[, c(1L, which(dec == "a") + 1)]) %>%
  melt(id.vars = "cyc") %>%
  ggplot(aes(x = cyc, y = value, color = variable)) +
  geom_line() +
  theme_bw() +
  xlab("Cycle") +
  ylab("Raw RFU") +
  ggtitle(paste0("ambiguous, ", "n = ", class[2])) + #qPCR curves
  theme(legend.position = "none")

# Ambiguous Curves
p1_amb
```

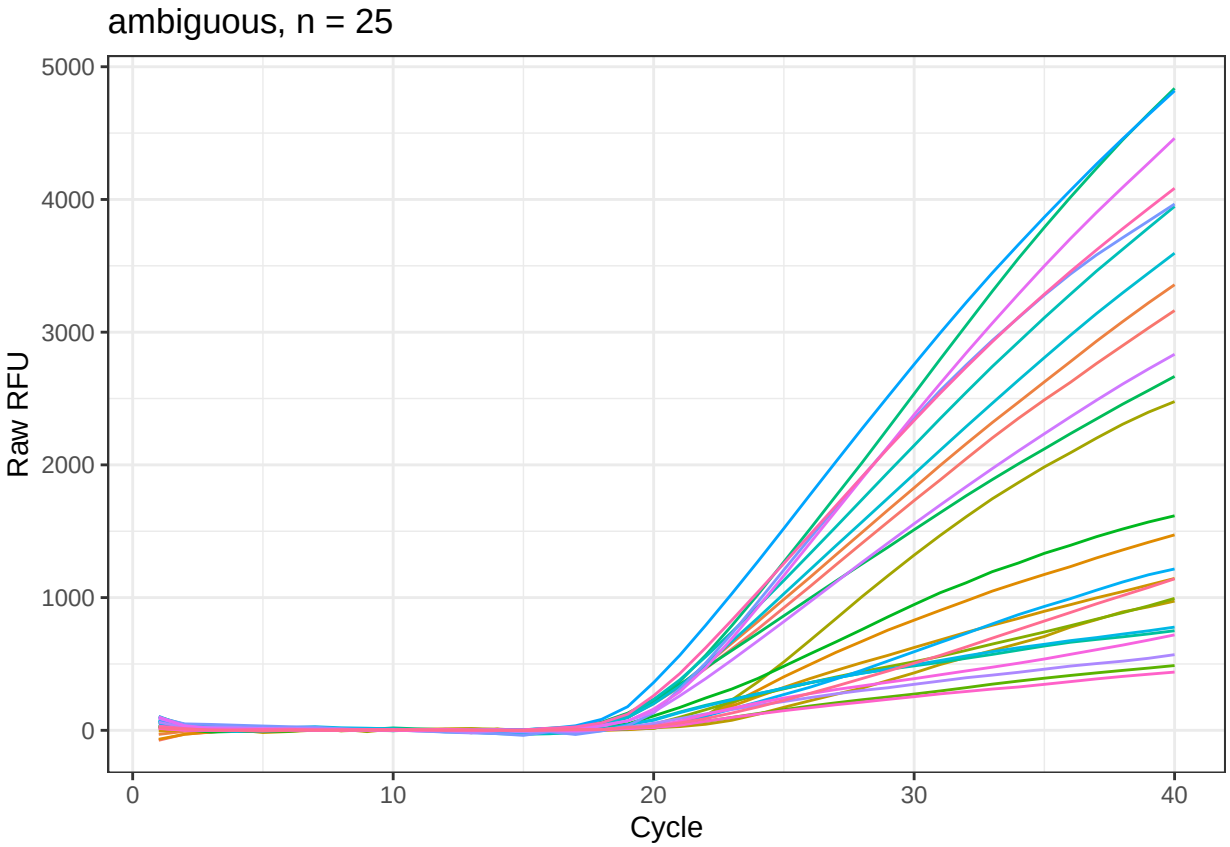


## 4.2 Calculating some parameters with the encu() function

The *encu()* function was used to calculate some parameters that are later used for the machine learning. Please be patient, this step will take some time.

```
res <- encu(kbqPCR[, 1L:curves])


head(res)
```

```
##                   runs  cpD1  cpD2 cpD2_approx cpD2_ratio      eff   sliwin
## 1    A01_p949_unkn_B2m 23.88 20.21    19.48311   1.037309 1.549925 1.191533
## 2  A01_p949_unkn_HA1_G 25.54 21.65    20.68362   1.046722 1.465490 1.835884
## 3  A01_p949_unkn_HA2_C 25.08 20.72    19.94307   1.038957 1.446608 1.923550
## 4 A01_p949_unkn_HER2_C 26.63 21.02    19.27053   1.090785 1.389097 1.083815
## 5 A01_p949_unkn_UTA2_T  0.00  0.00    21.85187   0.000000 0.000000 0.000000
## 6    A02_p949_unkn_B2m 22.36 19.37    18.48386   1.047941 1.637958 1.604790
##   cpDdiff loglin_slope cpD2_range top     f.top tdp     f.tdp bg.stop amp.stop
## 1    3.67    124.12115   6.564496  20 191.99698  30 1246.6052       9       35
## 2    3.89    232.87039   8.559779  18  88.30540  31 2517.3868      11       37
## 3    4.36    134.16144   7.122306  18  79.19799  29 1247.2282      10       36
## 4    5.61     94.29129  17.369068  20 175.74303  26  761.1615      11       32
## 5    0.00      0.00000   0.000000   0   0.00000  10    0.0000       5       40
## 6    2.99    123.83743   6.926792  17  55.05066  33 1278.1321       9       34
##      b_slope b_model_param c_model_param d_model_param e_model_param
## 1 -6.2669793    -5.9161291    -34.811525    1423.07220  4.856655e+00
## 2 -5.6178685    -5.4983218    -14.321637    3252.50156  1.182525e+01
```

```
## 3 -6.1404228    -6.1404228     17.813412    1429.67094  5.041502e+00
## 4 -3.2357222    -3.4137014    -24.572206    2433.98797  1.946989e+00
## 5 -0.3310897    -0.6547394  -8170.293866      65.80403  3.057075e-05
## 6 -6.7551476    -6.7551476     -7.633401    1383.39497  1.590588e+01
##   f_model_param  f_intercept k1_model_param k2_model_param convInfo_iteratons
## 1  10188.930930 12943.148321      1.1699973     0.08206191               387
## 2     59.059521    35.121106      0.5867746     0.05108700                84
## 3  13061.109729 13061.109729     -7.9001443     0.45594034               392
## 4   7662.295671  7815.746183     -1.5621517    -0.03899956               438
## 5     14.657164    10.353329     -5.3452465     0.02843339               978
## 6      8.452845     8.452845      1.2014996    -0.05736885                21
##   qPCRmodel qPCRmodelRF    minRFU      maxRFU      init2     fluo  slope_bg
## 1        l6          l7 -75.27223 1479.531956 0.02982747 209.3124 22.862132
## 2        l6          l7 -24.67726 3074.970854 0.11889888 466.3456  7.811147
## 3        l7          l7 -24.19175 1778.188143 0.11792800 247.7927  8.184786
## 4        l5          l7 -77.62262 1905.960553 0.24571796 245.8530 21.596083
## 5        l6          l7 -70.73830    4.869188 0.00000000   0.0000 15.781006
## 6        l7          l7 -12.98617 1315.806466 0.01441520 204.1098  4.135943
##   intercept_bg  sigma_bg       sd_bg head2tail_ratio mblrr_slope_pt
## 1   -100.17801 20.426454 0.028918879   -0.0071145854    24.94996119
## 2    -32.80573  7.019530 0.004293875   -0.0004162518    66.90746429
## 3    -33.53280  7.005349 0.005606004   -0.0013589145    46.47908239
## 4    -91.05474 24.955829 0.018320342   -0.0028962469    71.76004904
## 5    -67.18670 19.505107 0.000000000    0.0852400718     0.02638925
## 6    -16.52044  5.418389 0.005579370   -0.0005963721     5.22164784
##   mblrr_intercept_bg mblrr_slope_bg mblrr_cor_bg mblrr_intercept_pt
## 1          -9.012464      0.5321502            0        508.8259860
## 2           1.913971     -0.4062244            0        467.6648281
## 3          -6.771171      0.3759428            0        -46.5619771
## 4         -11.520993     -1.3225894            0       -914.8416511
## 5         -71.764671      0.2040505            0          0.5649513
## 6          -8.162882      0.3645041            0       1113.5585068
##   mblrr_cor_pt  polyarea peaks_ratio autocorrelation cp_e.agglo cp_bcp
## 1    0.9836875  5990.232  0.04577561       0.7546165          6      5
## 2    0.9816597 19110.654  0.01194417       0.7696127          6      6
## 3    0.9949512 10937.785  0.01037196       0.7908715          8      6
## 4    0.9990859 13693.926  0.62566786       0.8256833          6      6
## 5    0.0000000 -1300.574  1.63584385       0.8155676          5      4
## 6    0.9085009  3627.553  0.05106900       0.7119473          6      4
##   amptester_shapiro amptester_lrt amptester_rgt amptester_tht amptester_slt
## 1                 0             1             0             1             1
## 2                 0             1             0             1             1
## 3                 0             1             0             1             1
## 4                 0             1             1             1             1
## 5                 0             1             0             0             0
## 6                 0             1             1             1             1
##   amptester_polygon amptester_slope.ratio hookreg_hook hookreg_hook_slope
## 1      1.073298e+03            0.00000000            0           0.000000
## 2      2.037422e+03            0.00000000            0           0.000000
## 3      1.177453e+03            0.00000000            0           0.000000
## 4      1.128750e+03            0.00000000            0           0.000000
## 5      1.820168e-30            0.02344791            1          -3.047887
## 6      1.089792e+03            0.00000000            0           0.000000
##   hookreg_hook_delta central_angle number_of_cycles direction   range
```

```
## 1                 0     0.9988255              40         0 1554.80
## 2                 0     0.9994483              40         0 3099.65
## 3                 0     0.9986950              40         0 1802.38
## 4                 0     0.9901146              40         0 1983.58
## 5                27     0.0000000              40         1   75.61
## 6                 0     0.9986867              40         0 1328.79
##   polyarea_trapz        cor res_coef_pcrfit.b res_coef_pcrfit.c
## 1      21454.867  0.9366782         -8.750195         -22.35391
## 2      40741.685  0.9222086         -8.818435         -21.14469
## 3      23543.895  0.9304190         -7.760207         -20.86382
## 4      22560.189  0.9249606         -6.454944         -38.87111
## 5      -1046.235 -0.7821276          0.000000           0.00000
## 6      21793.258  0.9348263        -10.008578         -11.08716
##   res_coef_pcrfit.d res_coef_pcrfit.e   fitAIC fitIter segment_x segment_U1.x
## 1          1463.234          24.51221 399.9267       8         0            0
## 2          3094.805          26.20812 419.8412       8         0            0
## 3          1779.390          25.93003 416.2635       9         0            0
## 4          2036.645          27.94828 437.9552      10         0            0
## 5             0.000           0.00000   0.0000       0         0            0
## 6          1310.153          22.81194 345.2181       9         0            0
##   segment_U2.x segment_psi1.x segment_psi2.x sumdiff     poly_1    poly_2
## 1            0              0              0   0.800  553.95107 3606.3019
## 2            0              0              0   0.825 1056.93059 7115.2729
## 3            0              0              0   0.825  610.72001 4060.3402
## 4            0              0              0   0.750  587.26736 4103.7777
## 5            0              0              0   0.500  -27.67874 -133.2859
## 6            0              0              0   0.825  561.12319 3387.9028
##      poly_3      poly_4 window_Win_1 window_Win_2 window_Win_3 window_Win_4
## 1  872.9966  -746.20457    31.469059    0.6618874    1.4004229     2.263783
## 2 2369.6976 -1180.25015    11.219640    1.1038951    0.1986875     2.278015
## 3 1264.2151  -675.50249    10.914128    0.5829170    0.6424087     1.999203
## 4 1496.8162  -428.59920    31.331992    1.6589245    7.6713223    12.141069
## 5  -69.0824    64.70451    22.544336    0.5879814    0.3897482     1.367281
## 6  540.7952  -969.16711     6.208302    0.3473472    3.1325450     2.094407
##   window_Win_5 window_Win_6 window_Win_7 window_Win_8 window_Win_9
## 1    74.141602   167.063084   115.901699    61.129190    34.681545
## 2    76.144784   289.470520   290.942723   176.605525    93.690913
## 3    60.702949   174.703625   138.601431    84.863156    60.275200
## 4    71.981947   151.001317   126.597415   104.919691    85.713717
## 5     2.566092     6.130375     5.363068     2.756653     1.913734
## 6   111.802498   166.808714    92.466952    35.387147    11.491093
##   window_Win_10  sd_plateau detection_chemistry device
## 1    19.1112751 0.061779055                  NA     NA
## 2    52.4553746 0.067908059                  NA     NA
## 3    44.7725891 0.103778422                  NA     NA
## 4    76.6477174 0.185181365                  NA     NA
## 5     0.2712679 5.435171019                  NA     NA
## 6     2.8569137 0.008734311                  NA     NA
```

## 4.3 Merging decisions and features into one dataset

Since the parameters from the calculations with the *encu()* function and the decisions are known by now, we can merge them into a single dataframe.

```
dat <- cbind(res, decision = factor(c("ambiguous", "negative", "positive")[dec],
                                    levels = c("positive", "ambiguous", "negative"))) %>%
  select(cpD2, amptester_polygon, cpDdiff, decision) %>%
  filter(!is.na(dec))

head(dat)
```

```
##    cpD2 amptester_polygon cpDdiff  decision
## 1 20.21      1.073298e+03    3.67 ambiguous
## 2 21.65      2.037422e+03    3.89 ambiguous
## 3 20.72      1.177453e+03    4.36 ambiguous
## 4 21.02      1.128750e+03    5.61 ambiguous
## 5  0.00      1.820168e-30    0.00  negative
## 6 19.37      1.089792e+03    2.99 ambiguous
```

## 4.4 Visualizing the parameter calculations

Next we visualize the results of the parameter calculations.

```
p2 <- ggplot(data = dat %>%
               mutate(id = rownames(dat)) %>%
               melt(id.vars = c("id", "decision")),
             aes(x = decision, y = value)) +
  geom_boxplot() +
  theme_bw() +
  facet_wrap(~ variable, scales = "free_y") +
  scale_y_continuous("Value [A.U.]") +
  scale_x_discrete("Assessment") +
  ggtitle("B)") # Separation of types of curves by encu() parameters

p2
```

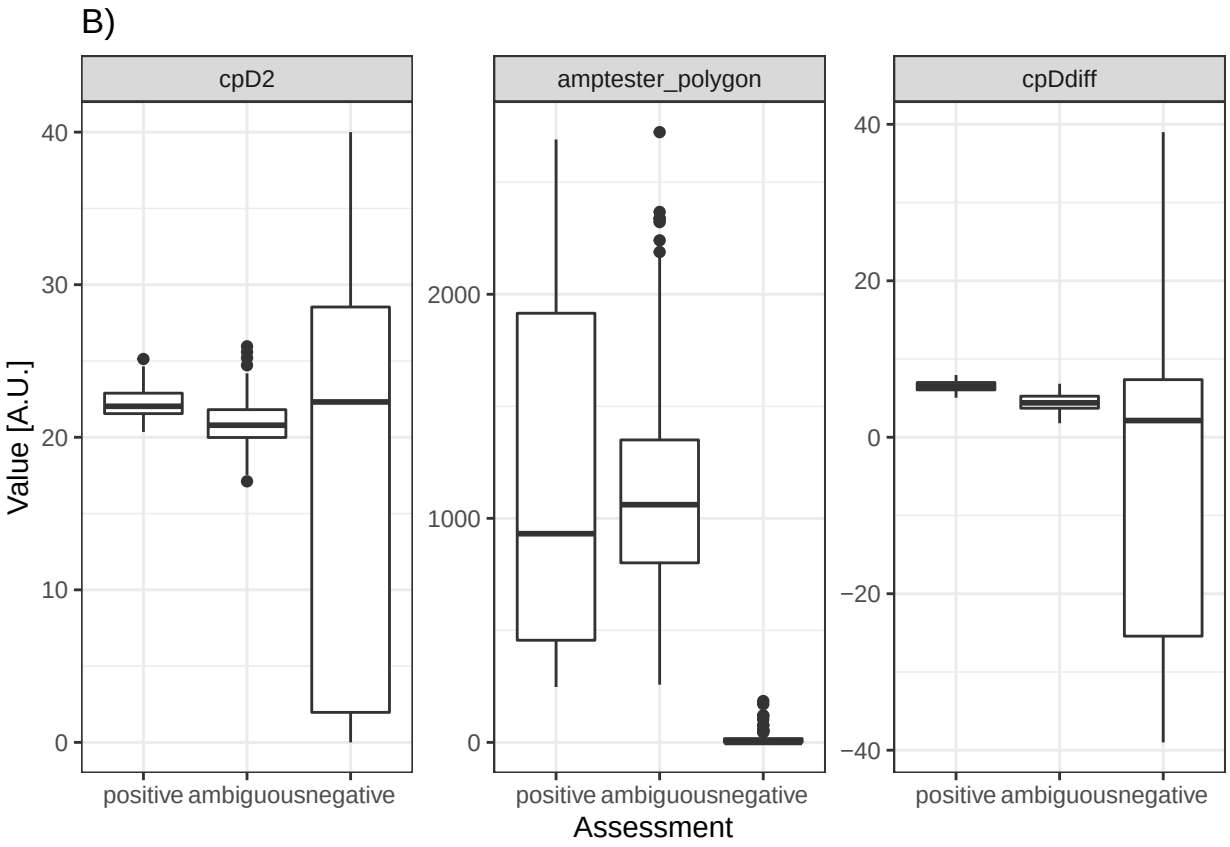


## 4.5 Modeling with different classifiers

Building the models follows the typical steps involving the definition of the splits, classifiers and their tasks. Here we use the *mlr* package. We want to classify only! As classifiers we use:

- Random Forest (classif.ranger),
- Support Vector Machines (classif.ksvm),
- linear discriminant analysis (classif.lda),
- Generalized Boosted Regression Models (classif.gbm),
- Multinomial Regression (classif.multinom) and
- Generalized Linear Regression with Lasso or Elasticnet Regularization (classif.glmnet).

```
tsk <- makeClassifTask("pcr_classif", data = dat, target = "decision")

mdls <- list()
mdls[[1]] <- makeLearner("classif.ranger", predict.type = "prob")
mdls[[2]] <- makeLearner("classif.ksvm", predict.type = "prob")
mdls[[3]] <- makeLearner("classif.lda", predict.type = "prob")
mdls[[4]] <- makeLearner("classif.gbm", predict.type = "prob")
mdls[[5]] <- makeLearner("classif.multinom", predict.type = "prob")
mdls[[6]] <- makeLearner("classif.glmnet", predict.type = "prob")

set.seed(4732)
results <- do.call(rbind, lapply(mdls, function(mdl) {
  res <- resample(mdl, tsk, cv10, measures = list(mmce, multiclass.au1u))
  cbind(model = res[["learner.id"]], res[["measures.test"]])
}))
```

```
## Distribution not specified, assuming multinomial ...
## Distribution not specified, assuming multinomial ...
## Distribution not specified, assuming multinomial ...
## Distribution not specified, assuming multinomial ...
## Distribution not specified, assuming multinomial ...
## Distribution not specified, assuming multinomial ...
## Distribution not specified, assuming multinomial ...
## Distribution not specified, assuming multinomial ...
## Distribution not specified, assuming multinomial ...
## Distribution not specified, assuming multinomial ...
## # weights:  15 (8 variable)
## initial  value 395.500424
## iter  10 value 92.447578
## iter  20 value 57.060568
## iter  30 value 31.171391
## iter  40 value 28.838469
## iter  50 value 28.672787
## final  value 28.672668
## converged
## # weights:  15 (8 variable)
## initial  value 395.500424
## iter  10 value 96.467572
## iter  20 value 59.395779
## iter  30 value 32.787908
## iter  40 value 31.974828
## iter  50 value 31.731572
## final  value 31.731568
## converged
## # weights:  15 (8 variable)
## initial  value 395.500424
## iter  10 value 93.258463
## iter  20 value 56.933428
## iter  30 value 29.346083
## iter  40 value 28.591188
## iter  50 value 28.516078
## final  value 28.512494
## converged
## # weights:  15 (8 variable)
## initial  value 395.500424
## iter  10 value 91.827440
## iter  20 value 55.112360
## iter  30 value 30.688026
## iter  40 value 28.792314
## iter  50 value 28.370631
## iter  60 value 28.358462
## final  value 28.356538
## converged
## # weights:  15 (8 variable)
## initial  value 395.500424
## iter  10 value 90.319676
## iter  20 value 50.753257
## iter  30 value 26.660289
## iter  40 value 24.123306
## iter  50 value 23.187871
```

```
## iter  60 value 23.187731
## final  value 23.187493
## converged
## # weights:  15 (8 variable)
## initial  value 395.500424
## iter  10 value 95.253170
## iter  20 value 56.517541
## iter  30 value 33.025200
## iter  40 value 30.364191
## iter  50 value 30.321314
## final  value 30.321209
## converged
## # weights:  15 (8 variable)
## initial  value 395.500424
## iter  10 value 92.104931
## iter  20 value 58.000138
## iter  30 value 31.155794
## iter  40 value 30.299997
## iter  50 value 30.186689
## iter  60 value 30.183198
## final  value 30.177296
## converged
## # weights:  15 (8 variable)
## initial  value 395.500424
## iter  10 value 90.320089
## iter  20 value 54.048927
## iter  30 value 31.309801
## iter  40 value 29.395258
## iter  50 value 28.681005
## iter  60 value 28.668026
## final  value 28.666493
## converged
## # weights:  15 (8 variable)
## initial  value 395.500424
## iter  10 value 95.825345
## iter  20 value 58.285315
## iter  30 value 34.371494
## iter  40 value 31.173327
## iter  50 value 31.129519
## final  value 31.129373
## converged
## # weights:  15 (8 variable)
## initial  value 395.500424
## iter  10 value 95.478753
## iter  20 value 61.682244
## iter  30 value 33.994258
## iter  40 value 29.766060
## iter  50 value 29.596974
## final  value 29.596888
## converged
```

```
results[["model"]] <- fct_recode(results[["model"]],
                                 `ranger::ranger` = "classif.ranger",
                                 `kernlab::ksvm` = "classif.ksvm",
```

```
                                `MASS::lda` = "classif.lda",
                                `gbm::gbm` = "classif.gbm",
                                `nnet::multinom` = "classif.multinom",
                                `glmnet::glmnet` = "classif.glmnet")
```

## 4.6 Visualizing the model results

```
p3 <- ggplot(data = results, aes(x = model, y = multiclass.au1u)) +
  geom_point(position = position_jitter(width = 0.2, seed = 4)) +
  geom_errorbar(data = results %>%
                  group_by(model) %>%
                  summarise(auc = median(multiclass.au1u)),
                aes(x = model, ymin = auc, ymax = auc),
                inherit.aes = FALSE, color = "#FC5E61",
                width = 0.5) +
  theme_bw() +
  xlab("Model") +
  ylab("Mean AUC (one vs all)") +
  ggtitle("C)") # Results of crossvalidating models trained on encu() parameters

p3
```

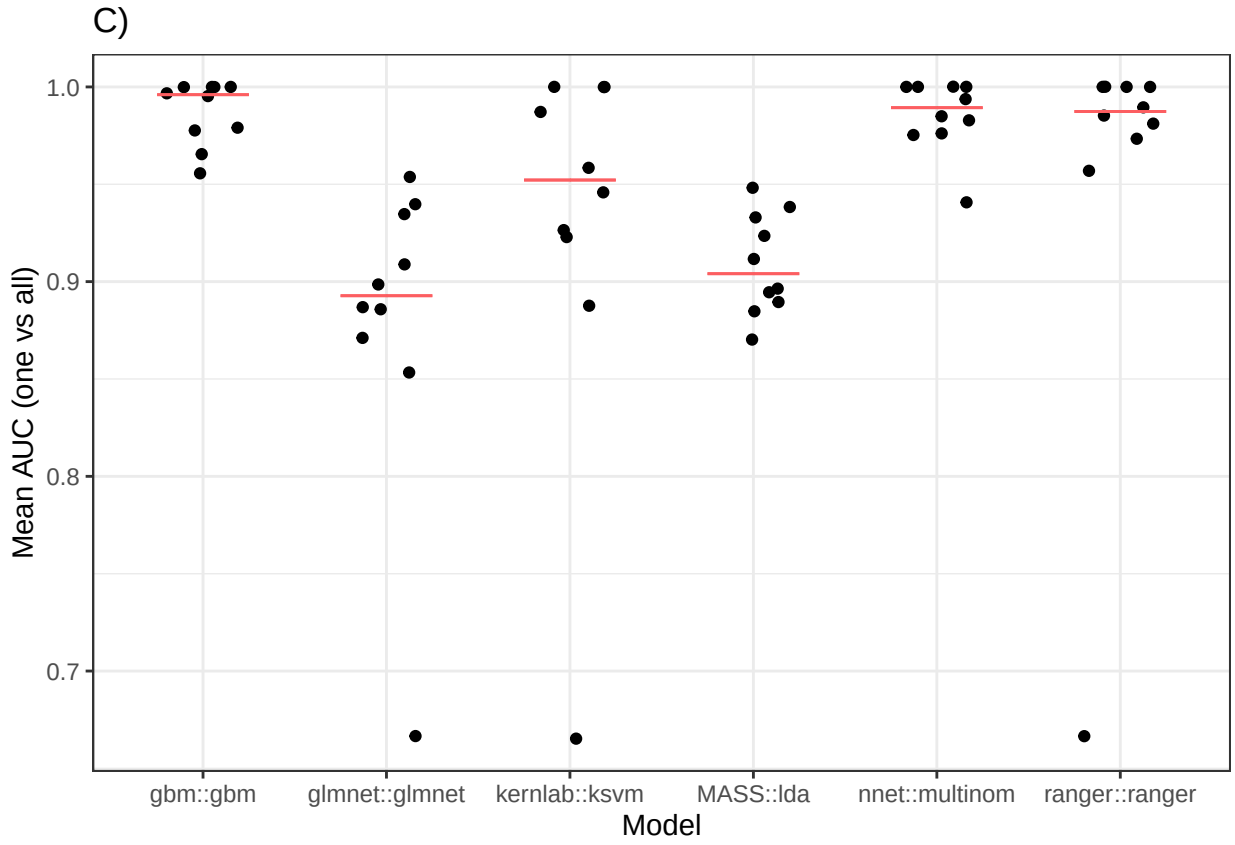


## 4.7 Final plot

Finally we plot all findings in a summary graphic.

```
cairo_ps("figure1.eps", width = 11, height = 3.1)
p1_pos + {
    p1_neg +
      p1_amb +
      plot_layout(ncol = 1)
  } + p2 + plot_layout(ncol = 3, widths = c(1, 1, 4))
dev.off()
```

```
## pdf
##   2
```

# 5 Summary and Conclusions

Extensive amounts of data represent a serious challenge in the analysis of qPCR amplification curves. In a manual classification (e. g. negative, positive), the result is usually characterized by the subjective perception of the experimenter. In addition, the time required for a manual analysis is high. An automatic system for amplification curve analysis might objectify and generalize the decision process. Interestingly, so far most authors focused on the extraction of single predictors from amplification curves. These are mainly the Cq and the amplification efficiency, which are used for the downstream processing such as expression analysis or genotyping (Pabinger et al. 2014).

Numerous software tools were developed, which deal with theses analytical steps. For example Baebler et al. (2017) published `quantGenius` and Mallona et al. (2017) published `Chainy`. However, none of them attempts to make use of characteristics of the amplification curve. Positive amplification curves usually exhibit a sigmoid shape, consisting of a ground phase, exponential phase, and plateau phase. Negative amplification curves resemble flat noisy signal. As a result, the experienced user is usually able to correctly interpret the curve shape. Similarly, outliers and measurement errors can also be identified. When setting up a qPCR assay, manual data analysis is a useful and necessary approach to familiarize oneself with the properties of the qPCR amplification curves.

It is challenging to analyze and classify amplification curves if they deviate substantially from the sigmoid shape or if their number is no longer feasible for manual analysis. Furthermore, the supposed objectivity of the user must also be questioned. In the scientific environment there is often the temptation - or rather the compulsion - to use all data for publications. As a result, amplification curves of rather poor quality are often provided. In Figure 27 it was demonstrated that a reproducible and objective analysis of amplification curves is not always given.

For a novice user, the quality of an amplification curve can be acceptable, for an experienced user, not. Ambiguous amplification curves are a big challenge for the user, as both classes (positive and negative) can be true. In most cases, however, the user is interested in an automatic distinction between positive and negative samples. This is important for screening applications. In subsubsection 3.2.2, further reasons were elaborated on why statistical methods are necessary for the objective and reproducible interpretation of the amplification curves.

A few scientific approaches have previously been shown in which machine learning was used for the analysis of amplification curves. The intention of Gunay, Goceri, and Balasubramaniyan (2016) was to improve the determination of Cq values, without dealing with classification. The authors postulated that they had developed an improved prediction of Cq values using a modified three-parameter model. One assumption of their approach was that their modified three-parameter model could be applied to any amplification curve. However, there are reasons why such an assumption is not valid. In chapters subsubsection 3.2.3 and Figure 27 it was described that a considerable proportion of amplification curves deviate clearly from a three-parameter model. Multiparametric models with more than four parameters are more frequently adapted to amplification curves. In addition, the multiparametric models tend to adapt to noise (Figure 2). Unsurprisingly, a Cq value is calculated for actually negative amplification curves, demonstrating that a three-parameter model alone cannot provide reliable predictions. However, a correct model is important for the extraction of Cq

values, for the determination of predictors from the curves and consequently for classification.

In addition to the determination of quantification points, the classification of amplification curves is necessary. For example, a diagnostician is interested in whether a sample is positive or negative. In research using high-throughput screening methods, it is important to classify large data sets quickly and cost-effectively. It is important to bear in mind that in manual classification, the classification result is influenced by the subjective perception of the experimenter and that it is comparatively time-consuming.

Here, an automatic computer-assisted classification of amplification curves is feasible because it renders the entire analysis process faster, more objective and more reproducible. The objectives were therefore to

1. create a collection of classified amplification curve data,
2. propose algorithms that can be used to calculate predictors from amplification curves,
3. to develop pipelines (e. g., machine learning, decision trees) that can be used for automatic classification of amplification curves,
4. evaluate pipelines that can be used for an automatic classification of amplification curves based on the curve shape and
5. to bundle and distribute the findings in a public repository open source software and open data package with an open data.class

for an automatic analysis of amplification curve data by machine learning.

For this purpose, the `PCRedux` package was developed. This package contains proof-of-concept algorithms and functions with which predictors (mathematically describable properties) of amplification curves can be calculated. The `pcrfit_single()` function is an extensible wrapper function for all algorithms and functions developed. `PCRedux` version 1.1.2 offers concepts to calculate 90 predictors from an amplification curve. In addition, predictors such as the employed chemistry, the qPCR device and further experimental details can be added by the user. Other parameters (e. g. hydrolysis probe, DNA binding dye) can be converted into binary classifiers and be used for modeling. Machine learning requires predictors to train a model (Saeys, Inza, and Larranaga 2007). The model should then be able to put new unknown data into a meaningful context. Predictors can have a significant influence on the accuracy of the prediction model. The predictors of the `PCRedux` package are a novelty in the literature for the classification of amplification curves, so that the collection probably constitutes the most extensive one at the time of the first release on https://github.com/devSJR/PCRedux (summer 2017).

It can be assumed that not all predictors are suitable or necessary for machine learning. Some **potential** predictors are more likely to be suitable for validation of data integrity (quality management) and data mining. The `maxRFU` predictors and `sigma_bg` (Figure 16) are to be mentioned here as examples. The predictor `maxRFU` should ideally be at a value of 1. If this is not the case, it can be assumed that a preprocessing problem was encountered. The `sigma_bg` value describes the standard deviation of the ground phase. It should be low ($sigma\_bg \leq 0.1$), otherwise it can be assumed that unusually high variations of the intensity values are present. Consequently, the relevance of the predictors must be determined independently by each user on the basis of domain knowledge, the objective, and the given data set.

At this point it should be mentioned that these approaches were deliberately sought and developed to make the approach and implementation more understandable. Self-learning machine-learning methods are expected to be included in the `PCRedux` package in future releases, from the necessity to design and test additional predictors.

To a modest extent, the usefulness of the predictors was tested on exemplary data sets, with the aim of achieving a high degree of objectivity and reproducibility. It is probably not possible to fulfill this ideal completely, since the algorithms were designed from a limited human perspective, which poses a generic problem in machine learning. In particular, data records can be distorted if the user excludes seemingly problematic data. Hence, it is advisable to perform a more comprehensive analysis of all predictors.

Several ROIs (see Figure 5) can be obtained from amplification curves. Sigmoidal amplification curves have turning points that can serve as an indicator of a positive amplification curve, and are mathematical and statistical starting points for calculating predictors. Amplification curves can have unique trajectories and

often deviate drastically from ideal sigmoid models (see Figure 4A and Figure 4B). Some amplification curves have only a slight increase with positive or negative signs lacking a sigmoid curvature.

Almost all real-time thermo-cyclers have built-in software that performs preprocessing steps such as smoothing, baseline correction and normalization on the amplification curves (Rödiger, Burdukiewicz, and Schierack 2015; Spiess et al. 2015, 2016). For this reason, it is nearly impossible to get access to informative raw data, so that the impact on the predictor extraction process cannot be adequately estimated.

The volume and classification of data sets needs to be representative (Herrera et al. 2016). The `PCRedux` package contains a large number of manually classified amplification curves. Here, data preparation is an important step,as it encompasses data cleansing, data transformation and data integration (Herrera et al. 2016). To assist, the `xray` package (Seibelt 2017) and `assertr` package (Fischetti 2019) can be used to analyze the distribution and variables in records for important anomalies such as missing values, zeros, empty strings (Blank) and infinite numbers (Inf). Users of the`PCRedux` package should use such tools before proceeding with the analysis. Even though the data records (qPCR runs) in the `PCRedux` package have a very similar structure, some records contain missing values or have different dimensions. For example, the data set `C127EGHP` comprises a matrix of 40 x 66 (35 cycles x observations (65 amplification curves)), while the data set `htPCR` comprises a matrix of 35 x 8859.

Talking about data sets, it is important to make sure that the volume of the data is representative. In this study amplification curves were categorized by hand and processed with the algorithms described in this study. Although this data set is fairly large in comparison to what existed before, there is no numeric evidence how well it reflects amplification curves in general. In particular, not all data sets have comparable case numbers. For example, the `htPCR` data set (Biomark HD, Fluidigm) encompass in total 8858 amplification curves, while the `C127EGHP` data set (iQ5, Bio-Rad) encompass in total 64 amplification curves. While most of the amplification curves of the `C127EGHP` data set have a classical sigmoid curve shape, amplification curves from the `htPCR` data set largely display noisy curvatures with non-sigmoid shape. One may question if the larger data set introduces a confirmation bias.

Although data sets in the `PCRedux` package are large compared to what has been previously available, there is no conclusive evidence of how well these represent amplification curves in other settings. Bellman coined the term "Curse of Dimensionality" in 1961 when he dealt with adaptive control processes, vaguely describing the practical difficulties of high-dimensional analysis and estimation. There is only a maximum number of predictors for a sample of a certain size. If there are too many, the performance of an algorithm decreases rather than improves. As a result, many data mining algorithms fail with high dimensionality because the data points are sparse (Herrera et al. 2016). Besides, the following applies:

- The user's knowledge, prejudices, and skills are reflected in the classified data. For example, an amplification can be classified as "ambiguous" by one and "positive" by another user.
- Not all data sets have a comparable number of cases as described above. The most of the amplification curves of the `C127EGHP` data set have an *ideal* sigmoid waveform. In contrast, the amplification curves from the `htPCR` data set are noisy and difficult to classify.
- The user decides
  - how the data is preprocessed,
  - which predictors are determined by the amplification curves,
  - which data set is used for machine learning and to what extent,
  - how the models are tested and
  - which results are reported.

Accordingly, the domain knowledge, biases and competences of the human operator are reflected by the software. For example, amplification that are classified by one human as 'ambiguous' might be classified as 'positive' by another human operator. This will affect (bias) the characteristics of the training data set. The model is intended to be in accordance with the human operator. The implications can be problematic. For example, amplification curves rated as false negative might lead to an adverse evidence in a forensic setting. As illustrated in subsection 3.2, every human operator will make an association between the shape of an amplification curve and the class it belongs to.

Measures to minimize errors in manual classification include the implementation of algorithms to detect them. This should preferably be done in the form of open source packages with publicly accessible data sets. In contrast to black box algorithms and hidden data sets, third parties can review and modify all elements. Many qPCR devices have built-in software that performs preprocessing steps like smoothing, base-lining and normalization and the data sets (Rödiger, Burdukiewicz, and Schierack 2015; Spiess et al. 2015, 2016). This will have an impact on the predictor extraction process. The same applies to the preprocessing steps in the `PCRedux` package, which have not been studied thoroughly.

For the examples in the `PCRedux` package, the question could not be clarified whether class imbalances in the data sets cause a confirmation distortion. However, a class imbalance may result in loss of prediction strength, because some classifiers make the assumption of similar class distributions (Herrera et al. 2016).

A new concept for the fast group-wise classification of amplification curves was introduced within the `PCRedux` package. Based on experience with the collected data sets it can be stated that only a few iterations are necessary to classify a large data set. This part of the software is intended as an assistance tool for the users of the package.

Measures to minimize these sources of error are based on the implementation of algorithms in the form of an open source package, and the publication of the data sets. Unlike black box algorithms and inaccessible data sets, every user can check and correct all steps. However, it is advised that users of the `PCRedux` package verify independently whether their models are objective. Failure to do so may have severe implications, for instance, amplification curves classified as false negative may lead to misleading inferences in a forensic analysis.

Machine-learning algorithms require careful data preprocessing and quality management. In a first step, relatively large data sets of known characteristic vectors have to be collected and depending on the machine learning approach, predictors calculated. In a second step, these characteristics are used to classify unknown characteristic vectors using the automatic learning algorithm. As an example, the amplification curves would need to be randomly split into training data and test data. Some examples were used in the `PCRedux` package to show how predictors of an amplification curve data set can be calculated and used for classifications.

The scope of the `PCRedux` package is wide. The quantitation of nucleic acids by curve parameters such as the Cq and amplification efficiency is meaningful only if the amplification curves have a sigmoid shape (Ruijter et al. 2013, 2014; Ritz and Spiess 2008), which in principle, can now be verified with the `PCRedux` package.

In this study, it was shown how a given data set of amplification curves with known classifications can be used to build a system that can predict the classification of amplification curves. The algorithms provide means for a sensitive and specific classification of amplification curves from qPCR experiments in both supervised an unsupervised analysis mode. However, this method might be applicable to melting analysis too. This needs to be investigated in further studies.

Importantly, the concepts elucidated in this work may also be applied to other bioanalytical methods (e. g. enzyme kinetics, receptor binding studies, ELISA results, biological growth curves) with sigmoidal structure, however this requires more detailed interrogation. The `PCRedux` software may also be coupled with other technologies like Next Generation Sequencing. qPCR is used for pretesting (DNA quality) and as a confirmation test for RNA-Seq quantification (Nassirpour et al. 2014). For this purpose, automated quality control and decision support are conceivable.

# References


Alonso, Antonio, and Oscar García. 2007. "Real-time quantitative PCR in forensic science." *Molecular Forensics*, 59.

Arlot, Sylvain, and Alain Celisse. 2010. "A survey of cross-validation procedures for model selection." *Statistics Surveys* 4: 40–79. https://doi.org/10.1214/09-SS054.

Bååth, Rasmus. 2012. "The State of Naming Conventions in R." *The R Journal* 4 (2): 74–75. http://journal.r-project.org/archive/2012-2/RJournal_2012-2_Baaaath.pdf.

Baebler, Miha Svalina, Marko Petek, Katja Stare, Ana Rotter, Maruša Pompe-Novak, and Kristina Gruden. 2017. "quantGenius: implementation of a decision support system for qPCR-based gene quantification." *BMC Bioinformatics* 18 (1). https://doi.org/10.1186/s12859-017-1688-7.

Barratt, Kevin, and John F. Mackay. 2002. "Improving Real-Time PCR Genotyping Assays by Asymmetric Amplification." *Journal of Clinical Microbiology* 40 (4): 1571–2. https://doi.org/10.1128/JCM.40.4.1571-1572.2002.

Beer. 1852. "Bestimmung der Absorption des rothen Lichts in farbigen Flüssigkeiten." *Annalen Der Physik* 162 (5): 78–88. https://doi.org/10.1002/andp.18521620505.

Berg, Jeremy M., John L. Tymoczko, and Lubert Stryer. 2002. "DNA, RNA, and the Flow of Genetic Information." https://www.ncbi.nlm.nih.gov/books/NBK21171/.

Bischl, Bernd, Michel Lang, Lars Kotthoff, Julia Schiffner, Jakob Richter, Erich Studerus, Giuseppe Casalicchio, and Zachary M. Jones. 2010. *mlr: Machine learning in R*. http://www.jmlr.org/papers/volume17/15-066/source/15-066.pdf.

Breiman, Leo. 2001. "Random forests." *Machine Learning* 45 (1): 5–32.

Brito, Paula, ed. 2008. *COMPSTAT 2008: Proceedings in Computational Statistics*. Physica-Verlag Heidelberg.

Burdukiewicz, Michał, Stefan Rödiger, Piotr Sobczyk, Mario Menschikowski, Peter Schierack, and Paweł Mackiewicz. 2016. "Methods for comparing multiple digital PCR experiments." *Biomolecular Detection and Quantification* 9 (September): 14–19. https://doi.org/10.1016/j.bdq.2016.06.004.

Burdukiewicz, Michał, Andrej-Nikolai Spiess, Konstantin A. Blagodatskikh, Werner Lehmann, Peter Schierack, and Stefan Rödiger. 2018. "Algorithms for Automated Detection of Hook Effect-Bearing Amplification Curves." *Biomolecular Detection and Quantification*, October. https://doi.org/10.1016/j.bdq.2018.08.001.

Bustin, Stephen. 2017. "The continuing problem of poor transparency of reporting and use of inappropriate methods for RT-qPCR." *Biomolecular Detection and Quantification* 12 (June): 7–9. https://doi.org/10.1016/j.bdq.2017.05.001.

Caudle, Kelly E., Roseann S. Gammal, Jason H. Karnes, Janna Afanasjeva, Keri C. Anderson, Erin F. Barreto, Craig Beavers, et al. 2019. "PRN OPINION PAPER: Application of Precision Medicine Across Pharmacy Specialty Areas." *JACCP: JOURNAL OF THE AMERICAN COLLEGE OF CLINICAL PHARMACY* 2 (3): 288–302. https://doi.org/10.1002/jac5.1107.

Chang, Winston, Joe Cheng, JJ Allaire, Yihui Xie, and Jonathan McPherson. 2019. *Shiny: Web Application Framework for R*. https://CRAN.R-project.org/package=shiny.

Charpiat, Guillaume, Olivier Faugeras, and Renaud Keriven. 2003. "Shape metrics, warping and statistics." In *Image Processing, 2003. ICIP 2003. Proceedings. 2003 International Conference on*, 2:II–627. IEEE. http://ieeexplore.ieee.org/abstract/document/1246758/.

Cook, Dianne, and Deborah F. Swayne. 2007. *Interactive and Dynamic Graphics for Data Analysis: With R and GGobi*. 2007 edition. 1st Ser. New York: Springer. https://doi.org/10.1007/978-0-387-71762-3.

Cristino, Alexandre S., Erica D. Tanaka, Mercedes Rubio, Maria-Dolors Piulachs, and Xavier Belles. 2011. "Deep Sequencing of Organ- and Stage-Specific microRNAs in the Evolutionarily Basal Insect Blattella

Germanica (L.) (Dictyoptera, Blattellidae)." *PLOS ONE* 6 (4): e19350. https://doi.org/10.1371/journal.pone.0019350.

Curran, James M. 2009. "Statistics in forensic science." *Wiley Interdisciplinary Reviews: Computational Statistics* 1 (2): 141–56. https://doi.org/10.1002/wics.33.

De Vries, Andrie, and Joris Meys. 2012. *R for Dummies*. 2nd ed. John Wiley & Sons.

Dvinge, Heidi, and Paul Bertone. 2009. "HTqPCR: high-throughput analysis and visualization of quantitative real-time PCR data in R." *Bioinformatics* 25 (24): 3325–6. https://doi.org/10.1093/bioinformatics/btp578.

Erdman, Chandra, John W. Emerson, and others. 2007. "bcp: an R package for performing a Bayesian analysis of change point problems." *Journal of Statistical Software* 23 (3): 1–13. https://www.jstatsoft.org/article/view/v023i03/v23i03.pdf.

Febrero-Bande, Manuel, and Manuel Oviedo de la Fuente. 2012. "Statistical Computing in Functional Data Analysis: The R Package fda.usc." *Journal of Statistical Software* 51 (4): 1–28. http://www.jstatsoft.org/v51/i04/.

Fernandez-Delgado, Manuel, Eva Cernadas, Senen Barro, and Dinani Amorim. 2014. "Do we Need Hundreds of Classifiers to Solve Real World Classification Problems?" *Journal of Machine Learning Research* 15: 3133–81. http://jmlr.org/papers/v15/delgado14a.html.

Feuer, Ronny, Sebastian Vlaic, Janine Arlt, Oliver Sawodny, Uta Dahmen, Ulrich M. Zanger, and Maria Thomas. 2015. "LEMming: A Linear Error Model to Normalize Parallel Quantitative Real-Time PCR (qPCR) Data as an Alternative to Reference Gene Based Methods." *PLOS ONE* 10 (9): e0135852. https://doi.org/10.1371/journal.pone.0135852.

Fischer, Bettina Maria, Daniel Neumann, Ann Liza Piberger, Sarah Fremgaard Risnes, Beate Köberle, and Andrea Hartwig. 2016. "Use of High-Throughput RT-qPCR to Assess Modulations of Gene Expression Profiles Related to Genomic Stability and Interactions by Cadmium." *Archives of Toxicology* 90 (11): 2745–61. https://doi.org/10.1007/s00204-015-1621-7.

Fischetti, Tony. 2019. *assertr: Assertive Programming for R Analysis Pipelines*. https://CRAN.R-project.org/package=assertr.

Geng, Tao, Richard Novak, and Richard A. Mathies. 2014. "Single-Cell Forensic Short Tandem Repeat Typing within Microfluidic Droplets." *Analytical Chemistry* 86 (1): 703–12. https://doi.org/10.1021/ac403137h.

George, Sandra, Stefan Rödiger, Christian Schröder, Michael Knaut, and Jan-Heiner Küpper. 2016. "Development of multiplex PCR systems for expression profiling of human cardiomyocytes induced to proliferate by lentivirus transduction of upcyte genes." *Journal of Cellular Biotechnology* 2 (1): 35–55. https://doi.org/10.3233/JCB-15025.

Giuliano, Kenneth A., Shinichiro Wachi, Lawrence Drew, Danijela Dukovski, Olivia Green, Cecilia Bastos, Matthew D. Cullen, et al. 2017. "Use of a High-Throughput Phenotypic Screening Strategy to Identify Amplifiers, a Novel Pharmacological Class of Small Molecules That Exhibit Functional Synergy with Potentiators and Correctors:" *SLAS DISCOVERY: Advancing Life Sciences R&D*, September. https://doi.org/10.1177/2472555217729790.

Gracz, Adam D., Ian A. Williamson, Kyle C. Roche, Michael J. Johnston, Fengchao Wang, Yuli Wang, Peter J. Attayek, et al. 2015. "A High-Throughput Platform for Stem Cell Niche Co-Cultures and Downstream Gene Expression Analysis." *Nature Cell Biology* 17 (3): 340–49. https://doi.org/10.1038/ncb3104.

Greene, Casey S., Jie Tan, Matthew Ung, Jason H. Moore, and Chao Cheng. 2014. "Big Data Bioinformatics." *Journal of Cellular Physiology* 229 (12): 1896–1900. https://doi.org/10.1002/jcp.24662.

Gunay, Melih, Evgin Goceri, and Rajarajeswari Balasubramaniyan. 2016. "Machine Learning for Optimum CT-Prediction for qPCR." In *Machine Learning and Applications (ICMLA), 2016 15th IEEE International Conference on Machine Learning and Applications (ICMLA)*, 588–92. IEEE. https://doi.org/10.1109/ICMLA.2016.0103.

Günther, Frauke, and Stefan Fritsch. 2010. "Neuralnet: Training of Neural Networks." *The R Journal* 2 (1): 30–38. http://journal.r-project.org/archive/2010-1/RJournal_2010-1_Guenther+Fritsch.pdf.

Halpern, Micah D., and Jack Ballantyne. 2011. "An STR Melt Curve Genotyping Assay for Forensic Analysis Employing an Intercalating Dye Probe FRET*." *Journal of Forensic Sciences* 56 (1): 36–45. https://doi.org/10.1111/j.1556-4029.2010.01549.x.

Herrera, Francisco, Sebastián Ventura, Rafael Bello, Chris Cornelis, Amelia Zafra, Dánel Sánchez-Tarragó, and Sarah Vluymans. 2016. *Multiple Instance Learning*. Cham: Springer International Publishing. https://doi.org/10.1007/978-3-319-47759-6.

Hester, Jim. 2018. *Covr: Test Coverage for Packages*. https://CRAN.R-project.org/package=covr.

Higuchi, Russell, Carita Fockler, Gavin Dollinger, and Robert Watson. 1993. "Kinetic PCR Analysis: Real-Time Monitoring of DNA Amplification Reactions." *Nature Biotechnology*, no. 9 (September): 1026–30. https://doi.org/10.1038/nbt0993-1026.

Horsman, Katie M., Joan M. Bienvenue, Kiev R. Blasier, and James P. Landers. 2007. "Forensic DNA Analysis on Microfluidic Devices: A Review." *Journal of Forensic Sciences* 52 (4): 784–99. https://doi.org/10.1111/j.1556-4029.2007.00468.x.

Hothorn, Torsten, and Brian S. Everitt. 2014. *A Handbook of Statistical Analyses using R, Third Edition*. 3rd ed. Oakville: Chapman; Hall/CRC.

Hothorn, Torsten, Kurt Hornik, and Achim Zeileis. 2006. "Unbiased Recursive Partitioning: A Conditional Inference Framework." *Journal of Computational and Graphical Statistics* 15 (3): 651–74. https://doi.org/10.1198/106186006X133933.

Igual, Laura, and Santi Seguí. 2017. *Introduction to Data Science*. Undergraduate Topics in Computer Science. Cham: Springer International Publishing. https://doi.org/10.1007/978-3-319-50017-1.

Isaac, Peter G. 2009. "Essentials of nucleic acid analysis: a robust approach." *Annals of Botany* 104 (2): vi–vi. https://doi.org/10.1093/aob/mcp135.

James, Gareth, Daniela Witten, Trevor Hastie, and Robert Tibshirani. 2013. *An Introduction to Statistical Learning*. Vol. 103. Springer Texts in Statistics. New York, NY: Springer New York. https://doi.org/10.1007/978-1-4614-7138-7.

James, Nicholas A., and David S. Matteson. 2013. "ecp: An R package for nonparametric multiple change point analysis of multivariate data." *arXiv Preprint arXiv:1309.3295*. https://arxiv.org/abs/1309.3295.

Jeffreys, A. J., V. Wilson, and S. L. Thein. 1985. "Individual-specific 'fingerprints' of human DNA." *Nature* 316 (6023): 76. https://doi.org/10.1038/316076a0.

Karsai, Albert, Sabine Müller, Stefan Platz, and Marie-Theres Hauser. 2002. "Evaluation of a Homemade SYBR Green I Reaction Mixture for Real-Time PCR Quantification of Gene Expression." *BioTechniques* 32 (4): 790–96. https://www.ncbi.nlm.nih.gov/pmc/articles/PMC4353838/.

Killick, Rebecca, and Idris A. Eckley. 2014. "changepoint: An R Package for Changepoint Analysis." *Journal of Statistical Software* 58 (3): 1–19. http://www.jstatsoft.org/v58/i03/.

Kitchin, Rob. 2014. *The data revolution : big data, open data, data infrastructures & their consequences*. Los Angeles, California London: SAGE Publications.

Knuth, D. E. 1984. "Literate Programming." *The Computer Journal* 27 (2): 97–111. https://doi.org/10.1093/comjnl/27.2.97.

Kruppa, Jochen, Yufeng Liu, Gérard Biau, Michael Kohler, Inke R. König, James D. Malley, and Andreas Ziegler. 2014. "Probability Estimation with Machine Learning Methods for Dichotomous and Multicategory Outcome: Theory." *Biometrical Journal*, no. 4 (July): 534–63. https://doi.org/10.1002/bimj.201300068.

Kuhn, Max. 2008. "Building Predictive Models in R Using the caret Package." *Journal of Statistical Software* 28 (5). http://www.jstatsoft.org/v28/i05/.

Lanubile, F., C. Ebert, R. Prikladnicki, and A. Vizcaíno. 2010. "Collaboration Tools for Global Software Engineering." *IEEE Software* 27 (2): 52–55. https://doi.org/10.1109/MS.2010.39.

Lee, Jae K. 2010. *Statistical Bioinformatics: For Biomedical and Life Science Researchers*. Wiley-Blackwell. https://www.wiley.com/en-sg/Statistical+Bioinformatics%3A+For+Biomedical+and+Life+Science+Researchers-p-9780471692720.

Lee, Seung-Hee, Daniel Cunha, Carlo Piermarocchi, Giovanni Paternostro, Anthony Pinkerton, Laurence Ladriere, Piero Marchetti, Decio L. Eizirik, Miriam Cnop, and Fred Levine. 2017. "High-Throughput Screening and Bioinformatic Analysis to Ascertain Compounds That Prevent Saturated Fatty Acid-Induced -Cell Apoptosis." *Biochemical Pharmacology* 138 (August): 140–49. https://doi.org/10.1016/j.bcp.2017.05.007.

Lefever, Steve, Jan Hellemans, Filip Pattyn, Daniel R. Przybylski, Chris Taylor, René Geurts, Andreas Untergasser, Jo Vandesompele, and RDML on behalf of the Consortium. 2009. "RDML: structured language and reporting guidelines for real-time quantitative PCR data." *Nucleic Acids Research* 37 (7): 2065–9. https://doi.org/10.1093/nar/gkp056.

Liaw, Andy, and Matthew Wiener. 2002. "Classification and Regression by randomForest." *R News* 2 (3): 18–22. http://CRAN.R-project.org/doc/Rnews/.

Luan, Shenghua, Lael J. Schooler, and Gerd Gigerenzer. 2011. "A signal-detection analysis of fast-and-frugal trees." *Psychological Review* 118 (2): 316–38. https://doi.org/10.1037/a0022684.

Lynch, Courtney, and Rachel Fleming. 2019. "A Review of Direct Polymerase Chain Reaction of DNA and RNA for Forensic Purposes." *Wiley Interdisciplinary Reviews: Forensic Science* 1 (4): e1335. https://doi.org/10.1002/wfs2.1335.

Maher, Robert L., Joseph T. Hanlon, and Emily R. Hajjar. 2014. "Clinical Consequences of Polypharmacy in Elderly." *Expert Opinion on Drug Safety* 13 (1). https://doi.org/10.1517/14740338.2013.827660.

Mallona, Izaskun, Anna Díez-Villanueva, Berta Martín, and Miguel A. Peinado. 2017. "Chainy: an universal tool for standardized relative quantification in real-time PCR." *Bioinformatics*. https://doi.org/10.1093/bioinformatics/btw839.

Mallona, Izaskun, Julia Weiss, and Marcos Egea-Cortines. 2011. "pcrEfficiency: a Web tool for PCR amplification efficiency prediction." *BMC Bioinformatics* 12: 404. https://doi.org/10.1186/1471-2105-12-404.

Martins, C., G. Lima, Mr. Carvalho, L. Cainé, and Mj. Porto. 2015. "DNA quantification by real-time PCR in different forensic samples." *Forensic Science International: Genetics Supplement Series* 5 (December): e545–e546. https://doi.org/10.1016/j.fsigss.2015.09.215.

Matz, Mikhail V., Rachel M. Wright, and James G. Scott. 2013. "No Control Genes Required: Bayesian Analysis of qRT-PCR Data." *PLoS ONE* 8 (8): e71448. https://doi.org/10.1371/journal.pone.0071448.

McCall, Matthew N., Helene R. McMurray, Hartmut Land, and Anthony Almudevar. 2014. "On non-detects in qPCR data." *Bioinformatics* 30 (16): 2310–6. https://doi.org/10.1093/bioinformatics/btu239.

McFadden, Daniel L. 1974. "Conditional Logit Analysis of Qualitative Choice Behavior." In *Frontiers in Economics*, Frontiers in Economics:105–42. P. Zarembka (ed.). New York: Academic Press. https://eml.berkeley.edu/reprints/mcfadden/zarembka.pdf.

Mestdagh, Pieter, Steve Lefever, Pieter-Jan Volders, Stefaan Derveaux, Jan Hellemans, and Jo Vandesompele. 2016. "Long Non-Coding RNA Expression Profiling in the NCI60 Cancer Cell Line Panel Using High-Throughput RT-qPCR." *Scientific Data* 3 (1): 1–6. https://doi.org/10.1038/sdata.2016.52.

Meyer, Hermann-Josef, Rebecca Turincio, Shirley Ng, Juan Li, Blair Wilson, Pamela Chan, Mark Zak, Dorothea Reilly, Maureen H. Beresini, and Athena W. Wong. 2017. "High Throughput Screening Identifies Novel, Cell Cycle-Arresting Small Molecule Enhancers of Transient Protein Expression." *Biotechnology Progress* 33 (6): 1579–88. https://doi.org/10.1002/btpr.2517.

Myers, Glenford J., Tom Badgett, Todd M. Thomas, and Corey Sandler. 2004. *The art of software testing*. 2nd ed. Hoboken, N.J: John Wiley & Sons.

Nassirpour, Rounak, Sachin Mathur, Mark M. Gosink, Yizheng Li, Ahmed M. Shoieb, Joanna Wood, Shawn P. O'Neil, Bruce L. Homer, and Laurence O. Whiteley. 2014. "Identification of Tubular Injury microRNA Biomarkers in Urine: Comparison of Next-Generation Sequencing and qPCR-Based Profiling Platforms." *BMC Genomics* 15 (June): 485. https://doi.org/10.1186/1471-2164-15-485.

Neve, Jan De, Joris Meys, Jean-Pierre Ottoy, Lieven Clement, and Olivier Thas. 2014. "unifiedWMWqPCR: the unified Wilcoxon–Mann–Whitney test for analyzing RT-qPCR data in R." *Bioinformatics* 30 (17): 2494–5. https://doi.org/10.1093/bioinformatics/btu313.

Nolan, Tania, Rebecca E Hands, and Stephen A Bustin. 2006. "Quantification of mRNA using real-time RT-PCR." *Nature Protocols* 1 (November): 1559. https://doi.org/10.1038/nprot.2006.236.

Olagnier, David, Cindy Chiang, and John Hiscott. 2017. "Evaluation of Innate Immune Gene Expression Following HDAC Inhibitor Treatment by High Throughput qPCR and PhosFlow Cytometry." In *HDAC/HAT Function Assessment and Inhibitor Development*, 245–55. Methods in Molecular Biology. Humana Press, New York, NY. https://doi.org/10.1007/978-1-4939-6527-4_18.

Oorschot, Roland AH van, Kaye N Ballantyne, and R John Mitchell. 2010. "Forensic Trace DNA: A Review." *Investigative Genetics*, no. 1: 14. https://doi.org/10.1186/2041-2223-1-14.

Pabinger, Stephan, Stefan Rödiger, Albert Kriegner, Klemens Vierlinger, and Andreas Weinhäusel. 2014. "A survey of tools for the analysis of quantitative PCR (qPCR) data." *Biomolecular Detection and Quantification* 1 (1): 23–33. https://doi.org/10.1016/j.bdq.2014.08.002.

Pabinger, Stephan, Gerhard G. Thallinger, René Snajder, Heiko Eichhorn, Robert Rader, and Zlatko Trajanoski. 2009. "QPCR: Application for real-time PCR data management and analysis." *BMC Bioinformatics* 10 (1): 268. https://doi.org/10.1186/1471-2105-10-268.

Perkins, James R., John M. Dawes, Steve B. McMahon, David LH Bennett, Christine Orengo, and Matthias Kohl. 2012. "ReadqPCR and NormqPCR: R packages for the reading, quality checking and normalisation of RT-qPCR quantification cycle (Cq) data." *BMC Genomics* 13 (1): 296. https://doi.org/10.1186/1471-2164-13-296.

Phillips, Nathaniel, Hansjoerg Neth, Jan Woike, and Wolfgang Gaissmaer. 2017. *FFTrees: Generate, Visualise, and Evaluate Fast-and-Frugal Decision Trees*. https://CRAN.R-project.org/package=FFTrees.

Quinlan, J. Ross. 1986. "Induction of decision trees." *Machine Learning* 1 (1): 81–106. https://doi.org/10.1007/BF00116251.

Rao, Prema S., Ryan Endicott, Randy Mullins, and U. Subrahmanyeswara Rao. 2018. "A 6-Week Laboratory Research Rotation in Pharmacogenomics: A Model for Preparing Pharmacy Students to Practice Precision Medicine." *The Pharmacogenomics Journal* 18 (4): 601–8. https://doi.org/10.1038/s41397-018-0019-3.

Richards, F. J. 1959. "A Flexible Growth Function for Empirical Use." *Journal of Experimental Botany* 10 (2): 290–301. https://doi.org/10.1093/jxb/10.2.290.

Ritz, Christian, and Andrej-Nikolai Spiess. 2008. "qpcR: an R package for sigmoidal model selection in quantitative real-time polymerase chain reaction analysis." *Bioinformatics* 24 (13): 1549–51. https://doi.org/10.1093/bioinformatics/btn227.

Rödiger, Stefan, Alexander Böhm, and Ingolf Schimke. 2013. "Surface Melting Curve Analysis with R." *The R Journal* 5 (2): 37–53. http://journal.r-project.org/archive/2013-2/roediger-bohm-schimke.pdf.

Rödiger, Stefan, Michał Burdukiewicz, Konstantin A. Blagodatskikh, and Peter Schierack. 2015. "R as an Environment for the Reproducible Analysis of DNA Amplification Experiments." *The R Journal* 7 (2): 127–50. http://journal.r-project.org/archive/2015-1/RJ-2015-1.pdf.

Rödiger, Stefan, Michał Burdukiewicz, and Peter Schierack. 2015. "chipPCR: an R package to pre-process raw data of amplification curves." *Bioinformatics* 31 (17): 2900–2902. https://doi.org/10.1093/bioinfor

matics/btv205.

Rödiger, Stefan, Michał Burdukiewicz, Andrej-Nikolai Spiess, and Konstantin Blagodatskikh. 2017. "Enabling reproducible real-time quantitative PCR research: the RDML package." *Bioinformatics*, August. https://doi.org/10.1093/bioinformatics/btx528.

Rödiger, Stefan, Thomas Friedrichsmeier, Prasenjit Kapat, and Meik Michalke. 2012. "RKWard: a comprehensive graphical user interface and integrated development environment for statistical analysis with R." *Journal of Statistical Software* 49 (9): 1–34. https://www.jstatsoft.org/article/view/v049i09/v49i09.pdf.

Rödiger, Stefan, Sandra George, Carsten Schmidt, Ulrike Frömmel, Mirko Ruhland, Ingolf Schimke, Peter Schierack, and Christian Schröder. 2011. "Alternative Nukleinsäureamplifikationsverfahren für die Multiparameteranalytik." In *Multiparameteranalytik in Forschung und Praxis*, 133–46. Pabst Science Publishers. https://doi.org/10.13140/RG.2.1.2766.1681.

Rödiger, Stefan, Claudia Liebsch, Carsten Schmidt, Werner Lehmann, Ute Resch-Genger, Uwe Schedler, and Peter Schierack. 2014. "Nucleic acid detection based on the use of microbeads: a review." *Microchimica Acta* 181 (11-12): 1151–68. https://doi.org/10.1007/s00604-014-1243-4.

Rödiger, Stefan, Peter Schierack, Alexander Böhm, Jörg Nitschke, Ingo Berger, Ulrike Frömmel, Carsten Schmidt, et al. 2013. "A highly versatile microscope imaging technology platform for the multiplex real-time detection of biomolecules and autoimmune antibodies." *Advances in Biochemical Engineering/Biotechnology* 133: 35–74. https://doi.org/10.1007/10_2011_132.

Romaniuk, Dmitrii S., Anna M. Postovskaya, Alexandra A. Khmelevskaya, Dmitry B. Malko, and Grigory A. Efimov. 2019. "Rapid Multiplex Genotyping of 20 HLA-A*02:01 Restricted Minor Histocompatibility Antigens." *Frontiers in Immunology* 10. https://doi.org/10.3389/fimmu.2019.01226.

Ronde, Maurice W. J. de, Jan M. Ruijter, David Lanfear, Antoni Bayes-Genis, Maayke G. M. Kok, Esther E. Creemers, Yigal M. Pinto, and Sara-Joan Pinto-Sietsma. 2017. "Practical data handling pipeline improves performance of qPCR-based circulating miRNA measurements." *RNA* 23 (5): 811–21. https://doi.org/10.1261/rna.059063.116.

Rote, Günter. 1991. "Computing the minimum Hausdorff distance between two point sets on a line under translation." *Information Processing Letters* 38 (3): 123–27. https://doi.org/10.1016/0020-0190(91)90233-8.

Ruijter, Jan M., Peter Lorenz, Jari M. Tuomi, Michael Hecker, and Maurice J. B. van den Hoff. 2014. "Fluorescent-increase kinetics of different fluorescent reporters used for qPCR depend on monitoring chemistry, targeted sequence, type of DNA input and PCR efficiency." *Microchimica Acta*, 1–8. https://doi.org/10.1007/s00604-013-1155-8.

Ruijter, Jan M., Michael W. Pfaffl, Sheng Zhao, Andrej N. Spiess, Gregory Boggy, Jochen Blom, Robert G. Rutledge, et al. 2013. "Evaluation of qPCR curve analysis methods for reliable biomarker discovery: Bias, resolution, precision, and implications." *Methods* 59 (1): 32–46. https://doi.org/10.1016/j.ymeth.2012.08.011.

Ruijter, Jan M., Adrián Ruiz Villalba, Jan Hellemans, Andreas Untergasser, and Maurice J. B. van den Hoff. 2015. "Removal of between-run variation in a multi-plate qPCR experiment." *Biomolecular Detection and Quantification*, Special Issue: Advanced Molecular Diagnostics for Biomarker Discovery – Part I, 5 (September): 10–14. https://doi.org/10.1016/j.bdq.2015.07.001.

Ruijter, J M, C Ramakers, W M H Hoogaars, Y Karlen, O Bakker, M J B van den Hoff, and A F M Moorman. 2009. "Amplification efficiency: linking baseline and bias in the analysis of quantitative PCR data." *Nucleic Acids Research* 37 (6): e45. https://doi.org/10.1093/nar/gkp045.

Rutledge, R. G., and C. Côté. 2003. "Mathematics of Quantitative Kinetic PCR and the Application of Standard Curves." *Nucleic Acids Research*, no. 16 (August): e93.

Saeys, Y., I. Inza, and P. Larranaga. 2007. "A review of feature selection techniques in bioinformatics." *Bioinformatics* 23 (19): 2507–17. https://doi.org/10.1093/bioinformatics/btm344.

Sauer, Eva, Ann-Kathrin Reinke, and Cornelius Courts. 2016. "Differentiation of five body fluids from forensic samples by expression analysis of four microRNAs using quantitative PCR." *Forensic Science International: Genetics* 22 (May): 89–99. https://doi.org/10.1016/j.fsigen.2016.01.018.

Scott, A. J., and M. Knott. 1974. "A Cluster Analysis Method for Grouping Means in the Analysis of Variance." *Biometrics* 30 (3): 507. https://doi.org/10.2307/2529204.

Seibelt, Pablo. 2017. *xray: X Ray Vision on your Datasets*. https://CRAN.R-project.org/package=xray.

Shin, Hoo-Chang, Holger R. Roth, Mingchen Gao, Le Lu, Ziyue Xu, Isabella Nogues, Jianhua Yao, Daniel Mollura, and Ronald M. Summers. 2016. "Deep Convolutional Neural Networks for Computer-Aided Detection: CNN Architectures, Dataset Characteristics and Transfer Learning," February. http://arxiv.org/abs/1602.03409.

Silva, Sarah S., Cátia Lopes, A. L. Teixeira, M. J Carneiro de Sousa, and R. Medeiros. 2015. "Forensic miRNA: Potential biomarker for body fluids?" *Forensic Science International: Genetics* 14 (January): 1–10. https://doi.org/10.1016/j.fsigen.2014.09.002.

Sing, Tobias, Oliver Sander, Niko Beerenwinkel, and Thomas Lengauer. 2005. "ROCR: visualizing classifier performance in R." *Bioinformatics* 21 (20): 3940–1. https://doi.org/10.1093/bioinformatics/bti623.

Singer, V. L., L. J. Jones, S. T. Yue, and R. P. Haugland. 1997. "Characterization of PicoGreen reagent and development of a fluorescence-based solution assay for double-stranded DNA quantitation." *Analytical Biochemistry* 249 (2): 228–38. https://doi.org/10.1006/abio.1997.2177.

Spiess, Andrej-Nikolai, Claudia Deutschmann, Michał Burdukiewicz, Ralf Himmelreich, Katharina Klat, Peter Schierack, and Stefan Rödiger. 2015. "Impact of Smoothing on Parameter Estimation in Quantitative DNA Amplification Experiments." *Clinical Chemistry* 61 (2): 379–88. https://doi.org/10.1373/clinchem.2014.230656.

Spiess, Andrej-Nikolai, Caroline Feig, and Christian Ritz. 2008. "Highly accurate sigmoidal fitting of real-time PCR data by introducing a parameter for asymmetry." *BMC Bioinformatics* 9 (1): 221. https://doi.org/10.1186/1471-2105-9-221.

Spiess, Andrej-Nikolai, Stefan Rödiger, Michał Burdukiewicz, Thomas Volksdorf, and Joel Tellinghuisen. 2016. "System-specific periodicity in quantitative real-time polymerase chain reaction data questions threshold-based quantitation." *Scientific Reports* 6 (December): 38951. https://doi.org/10.1038/srep38951.

Swango, Katie L., William R. Hudlow, Mark D. Timken, and Martin R. Buoncristiani. 2007. "Developmental validation of a multiplex qPCR assay for assessing the quantity and quality of nuclear DNA in forensic samples." *Forensic Science International* 170 (1): 35–45. https://doi.org/10.1016/j.forsciint.2006.09.002.

Taylor, Sean C., Katia Nadeau, Meysam Abbasi, Claude Lachance, Marie Nguyen, and Joshua Fenrich. 2019. "The Ultimate qPCR Experiment: Producing Publication Quality, Reproducible Data the First Time." *Trends in Biotechnology* 37 (7): 761–74. https://doi.org/10.1016/j.tibtech.2018.12.002.

Therneau, Terry, Beth Atkinson, and Brian Ripley. 2017. *rpart: Recursive Partitioning and Regression Trees*. https://CRAN.R-project.org/package=rpart.

Tichopad, Ales, Michael Dilger, Gerhard Schwarz, and Michael W Pfaffl. 2003. "Standardized determination of real-time PCR efficiency from a single reaction set-up." *Nucleic Acids Research* 31 (20): e122.

Tierney, Nicholas. 2017. "Visdat: Visualising Whole Data Frames." *The Journal of Open Source Software* 2 (16).

Tolson, Edward. 2001. "Machine Learning in the area of image analysis and pattern recognition." *Advanced Undergraduate Project, Spring*. https://stuff.mit.edu/afs/athena/course/urop/profit/PDFS/EdwardTolson.pdf.

Vennemann, Marielle, and Antje Koppelkamm. 2010. "mRNA profiling in forensic genetics I: Possibilities and limitations." *Forensic Science International* 203 (1-3): 71–75. https://doi.org/10.1016/j.forsciint.2010.07.006.

Walsh, Ian, Gianluca Pollastri, and Silvio C. E. Tosatto. 2015. "Correct machine learning on protein sequences: a peer-reviewing perspective." *Briefings in Bioinformatics*, September, bbv082. https://doi.org/10.1093/bib/bbv082.

Westermeier, Reiner. 2004. *Electrophoresis in Practice: A Guide to Methods and Applications of DNA and Protein Separations, Fourth Edition*. Wiley-Blackwell. https://doi.org/10.1002/3527603468.

Wickham, Hadley. 2011. "testthat: Get Started with Testing." *The R Journal* 3 (1): 5–10. http://journal.r-project.org/archive/2011/RJ-2011-002/index.html.

Williams, Graham J. 2009. "Rattle: A Data Mining GUI for R." *The R Journal* 1 (2): 45–55. http://journal.r-project.org/archive/2009-2/RJournal_2009-2_Williams.pdf.

Wilson, Greg, Jennifer Bryan, Karen Cranston, Justin Kitzes, Lex Nederbragt, and Tracy K. Teal. 2017. "Good enough practices in scientific computing." *PLOS Computational Biology* 13 (6): e1005510. https://doi.org/10.1371/journal.pcbi.1005510.

Wurmb-Schwark, N. von, R. Higuchi, A. P. Fenech, C. Elfstroem, C. Meissner, M. Oehmichen, and G. A. Cortopassi. 2002. "Quantification of human mitochondrial DNA in a real time PCR." *Forensic Science International* 126 (1): 34–39. https://doi.org/10.1016/S0379-0738(02)00026-9.

Yang, Yaran, Bingbing Xie, and Jiangwei Yan. 2014. "Application of Next-generation Sequencing Technology in Forensic Science." *Genomics, Proteomics & Bioinformatics*, Special Issue: Translational Omics, 12 (5): 190–97. https://doi.org/10.1016/j.gpb.2014.09.001.

Zielesny, Achim. 2011. *From Curve Fitting to Machine Learning*. Edited by Janusz Kacprzyk and Lakhmi C. Jain. Vol. 18. Intelligent Systems Reference Library. Berlin, Heidelberg: Springer Berlin Heidelberg. https://doi.org/10.1007/978-3-642-21280-2.